UNIVERSITÀ CATTOLICA del Sacro Cuore

Dottorato per il Sistema Agro-alimentare

Ph.D. in Agro-Food System

cycle XXXIII

S.S.D: AGR/11

Study of airborne particulate matter (PM) contaminating the honey bee *Apis mellifera* Linnaeus, 1758 and bee products

Coordinator: Ch.mo Prof. Paolo Ajmone Marsan

Candidate: Giulia Papa

Matriculation n.: 4713488

Tutor: Dr. Ilaria Negri

Academic Year 2019/2020

Go to the bee, thou poet:
consider her ways and be
wise.

George Bernard Shaw,
Man and Superman, 1903 p.96

Alla mia famiglia,

e a Mario.

Contents

Abstract

Apis mellifera Linnaeus (1758) order Hymenoptera family Apidae, is a eusocial insect widely known for its role in pollination, a fundamental ecosystem service for plant biodiversity and ultimately for the planet. During flight and foraging activity, the honey bee can collect airborne particulate matter (PM) on their own body, especially on the forewings, and can also contaminate bee products as pollen and honey. Particulate matter can originate from natural or anthropic sources, and is characterised by size (e.g., PM_{10}, $PM_{2.5}$, $PM_{0.1}$), chemical composition, and morphology.

In this thesis, honey bee, pollen and honey were used as bioindicator of PM – from coarse to ultrafine – in industrial areas of the Po Valley, Italy (Chapter 2 and Chapter 3). The (sub-lethal) effects of Titanium dioxide – a widespread airborne PM_1 pollutant – on the honey bee through oral exposure was then investigated (Chapter 4).

The technique used to analyse the PM contaminating bees and bee products is the scanning electron microscopy (SEM) coupled with X-ray spectrometer (EDX). EDX spectra allowed us to obtain chemical information from specimens, while backscattered-electron (BSE) imaging and elemental mapping provided both compositional and topographic information of PM.

Chapter 1 General introduction

1.1 Bees in the world

Apis mellifera Linnaeus (1758) is a eusocial insect that belongs to the family Apidae. This family is composed of subfamily Apinae with only one tribe Apini, with seven species of the genus *Apis* (Table 1), three of which are extinct species (Engel, 1999; Michener, 2007). The honey bees are a tropical group and arose in the Indo-Malayan region during the early Oligocene (Engel, 1999); the species that is distributed worldwide by human activity is *A. mellifera* Linnaeus (Michener, 2007).

Table 1. Distribution of genus *Apis*. **A. mellifera* Linnaeus has been distributed worldwide by human activity.

Species of the genus *Apis*			
Species	**Author**	**Year**	**Distribution**
Apis mellifera	Linneus	1758	Worldwide*
Apis florea	Fabricius	1787	South Asia
Apis dorsata	Fabricius	1793	Indo-Malayan
Apis cerana	Fabricius	1793	North Asia and East Asia
Apis henshawi †	Cockerell	1907	Europe
Apis armbrusteri †	Zeuner	1931	Europe
Apis vetusta †	Engel	1998	Europe

Most "varieties" of *A. mellifera* that can be easily identified by their general aspect, have been recognized as subspecies for a long time (Ruttner, 1988). However, a clear classification of the whole species was achieved only by a morphometric survey of specimens from all the accessible regions of the mellifera area, using a set of carefully selected characters, leading numerous taxa to be suppressed (Ruttner, 1988). In Biogeography and Taxonomy of Honeybees (Ruttner, 1988), Ruttner gathered the distinct taxonomic groups of *A. mellifera* in three groups for convenience: Near East, Tropical Africa and Mediterranean.

The Mediterranean group is divided in two subgroups (Table 2; Figure 1.1): West Mediterranean (North Africa, and West Mediterranean and North Europe), and Central Mediterranean and Southeast European. Within the latter, the taxonomic group including the subspecies of the peninsular Italian bee *Apis mellifera ligustica* Spinola, 1806, is present. The peninsular Italian honey bee is one of the most commercialized subspecies in the world, although it is mostly hybridized with *Apis mellifera mellifera* and *Apis mellifera carnica* typical of Northern Europe, and the Alps, Ex-Yugoslavia and Romania, respectively (Table 2; Figure 1.1) (Engel, 1999).

Table 2. Species within of the Mediterranean group by Ruttner. N.A.= North Africa; W.M. and N.E.= West Mediterranean and North Europe.

Mediterranean group of the *Apis mellifera*				
Species	**Groups**	**Sub-groups**	**Author**	**Year**
A. m. sahariensis	West Mediterranean	N.A.	Baldensperger	1924
A. m. intermissa		N. A.	Buttel-Reepen	1906
A. m. iberica		W.M.and N.E.	Goetze	1964
A. m. mellifera		W.M.and N.E.	Linnaeus	1758
A. m. sicula	Central Mediterranean and Southeast Europe		Montagano	1911
A. m. ligustica			Spinola	1806
A. m. cecropia			Kiesenwetter	1860
A. m. macedonica			Ruttner	1987
A. m. carnica			Pollmann	1879

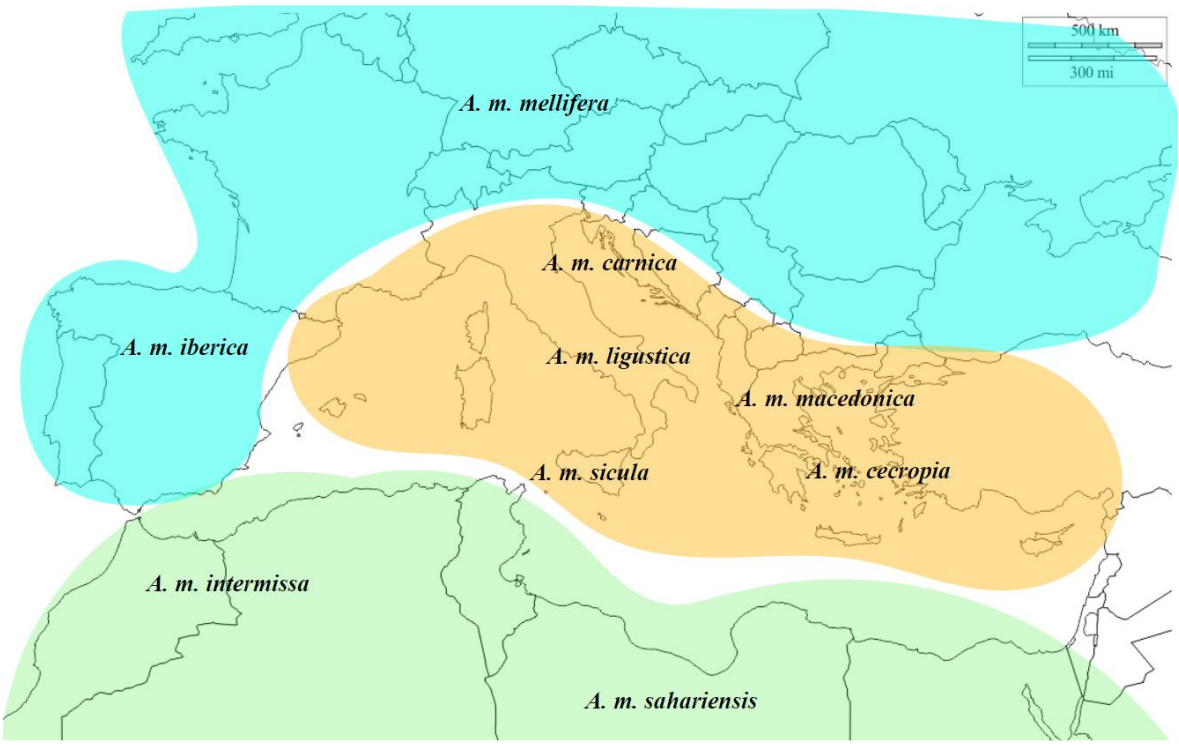

Figure 1.1 Bio-geographical distribution of *Apis mellifera* by Ruttner 1988. Light blue shows the West Mediterranean and North Europe subgroup, green shows the North Africa subgroup, and orange shows the Central Mediterranean and Southeast Europe subgroup.

1.2 A brief introduction on the honey bees world

1.2.1 Sex determination and castes

The honey bee lives in colonies, and the social organisation within a colony consists of three castes: the queen, workers, and drones (Figure 1.2). The queen is the only prolific female and can lay two types of eggs: unfertilized and fertilized, hence leading to haplodiploidy (Mackensen, 1951; Tautz, 2008; Contessi, 2009). Eggs are white and rod-shaped, with diameter 0.3 mm and length 1.5 mm (Contessi, 2009). Unfertilized haploid eggs will generate males or drones, whereas fertilized diploid eggs will generate female workers (sterile) or queens (fertile). The queen larva is fed exclusively with royal jelly throughout her life, whereas the worker larva is fed with royal jelly only the first three days after hatching, and then with bee bread (Contessi, 2009). Drones are fed with same diet of workers.

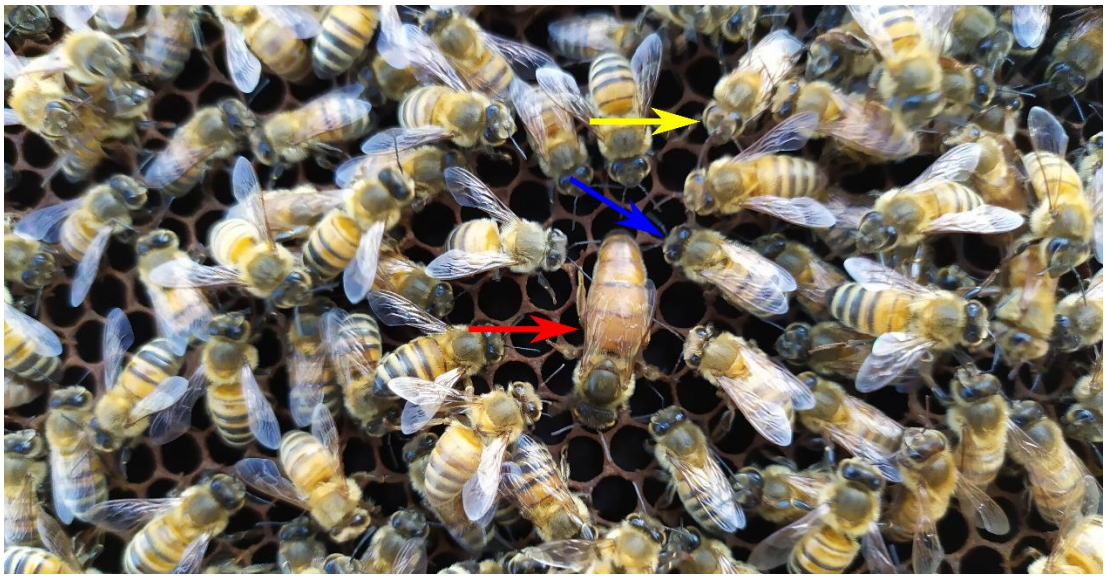

Figure 1.2 A colony of honey bees. The yellow, blue, and red arrows indicate the worker, the drone and the queen respectively (Photo by Alessandro Tinozzi).

1.2.2 Hive

The colony includes one queen, ~11-60 thousand workers, and ~1-2 thousand drones (Contessi, 2009). The whole colony lives into the hive. The hive is made of wax honeycombs built by the workers; cells in the honeycomb are used to either lay eggs or store food. The cells used to lay eggs differ depending on the caste of the bee which will be raised in it. With the exclusion of a 'queen' cell, all cells are hexagonal in shape (Figure 1.3 a; Figure 1.4) and sloped upward of 9-14° (Figure 1.3 b), the bottom walls are not flat and they are angled at 120° with the lateral walls (Figure 1.3 a). Cells having different purpose tend to be found in specific areas of the honeycomb. Specifically, 'food cells' are found in the upper part, 'worker cells' in the central part, and drone cells – that are slightly larger than worker cells – in the lateral and bottom parts. When new queens are needed, worker bees will build special elongated cells, resembling a peanut shell, at the bottom of the honeycomb in which queens are reared.

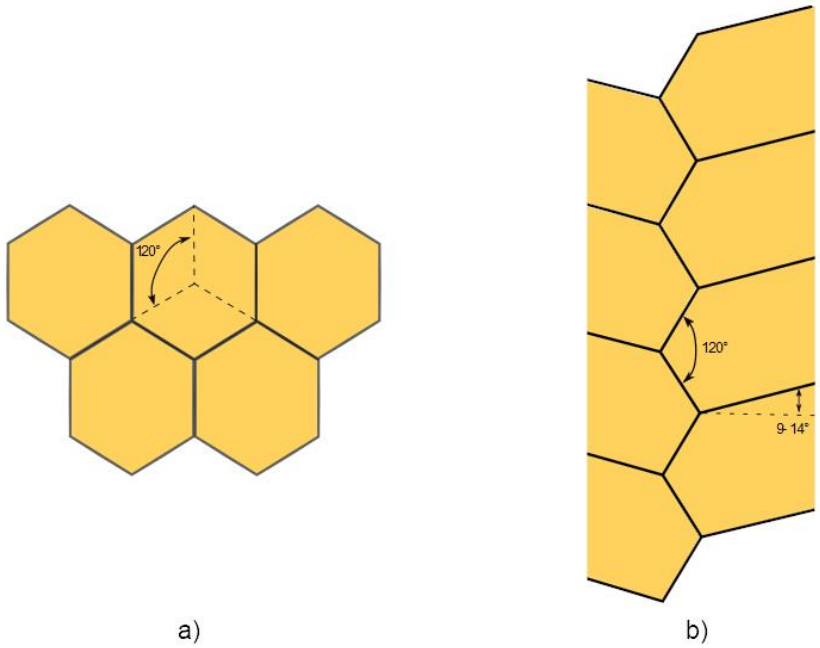

Figure 1.3 Geometry of the cells. a) Front view of the cells. b) Sagittal section of the honeycomb (figure based on Contessi, 2009).

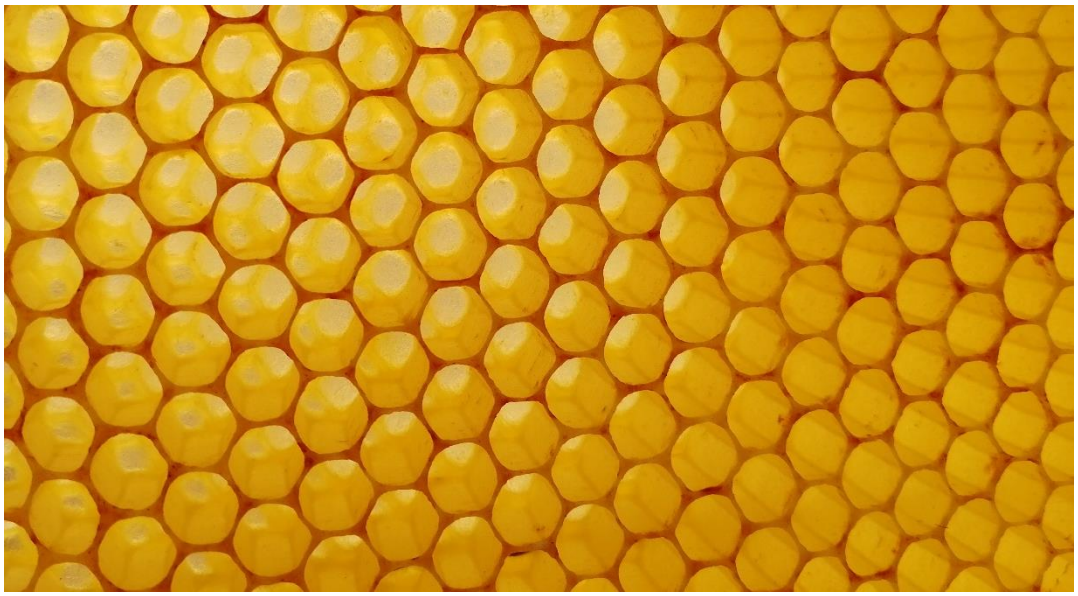

Figure 1.4 Cells of a honeycomb (Photo by Giulia Papa).

1.2.3 Life cycle of workers

Workers originate from fertilized eggs. The queen lays an egg at the bottom of the cell, which gets covered by a drop of royal jelly secreted by nurse bees. The egg hatches after three days and will be nursed and fed by nurse bees until pupation. A worker larva is fed

with royal jelly through the first three days after hatching and with bee bread (honey and pollen) afterwards. The larva goes through four moults, at 12, 36, 60, and 84 hours after hatching, respectively; a last moult occurs 11 days after hatching when the larva is covered. The covering starts seven days from laying when the larva body completely occupies the cell, then the workers close the cell with an air-permeant wax cover called operculum. After the last moult, the larva transforms into a pupa starting the metamorphosis. After ~21 days from laying, the young worker nibbles the operculum and comes out the cell as an adult. The values reported here on the life cycle of the workers are average values which can be affected by several factors, e.g., temperature. See Figure 1.5 for a schematic of bees' life cycle.

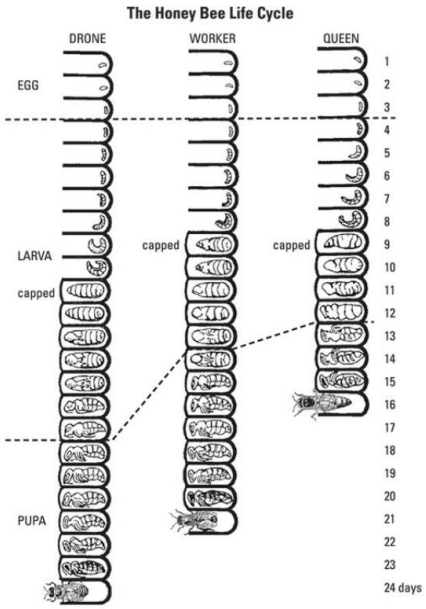

Figure 1.5 Life cycle of the drone, worker and queen bee (figure from Yadav, Kumar & Jat, 2017).

1.2.4 Tasks of the worker bee

When the worker bee becomes an adult, it conducts several tasks within and outside the hive (Figure 1.6) (Contessi, 2009). The first task is to clean and cover with propolis – that has antibacterial and antifungal properties (Ghisalberti, 1979) – the cells that will host the new eggs; the task will last about three days. Then, during the next ~10 days the worker

becomes able to produce royal jelly through the hypopharynx and mandibles glands which develops and become functional during this period exclusively. The worker bee uses the royal jelly to feed and nurse the new-born larvae and the queen. Hence, during this time, the worker bee is commonly called ‘nurse bee’. The nurse bees also take care of the old larvae (older than three days) feeding them with water, honey, and pollen. From day 10 to day 16 of adulthood the worker bee starts producing the wax from wax glands located in the ventral part of the abdomen (Figure 1.7). During this time, the worker bee builds and repairs the hive. For a few days, the worker bee becomes the nectar-receiving bee, i.e., it takes the nectar from the foragers and deposits it in the cells. At day 20 from adulthood the worker bee commits to defend the colony. Finally, as last task in life the worker bee becomes a forager.

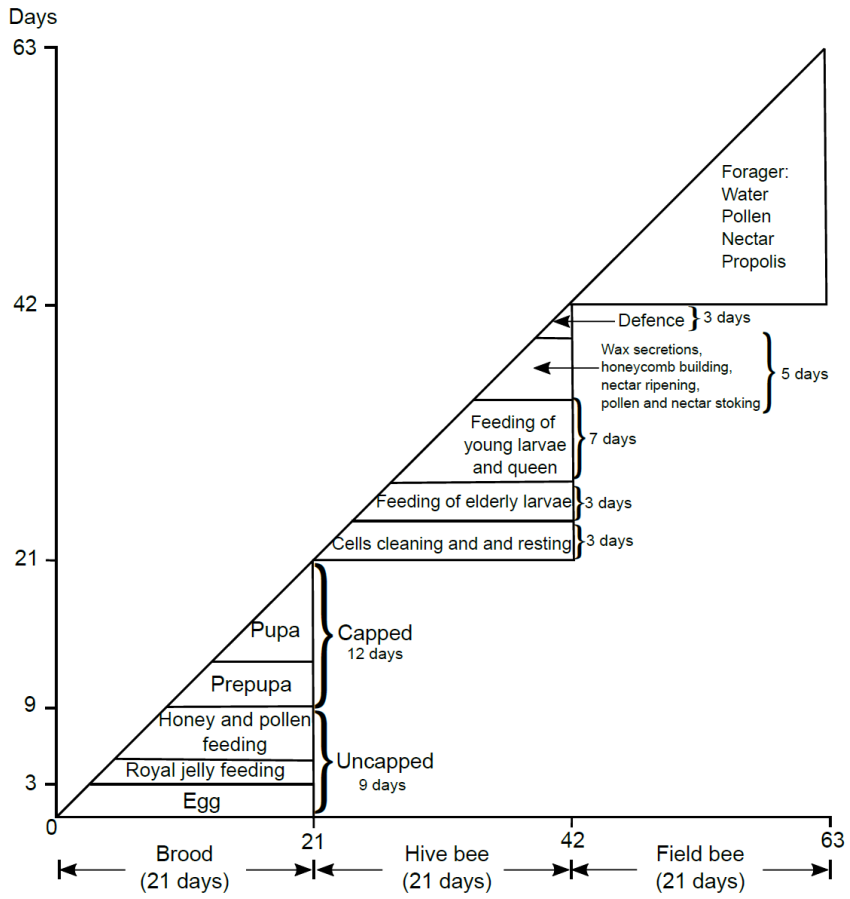

Figure 1.6 Sequence of duties of worker bees (figure modified from Contessi, 2009).

Figure 1.7 Worker Bee activating the wax glands in the ventral part of the abdomen (photo from Tautz, 2008).

1.2.5 Forager bees

The forager bees (Figure 1.8) are ~21 days old workers that collect water, nectar, pollen and plant resins. Forager bees can be classified into two categories: the scout bees and the reticent bees. The scout bees search for the best food resource and the reticent bees wait in the beehive until the scout bees return and give them information about the food source by dancing (von Frisch, 1967). The foraging activity of honey bees starts early in morning and finishes in the evening. Usually, the foraging activity fluctuates during the day with high pollen collection in the early morning and low amounts of pollen collected in the afternoon (Abou-Shaara, 2014). Foraging tends to happen within 2 km from the beehive, especially if there are attractive floral resources in the vicinity. However, scout bees can travel more than 10 km in search of desirable floral sources (Hagler et al., 2011).

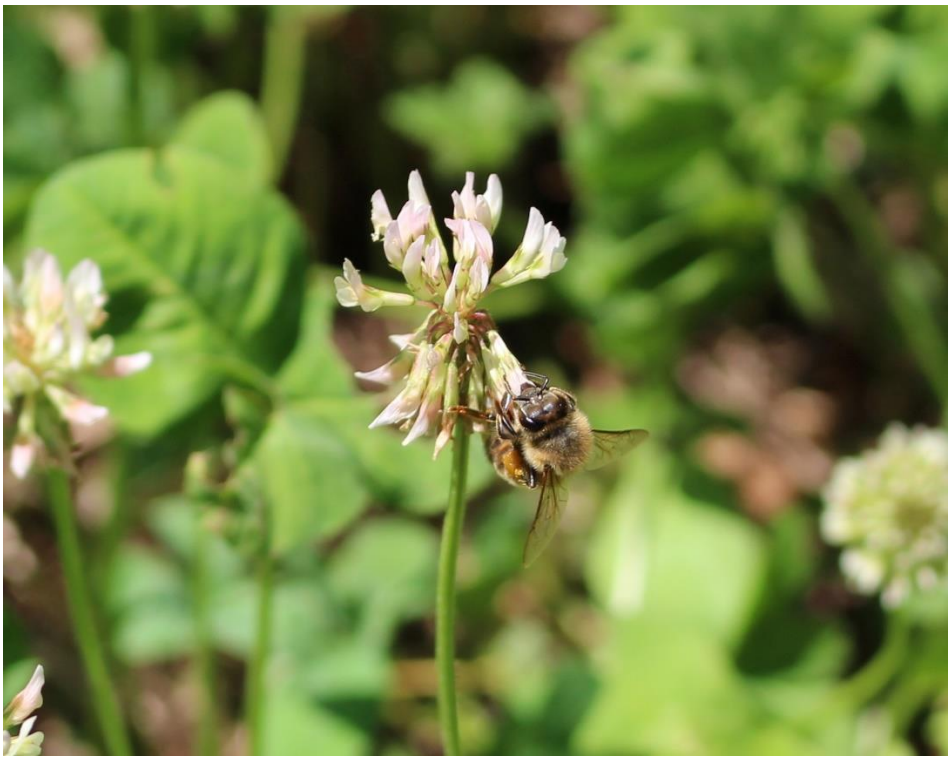

Figure 1.8 Forager bee. Forager bee in the field while collecting the nectar (Photo by Giulia Papa).

1.2.6 The products of the honeybees: honey and pollen

Honey is the principal and best-known product of bees and is their principal source of sugar. Honey derives from the nectar of the flowers that forager bees collect during the foraging activity. Nectar is a sugary solution that derives from the phloem sap and is collected from flowers nectaries, i.e., specialized tissues that secrete a sugary solution involved in interactions with animals (Nicolson, Nepi & Pacini, 2007). Various types of nectary exist, e.g., floral and extrafloral, located anywhere in the flower or in different parts of the plants. The constituents of nectar are water, carbohydrates (primarily of sugars which fructose, glucose and saccharose with total concentration ranges from 5% to 80%), amino acids, ions, organic acids, vitamin, enzyme and aromatic substances (Nicolson, Nepi & Pacini, 2007; Bortolotti & Marcazzan, 2017). The nectar composition varies from plant to plant and this variability is reflected by differences in colours, flavours and smell of the corresponding honey type.

When a bee reaches the flower, it extends the ligula, which is ~7 mm long, to reach the nectaries and suck the nectar (Bortolotti & Marcazzan, 2017). It is in this phase that the nectar is enriched with enzymes and other substances produced by the hypopharyngeal glands while it moves from the nectaries to the bee mouth before being stocked in the crop. When the bee returns to the hive, it regurgitates drops of the nectar solution stored in the crop to another bee. Such a phenomenon is called trophallaxis, it lasts 15-20 minutes and has the effect of reducing the water present in the droplet while adding enzymes such as invertase, diastase, glucose oxidase, catalase and phosphatase (Persano Oddo, Piazza & Pulcini, 1999; Bortolotti & Marcazzan, 2017). In particular, invertase is responsible for converting sucrose to fructose and glucose, which are the main sugars in honey (Persano Oddo, Piazza & Pulcini, 1999). Following trophallaxis, the nectar drop is deposited into a cell of the hive for the second phase of maturation (Figure 1.9). By moving their wings bees within the hive create air currents that favours the evaporation of the water. This activity allows the honey maturation, which is completed when the water percentage falls below 18%. At this point, the bees cover the honey with a wax lid as a protection and to prevent unwanted fermentation and spoilage (Bortolotti & Marcazzan, 2017).

Figure 1.9 Details of the honeycomb with immature honey (Photo by Giulia Papa).

Pollen represents the principal source of protein for bees and larvae. The collection of pollen is carried out by specialised forager bees (Contessi, 2009; Bortolotti & Marcazzan, 2017). While visiting a flower's blossom or inflorescence a forager bee covers its body with pollen dust. Once the bee takes off from the last flower visited, it uses the antenna cleaner present in its foreleg to collect any pollen dust from head and neck. The collected pollen is then kneaded with the available content from the crop to make a conglomerated pollen. The conglomerated pollen is then moved to the second pair of legs. In the meantime, the bee uses the second pair of legs to collect the pollen dust from the thorax. Then, using the hind legs the bee collects the pollen dust from its abdomen, the conglomerated pollen is then kneaded with the one coming midleg. Finally, the bee rubs its pollen brushes to aid the transfer of the conglomerated pollen to the pollen baskets using the auricle (Figure 1.10) (Contessi, 2009; Bortolotti & Marcazzan, 2017). Once the forager bee arrives in the hive it detaches the pollen using the spur present in the midleg. Other bees collect the pollen and store it in the cells of the hive (Figure 1.11) (Contessi, 2009; Bortolotti & Marcazzan, 2017).

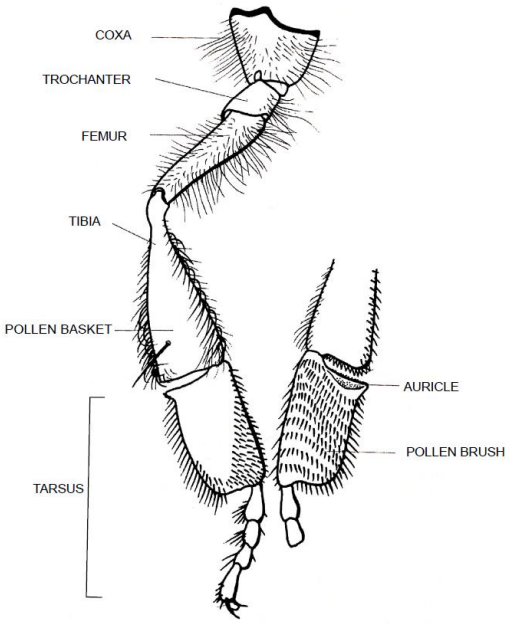

Figure 1.10 Anatomy of the bee leg (figure modified from Bortolotti & Marcazzan, 2017).

Figure 1.11 Pollen within the comb (Photo by Giulia Papa).

1.3 Honey bee and the ecosystem services

Ecosystem services are all the components of an ecosystem and the processes occurring in the ecosystem itself that sustain and fulfil human life (Daily, 1997). Ecosystem services include provisioning, regulating, cultural, and supporting services (Figure 1.12) (Millennium Ecosystem Assessment, 2005). Specifically:

- The provisioning services are the products obtained from the ecosystem (e.g., food, genetic resources, fuel, etc.).
- The regulating services are the benefits obtained from the regulation of ecosystem processes (e.g., pollination, climate regulation, water regulation, pest regulation, etc.).
- The cultural services are the nonmaterial benefits people obtain from ecosystem through spiritual enrichment, cognitive development, reflection, recreation, and aesthetic.

- The supporting services are necessary to produce all ecosystem services (e.g., photosynthesis).

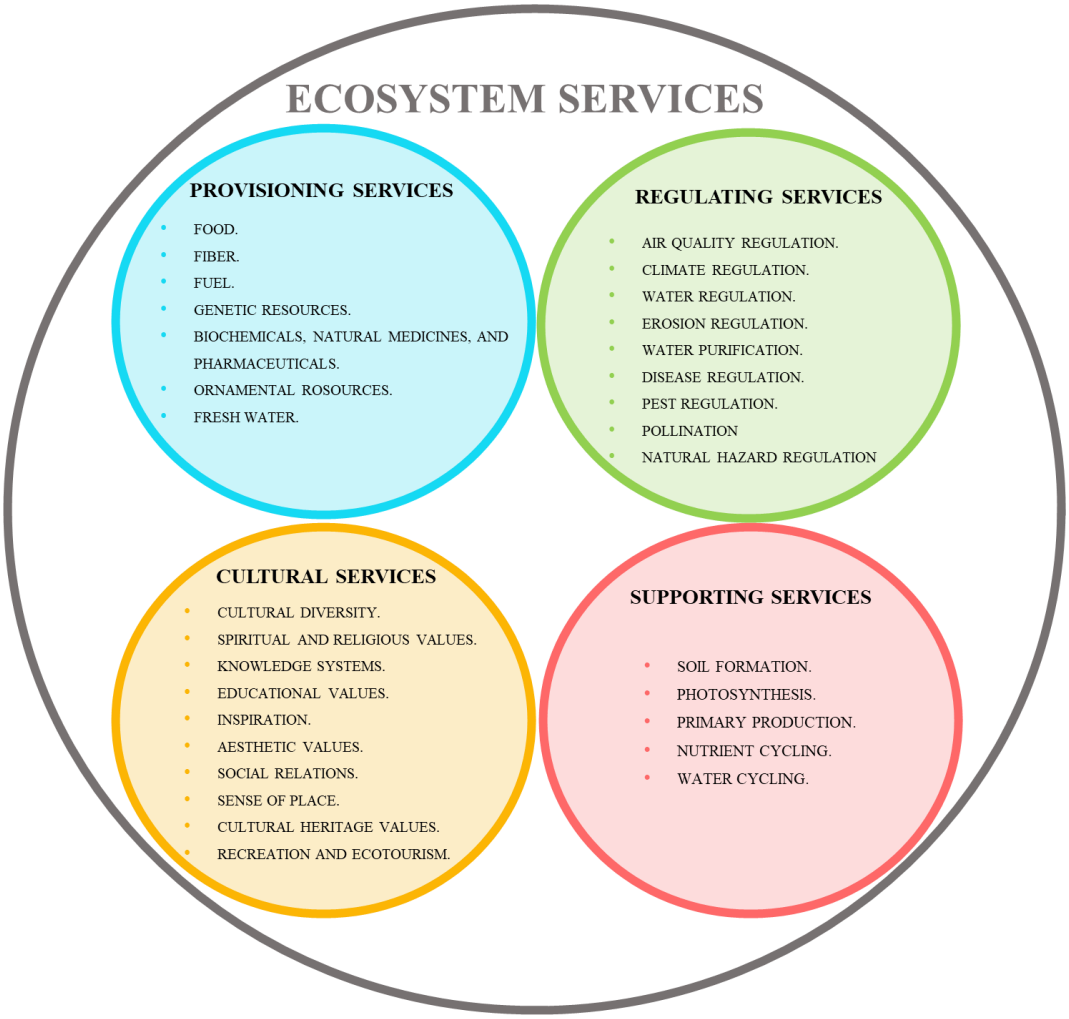

Figure 1.12 The four groups of ecosystem services.

Pollination is one of the regulating services, with animal pollination playing a key role in the sexual reproduction of many crops – 35% of global crop production – and wild plants (Klein et al., 2007). Pollination services are provided both by wild, free-living organisms (e.g., bee, moths, butterflies, wasps, bird, and mammals) and by commercially managed bee species. Honey bee is the most economically valuable pollinator of several crop monocultures worldwide and promotes the yields of fruit, seed, and nut crops. It is a common farming practice to ask beekeepers to relocate their beehives in the fields to ensure

crop pollination due to the scarcity or absence of wild pollinators (Klein et al., 2007; Kremen et al., 2007).

Albeit honey bee is commonly identified with pollination, this ecosystem service is performed also by other taxa as Diptera, Lepidoptera, Coleoptera, Formicidae and Vespoidea, often providing pollination services at times of the day and weather conditions when bees are unable to forage. Moreover, some non-bee taxa may be specific pollinators for some crops under certain conditions and/or carry pollen further distances than bees (Rader et al., 2016).

Loss of pollinators has directly affected the reproductive ability of some rare plants, ultimately leading to their extinction (Millennium Ecosystem Assessment, 2005; Christmann, 2020). Importantly, the abundance, distribution and success of pollinators are affected by ecosystem changes (Millennium Ecosystem Assessment, 2005).

1.4 Honey bee as bioindicator

Living organisms can be used to define the characteristics of the biosphere. These are referred to as biomonitors or bioindicators when the organism (or part of it) provides information on the quantitative or qualitative aspects of the quality of the environment, respectively. (Markert, Breure, & Zechmeister, 2003). Importantly, a biomonitor is always a bioindicator, whereas a bioindicator does not necessarily meet the requirements of a biomonitor (Markert, Breure & Zechmeister, 2003).

Bioindicators are used to assess both the health and changes in the environment they inhabit (Parmar, Rawtani & Agrawal, 2016). Three types of bioindicators can be distinguished: plants (e.g., diatoms, lichens), animals (e.g., aquatic invertebrates), and microbial (e.g., *Vogesella indigofera*). Bioindicators can be further distinguished in four categories depending on different application, namely: ecological bioindicator,

environmental bioindicator, biodiversity bioindicator, and pollution bioindicator (Figure 1.13) (Parmar, Rawtani & Agrawal, 2016).

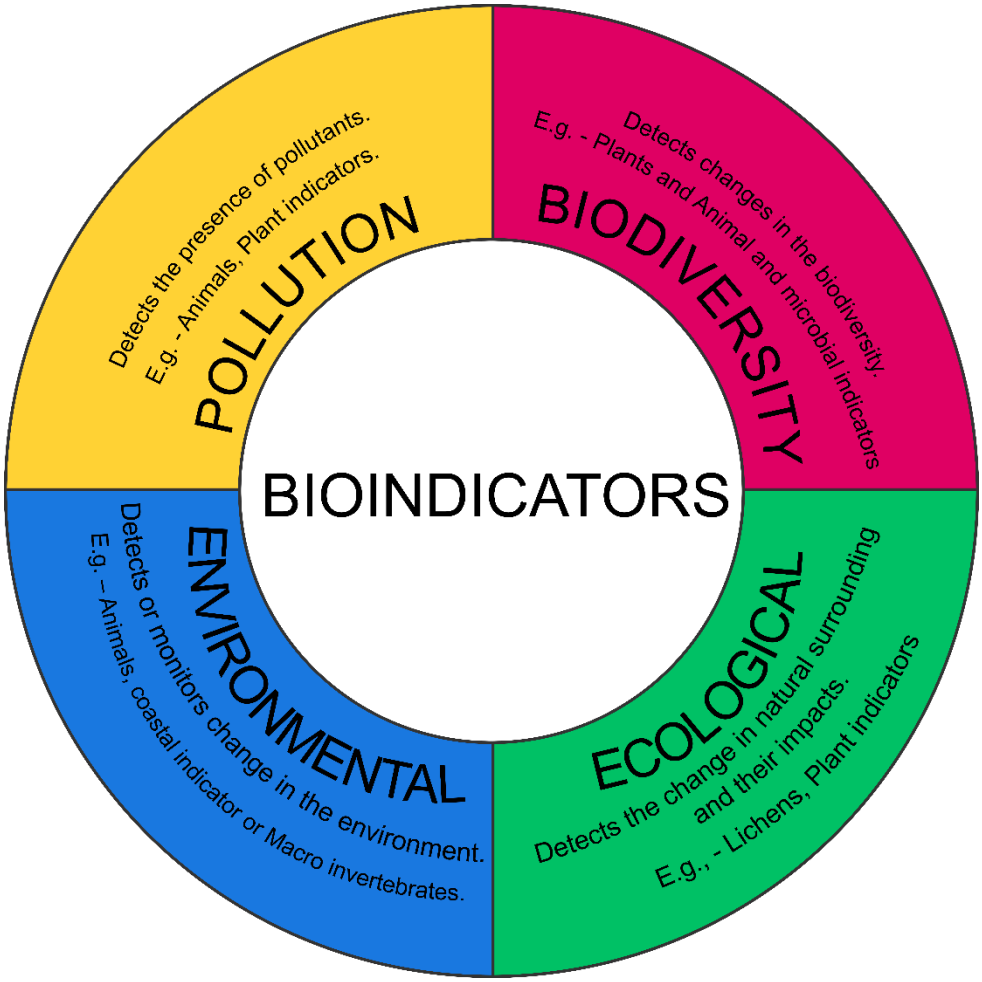

Figure 1.13 Different categories of bioindicators (figure based on Parmar, Rawtani, & Agrawal, 2016).

Honey bees and bee products (honey, pollen and wax) are frequently used as biomonitors of pollutant: e.g., pesticides, low-level radioactivity and heavy metals (Bromenshenk et al., 1985; Chemistry et al., 1990; Leita et al., 1996; Satta et al., 2012; Saunier et al., 2013; Bommuraj et al., 2019). Many studies were made to detect heavy metals in trace elements (TE) in bees and honey, as in Smith et al. (2019) where the honey bee and honey were also used to monitor isotopic lead ($^{206}Pb/Pb^{207}$ and $^{207}Pb/Pb^{208}$) (Zhou, Taylor & Davies, 2018; Smith et al., 2019).

Since 2015 the honey bee has been used as bioindicator of airborne particulate matter (PM) (Negri et al., 2015; Pellecchia & Negri, 2018). In these studies, the PM deposited on honey bees during their wide-ranging foraging activity was studied through scanning electron microscope coupled with X-ray spectroscopy (SEM-EDX) to investigate the morphology and the chemical composition of the PM deposit, and identify the different sources of emission.

1.5 Particulate matter

Particulate matter (PM) is an air pollutant, consisting of a heterogeneous mixture of soil and liquid particles suspended in the air (World Health Organization, 2013). Particulate pollution includes both natural and anthropogenic sources. Natural sources contain: sea salt, volcanic ash, wind-blown dust, soil particles, fungal spores, pollen, the products of forest fires and the oxidation of biogenic reactive gases (Kelly & Fussell, 2012; Kim, Kabir & Kabir, 2015). Anthropogenic sources include fossil fuel combustion (e.g., vehicles and power plants), erosion of the pavement by road traffic, and abrasion of brakes and tires, industrial process (e.g., cement factory, producing metals, ceramic and bricks), building, smelting, quarrying and mining activities, agricultural activities, cigarette smoking and wood stove burning (Kelly & Fussell, 2012; World Health Organization, 2013; Kim, Kabir & Kabir, 2015).

Primary PM is directly emitted into the atmosphere and may derive from both anthropogenic and natural sources. The main sources of anthropogenic primary PM are road transport and fossil fuel combustion processes from power and heat generation industries and residential sector. The main sources of natural primary PM are marine aerosol particles and soil dusts carried by the wind (Harrison et al., 2000; Juda-Rezler, Reizer & Oudinet, 2011; Kelly & Fussell, 2012; World Health Organization, 2013; Kim, Kabir & Kabir, 2015).

Secondary PM is generated in the atmosphere by photochemical gas-to-particle reactions, such as sulphur dioxide, oxide if nitrogen, ammonia, and non-methane volatile organic compounds, that produce low-volatility substances which condense into solid or liquid phase, thereby becoming submicron PM (d_a < 1.0 μm) (Harrison et al., 2000; Juda-Rezler, Reizer & Oudinet, 2011; Kelly & Fussell, 2012; World Health Organization, 2013; Kim, Kabir & Kabir, 2015).

PM is classified according to its aerodynamic diameter as: coarse PM_{10} ($d_a \geq 2.5$ μm and d_a < 10 μm), fine $PM_{2.5}$ (d_a < 2.5 μm), and ultrafine $PM_{0.1}$ (d_a < 100 nm) (Brook et al., 2010; Juda-Rezler, Reizer & Oudinet, 2011; Kelly & Fussell, 2012). The coarse particles (PM_{10}) include black smoke, soil, large salt particles from sea spray, dust from roads/tyres and building sites, but also pollen, mould, spores and other biological fragments (Juda-Rezler, Reizer & Oudinet, 2011; Kelly & Fussell, 2012). Fine particles ($PM_{2.5}$) may be generated by primary combustion processes (of fossil fuels), brake abrasion (Juda-Rezler, Reizer & Oudinet, 2011; Liati et al., 2019), and as product of the gas-to-particle conversion that generates secondary particles. Ultrafine particles (UFP; $PM_{0.1}$) arise largely from primary combustion emissions and secondary particles produced by gas-to-particle conversion processes. These particles are predominantly sulphates, nitrates, elemental carbon (EC) and organic carbon (OC) (Kelly & Fussell, 2012). A recent study showed that particles from brake wear occur in a wide-size spectrum including PM_{10}, $PM_{2.5}$ and $PM_{0.1}$ (Liati et al., 2019). PM between 0.1 and 1 μm in diameter may remain in the atmosphere for days or weeks and thus be subject to long-range transboundary transport in the air (Juda-Rezler, Reizer & Oudinet, 2011; World Health Organization, 2013).

Major chemical constituents in PM include sulphates, nitrates, ammonium, soil/minerals, and other inorganic ions, such as ions of sodium potassium, calcium, magnesium and chloride, organic and elemental carbon, particle-bound water, metals and polycyclic

aromatic hydrocarbons (PAH) (Kelly & Fussell, 2012; World Health Organization, 2013; Kim, Kabir & Kabir, 2015; Harrison, 2020). Moreover, biological components such as bacteria, viruses, fungi, mould, bacterial spores, and pollen may also be found (World Health Organization, 2013; Manisalidis et al., 2020).

Airborne particles may have a significant impact on human health, as they can penetrate within the respiratory system depending on their size (Figure 1.14) (Kim, Kabir & Kabir, 2015; Manisalidis et al., 2020). Epidemiological studies suggest that airborne PM is responsible of several respiratory and cardiovascular diseases, which might develop into lethal consequences (Wu et al., 2019). Furthermore, neurological effects (e.g., Alzheimer's disease, Parkinson's disease, and neurodevelopmental disorders) have been observed in adults and children after long-term exposure to air pollutants (Maher et al., 2016; Manisalidis et al., 2020).

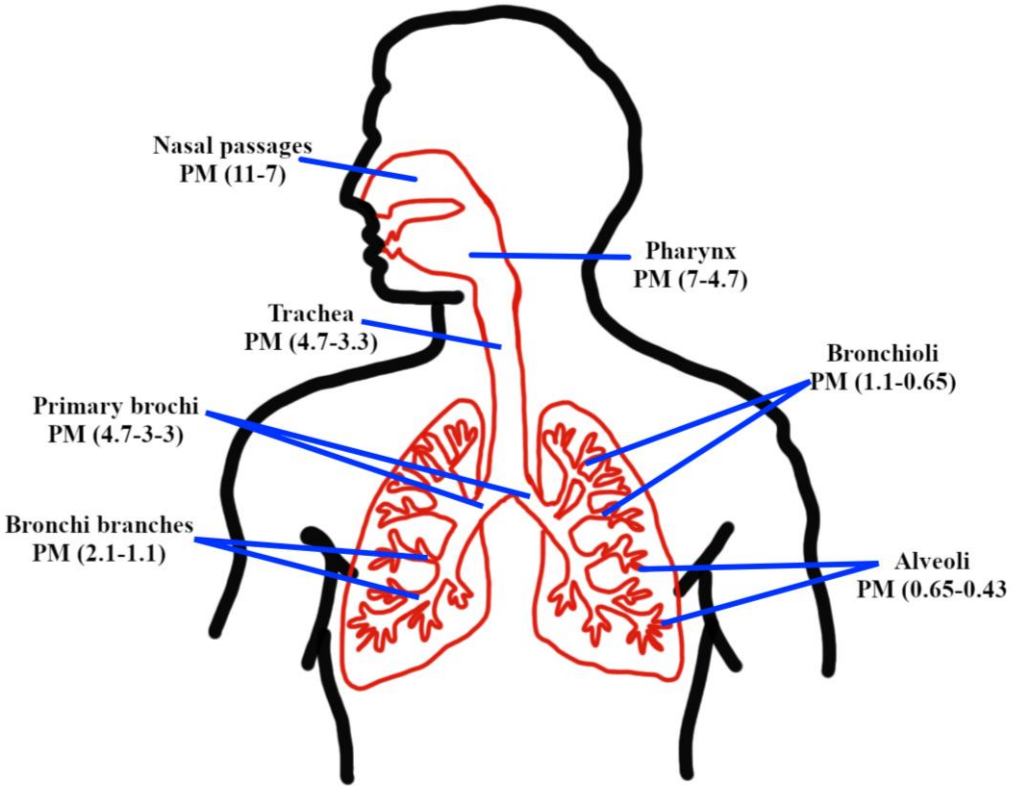

Figure 1.14 Penetrability according to particle size (figure based on Kim, 2015).

1.5.1 Honey bee and PM

The abundant pubescence on the body of the honey bee renders bees more likely to accumulate and retain small airborne particles during the flight, along with creating electrostatic-friction which enhances the attraction of such small particles to the bee body (Vaknin et al., 2000; Bonmatin et al., 2015). The airborne particulate matter deposits preferably on the head, wings, and hind legs of a bee (Figure 1.15) (Negri et al., 2015). It has been hypothesised that the presence of PM on the wings is due to the leading-edge vortex (LEV) (Figure 1.16) (Negri et al., 2015). The LEV is an aerodynamic mechanism generated by the insect wings motion which promotes the formation of a coherent vortical structure over the suction surface of the wings (Bomphrey, Taylor & Thomas, 2009). This vortex is typically generated through separation at the leading edge and generates high lift forces (Bomphrey et al., 2006; Bomphrey, Taylor & Thomas, 2009). Consequently, it is possible that the airborne dusts are continuously entrapped and canalized by the air flow, eventually becoming in contact with the wing edge where they adhere to the epicuticular wax and the hairs (Negri et al., 2015).

Figure 1.15 Higher concentration areas of Airborne PM deposition on a honey bee body are highlighted in red (figure from Negri et al. 2015).

Figure 1.16 Schematics of Leading Edge Vortexes on a honey bee wings during flight (figure from Negri et al. 2015).

1.6 Scanning electron microscope (SEM) with X-ray (EDX)

1.6.1 Introduction

The scanning electron microscope (SEM) is a versatile instrument for the examination and analysis of the microstructural morphology and chemical composition of samples (Zhou et al., 2006). The primary function of the SEM is to visualise small objects – otherwise invisible to human sight – by scanning high-energy electron beams on the surface of the object to form an image (Ul-Hamid, 2018).

The major sections of the SEM are the electron column, the specimen chamber, and the computer/electronic controls (Figure 1.17). On the top of the electron column is the electron gun that generates the electron beam. The beam penetrates a few microns into the surface of the sample. Into the column electromagnetic lenses are used to focus and reduce the electron beam into a small diameter probe. The specimen is kept under vacuum environment to allow electrons to travel without scattering (Zhou et al., 2006; Ul-Hamid, 2018).

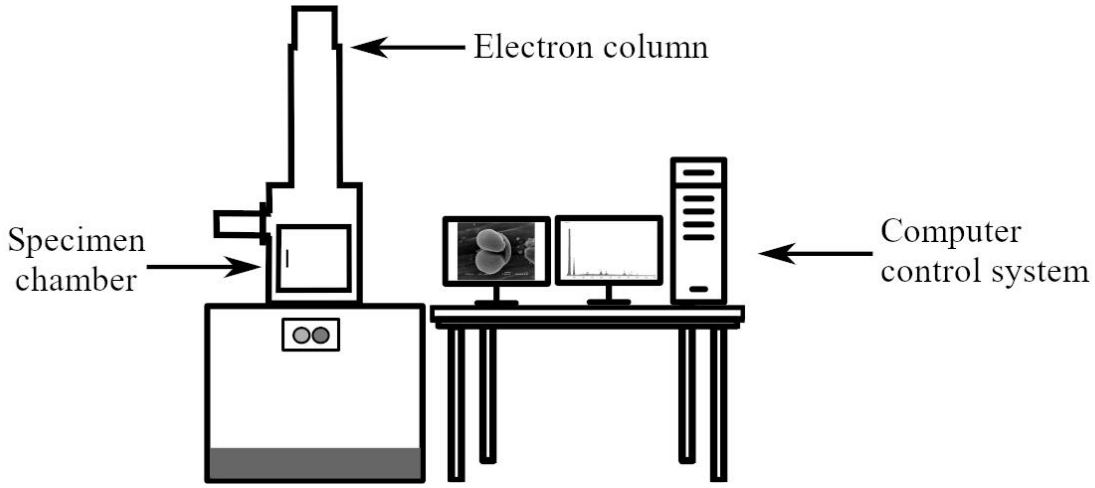

Figure 1.17 Three major sections of the SEM.

The interaction between the electron beam and the surface atoms of a sample generates a diversity of signals such as secondary and backscattered electrons, and characteristic X-rays are collected and processed to obtain images and the chemistry composition of the specimen surface (Zhou et al., 2006; Ul-Hamid, 2018).

Image creation in the SEM depends on the acquisition of signals produced from the electron beam, and specimen interactions (Figure 1.18) can be divided in elastic interactions and inelastic interactions (Zhou et al., 2006; Ul-Hamid, 2018).

Elastic scattering results from the deflection of the incident electron by the specimen atomic nucleus or by outer shell electrons of similar energy. This type of interaction is characterized by unimportant energy loss during the collision and by a wide-angle directional change of the scattered electron. Incident electrons that are elastically scattered through an angle of more than 90° are called backscattered electrons (BSE) and yield a useful signal for imaging the sample (Zhou et al., 2006).

Inelastic scattering occurs through interactions between the incident electrons and the electrons and atoms of the sample, resulting in the primary beam electron transferring a considerable amount of energy to that atom (Zhou et al., 2006). The quantity of energy loss

is dependent on whether the specimen electrons are excited singly or collectively and on the binding energy of the electron to the atom. Consequently, the excitation of the specimen electrons during the ionization of atoms leads to the generation of secondary electrons (SE). SE are commonly defined as electrons possessing energies of less than 50 eV and can be used to image or analyse the sample (Zhou et al., 2006). The best image resolution in the SEM corresponds to the diameter of the electron probe; in the new SEM generation the image resolution can be of the order of <1 nm (Ul-Hamid, 2018).

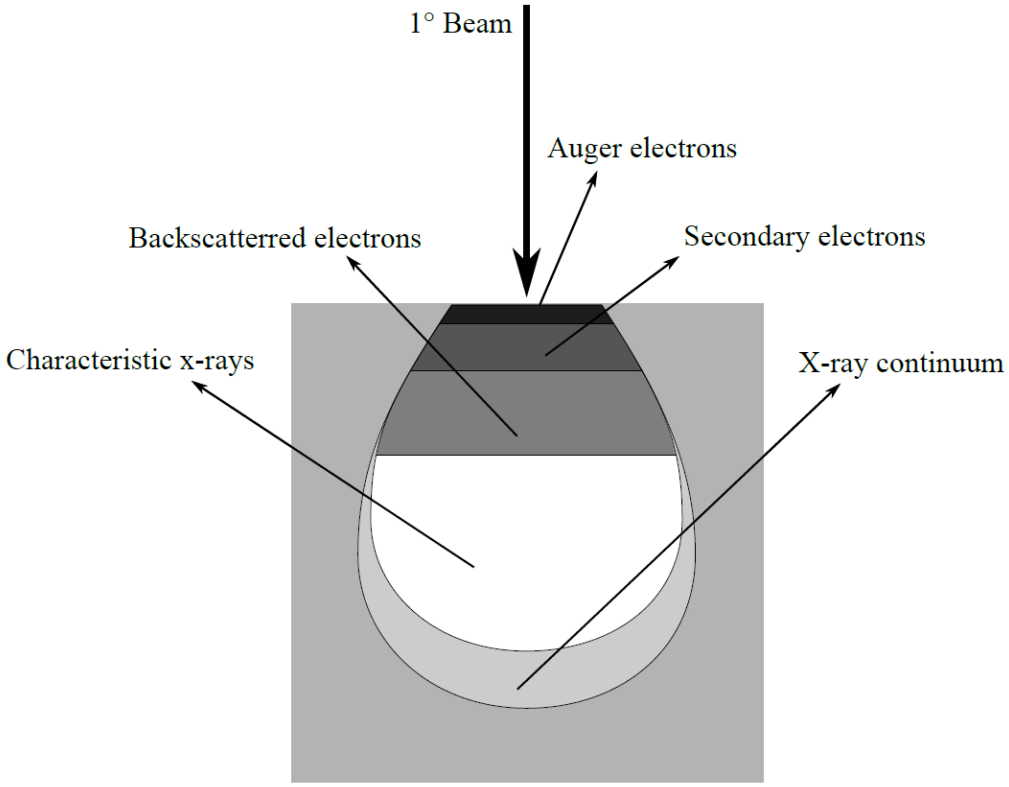

Figure 1.18 Signals that are utilized to form an image by electron beam-specimen interaction in SEM (figure based on Zhou et al., 2006).

1.6.2 Sample preparation

If the sample is either inorganic (conductive) or organic (nonconductive), it is necessary to prepare the sample accordingly. If the sample is inorganic (e.g., nanomaterials or geological samples) it can be observed by SEM directly by loading them on carbon tape. Biological samples need to be dried before receiving the metal coating (e.g., gold, silver

etc.) to render the specimen conductive (Zhou et al., 2006). Sputter coating (Figure 1.19) is used to cover the specimen with a uniform distribution of metal coating. This method works under lower vacuum in an argon atmosphere to reduce specimen surface damage (Zhou et al. 2006; Ul-Hamid 2018). Gold coating is preferred for topography, while carbon coating is preferred for elemental analysis because carbon does not interfere with the detection of other elements in energy dispersive X-ray spectrometer/spectrometry EDX/EDS analysis (Ul-Hamid, 2018). Evaporated carbon is used to cover the specimen with a fine grain size carbon layer, which makes it suitable for use at high magnifications. The optimal thickness of the carbon layer is around 20 nm and in this case the method is appropriate for flat surfaces (Ul-Hamid, 2018). In addition, granular morphology of the coating does not appear as an artifact during high-resolution imaging.

Figure 1.19 Quorum Q150T ES Plus combined sputtering and carbon coating system (photo from www.quorumtech.com).

1.6.3 BSE imaging

Incident electrons that are elastically scattered at an angle >90° are called backscattered electrons (BSE) (Zhou et al., 2006; Ul-Hamid, 2018). Detection by BSE provides both compositional and topographic information in SEM. Briefly, significant amount of beam energy is removed from the sample due to the leakage of backscattered electrons from the

specimen (Figure 1.20) (Ul-Hamid, 2018). Once out in the vacuum, these electrons can be captured by a detector and used to form an image called backscattered electron image. The contrast exhibited by the image is called compositional or atomic number (Z) contrast (Ul-Hamid, 2018). The result of the BSE image is a contrast picture where the phase with a high atomic number will appear relatively brighter, while phase with a low atomic number will appear relatively dark (Figure 1.21) (Ul-Hamid, 2018). Conversely, SE images are used for topographic contrast suitable for surface morphology examination i.e., for the visualization of surface texture and roughness (Zhou et al., 2006; Ul-Hamid, 2018). That is due to secondary electrons that are prevented from reaching the detector and will generate shadows or be darker in contrast than those regions that have an unobstructed electron path to the detector (Zhou et al., 2006).

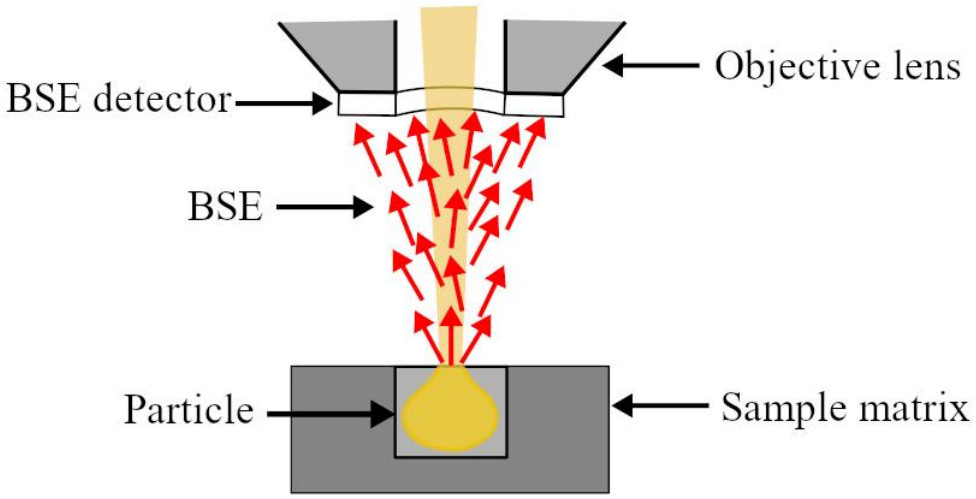

Figure 1.20 Schematics of BSE analyses (figure based on Ul -Hamid, 2018).

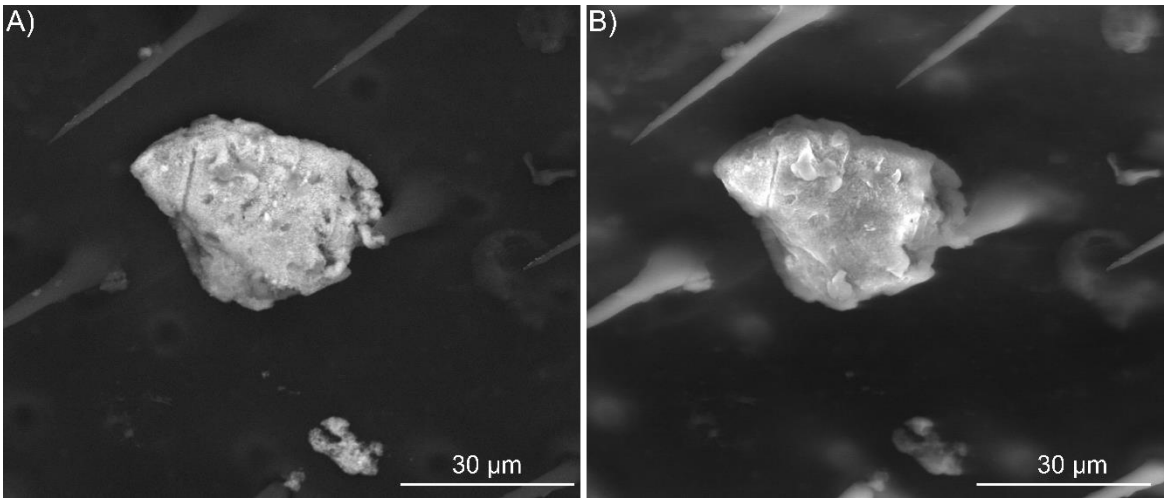

Figure 1.21 BSE and SE images. A) The black and white contrasts of the BSE image are based on the composition; B) the SE image allows surface morphology examination (Photos courtesy of I. Negri).

1.6.4 EDX/EDS analysis

The energy dispersive X-ray spectrometer/spectrometry (EDX or EDS) technique (Figure 1.22) can be applied to obtain chemical information from specimens examined using the SEM (Zhou et al., 2006; Ul-Hamid, 2018). The integration of an EDX detector in the SEM column enables to determine the localized chemistry of a region (Ul-Hamid, 2018). The EDX identifies the quantum characteristic X-ray energy and wavelength, respectively for elemental analysis (Ul-Hamid, 2018). In addition, the EDX detector is incorporated so that does not disturb or affect the imaging capability of the instrument.

Figure 1.22 Bruker XFlash 6|30 EDX detector mounted on the SEM (Photo by Giulia Papa).

The X-ray detector is used to obtain an X-ray signal, which is the combination of X-rays and white radiation (background X-rays). The X-ray signal is produced by interaction of the primary electron beam with the specimen material. Moreover, by measuring energy and intensity distribution, the X-ray detector can identify elements and determine their respective concentrations in the focal region of the specimen (Figure 1.23) (Ul-Hamid, 2018).

Element	At. No.	Netto	Mass [%]	Mass Norm. [%]	Atom [%]	Comp.	Sto. [%]	Sto. Norm. [%]	abs. error [%] (1 sigma)	rel. error [%] (1 sigma)
Carbon	6	322042	0.00	0.00	0.00		0.00	0.00	0.00	0.00
Oxygen	8	0	0.61	20.58	47.79		0.00	0.00	0.09	14.09
Chromium	24	2949	0.45	15.14	10.82	Cr2O3	0.66	22.13	0.04	8.96
Iron	26	6068	1.41	47.45	31.56	FeO	1.81	61.04	0.07	4.79
Copper	29	1156	0.50	16.83	9.84		0.50	16.83	0.05	9.23
		Sum	**2.97**	**100.00**	**100.00**		**2.97**	**100.00**		

Figure 1.23 Example of a quantitative microchemical analysis.

The EDX analyses provides micro-chemical information in the shape of an EDX spectrum (Figure 1.24). In the EDX spectrum the x-axis displays X-ray energy in keV (usually up to 20 keV), and the y-axis shows intensity in counts or counts per second (Zhou et al., 2006; Ul-Hamid, 2018). Elements are identified based on X-ray energies that will show specific peak positions according to each element identified. The computer compares peak energies against a database where the energy profiles of several elements are stored, enabling the labelling of the query peak (Ul-Hamid, 2018). An element can be characterised by several specific peaks, e.g., heavy elements often generate many X-ray peaks (Figure 1.24).

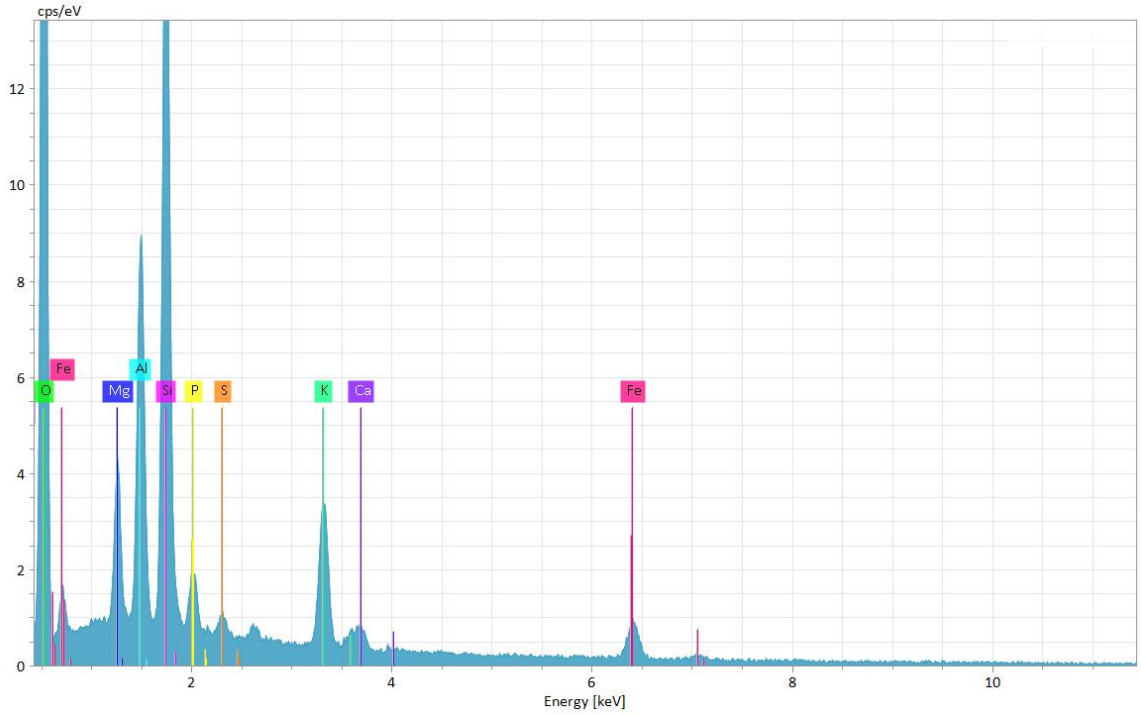

Figure 1.24 An EDX spectrum obtained from PM with heavy elements.

High-intensity peaks are identified as Kα, Lα or Mα depending on the atomic numbers of the elements present in the specimen (Ul-Hamid, 2018). This is followed by the identification of the corresponding Kβ, Lβ, or Mβ whose intensity is significantly lower (Ul-Hamid, 2018). The advantages of the EDX technique are: the non-destructive analysis of samples, small analysis time, sensitivity to light elements as well as heavy elements, and the ability to identify heterogeneity or segregation in specimens and determine the chemistry of small objects or areas of interest (Ul-Hamid, 2018).

1.6.5 X-ray maps

X-ray mapping allows the visual distribution of elements in a focal area of the specimen by means of X-ray spectra (Figure 1.25).

To obtain an X-ray map the sample is scanned by the electron beam from each discrete location (pixel), and an EDX spectrum is obtained and stored (Ul-Hamid, 2018). Data for all elements are captured in each pixel allowing different elements to be mapped simultaneously (Ul-Hamid, 2018). Several frames (hundreds) are taken from the same area

to improve map resolution. High probe currents are employed for X-ray mapping to attain good contrast (Ul-Hamid, 2018).

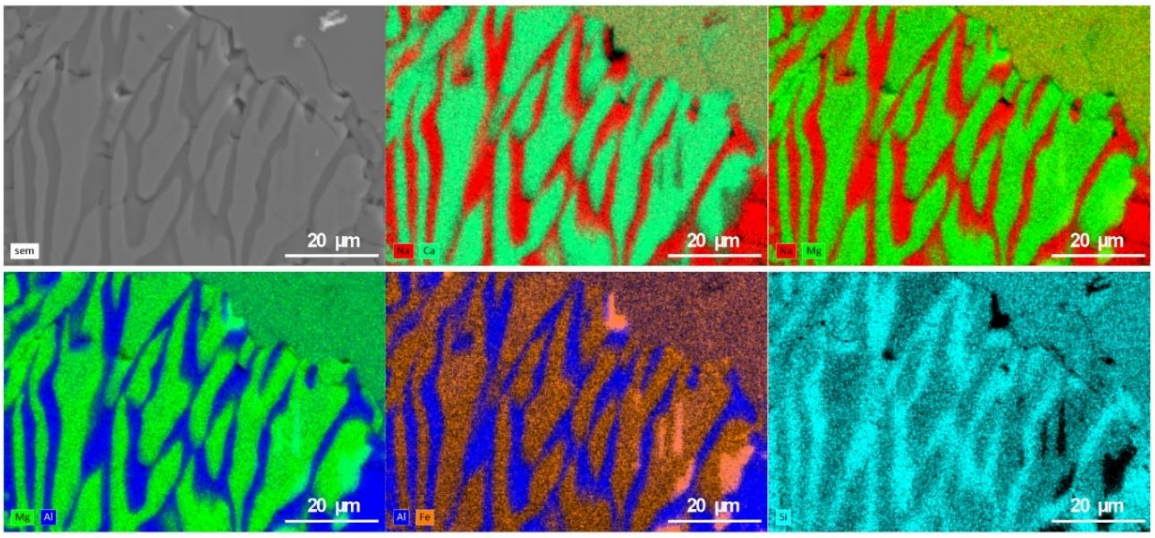

Figure 1.25 X-ray or EDX maps. EDX maps showing elemental distribution in plagioclase-diopside symplectites (solid state reaction microstructure) in eclogites from Alpe Arami (Locarno, Switzerland), one of the few localities in the Alps where ultra-high pressure rocks related to the Alpine orogenesis occur (figure courtesy of G. Capitani).

1.7 Aim of the thesis

The general aim of this work is to assess the contamination of *A. mellifera* and its products by airborne PM in highly-anthropized areas.

Within such a context, this thesis aims at achieving three specific goals:

1. Characterize the fine and ultrafine airborne PM in highly-anthropized area (Chapter 2 and Chapter 3). The honey bee was used as an alternative sampling system of PM in an area of the Po Valley (Northern Italy), which is subject to intense traffic. The characterization of PM was carried out by SEM-EDX.
2. Assess the presence of fine and ultrafine airborne PM pollutants in honey and pollen (Chapter 3). Pollen collected by forager bees and honey produced by the bee colony displayed contamination by nanosized Fe-oxides/hydroxides and baryte. Such a contamination exposes pollinators and humans to UFP ingestion, endangering the safety of food produced at traffic-influenced sites.
3. Verify microbiota alterations caused by fine and ultrafine PM on *A. mellifera* specimens using ecotoxicology essay (Chapter 4).

Chapter 2 Disentangling multiple PM emission sources in the Po Valley (Italy) using honey bees

Published in *Heliyon*

https://doi.org/10.1016/j.heliyon.2021.e06194

Giancarlo Capitani[1], Giulia Papa[2], Marco Pellecchia[3], Ilaria Negri[2]*

[1] DISAT – Università Milano Bicocca, Milano, Italy

[2] DIPROVES – Università Cattolica del Sacro Cuore, Piacenza, Italy

[3] KOINE'– Consulenze Ambientali, Montechiarugolo (Parma), Italy

*Corresponding author

Article history:

Received 16 June 2020

Revised 28 June 2020

Accepted 1 February 2021

Available online 10 February 2021

2.1 Abstract

Particulate matter (PM) is a complex mixture of airborne chemical compounds commonly classified by their aerodynamic diameter. Although PM toxicity strongly depends on the morphology, chemical composition, and dimensions of particles, exposure limits set by environmental organisations only refer to the mean mass concentration of PM sampled daily or annually by monitoring stations.

In this study, we used honey bees as sensors of airborne PM_{10} and $PM_{2.5}$ in a highly polluted area of the Po Valley, northern Italy. Honey bees are an efficient sampler of airborne PM because, during flight and foraging activities, their pubescence promotes the accumulation of electrical charge on the body surface owing to air resistance, thus enhancing airborne PM attraction. Particles attached to the body of bees are readily accessible for physico-chemical characterisation using a scanning electron microscope coupled with X-ray spectroscopy (SEM/EDX). Our results demonstrate that residents in the study area are intermittently but chronically exposed to a well-defined spectrum of metal-bearing particles and mineral phases known to induce specific health outcomes.

The morphology, size, and chemical composition of PM_{10} and $PM_{2.5}$ detected on bees in the monitoring area were indicative of traffic, agricultural operations, and high-temperature combustion processes. The contribution of the A1 Milano-Bologna highway, local wheat and alfalfa cultivation, and the Parma incineration plant were clearly distinguishable. Our data also demonstrated that PM exposure levels may vary sharply throughout the year based on recurrent local activities.

2.2 Introduction

Particulate matter (PM) is an air pollutant consisting of a mixture of suspended solid and liquid particles that originate directly from natural sources (e.g., volcanic eruptions, forest fires, and sea spray) and anthropogenic sources (e.g., motor vehicles, factories, and agriculture) and indirectly from chemical reactions that convert atmospheric precursors into secondary PM. Airborne PM is commonly classified according to particle size; inhalable PM includes particulates with an aerodynamic diameter $\leq 10\,\mu m$ (PM_{10}), which can penetrate the respiratory tract below the larynx, while respirable PM $\leq 2.5\,\mu m$ ($PM_{2.5}$) may penetrate the gas-exchange region of the lungs (Brown et al., 2013).

The human health hazards associated with PM exposure are universally acknowledged both in terms of the effects of their components and the enhanced transmissibility of pathogens (Wang, Eliot & Wellenius, 2014; van Doremalen et al., 2020; Setti et al., 2020). Although the toxicity of PM strongly depends on its morphology, chemical composition, and dimensions (Wang, Eliot & Wellenius, 2014; Maher et al., 2016; Bencsik, Lestaevel & Guseva Canu, 2018), exposure limits set by environmental organisations only refer to the mean mass concentrations of PM sampled daily or annually at monitoring stations, with no specific indicators regarding the chemical nature of the particles (see, for example, Directive 2008/50/EC of the European Parliament and of the Council of 21 May 2008 on ambient air quality and cleaner air for Europe).

In the present study, honey bees (*Apis mellifera* L.) were used as an alternative sampling system for airborne PM_{10} and $PM_{2.5}$ in a highly polluted area of the Po Valley, northern Italy, near the city of Parma. Besides being a key provider of ecosystem services through the provision of many products, such as honey, pollen, wax, and propolis, and the pollination of many wild and cultivated plants, honey bees are important bioindicators of environmental contamination (Devillers & Pham-Delegue, 2002; Bargańska, Ślebioda &

Namieśnik, 2016). Bees and their products are commonly used for the detection of environmental pollutants including pesticides, heavy metals, radionuclides, volatile organic compounds, polynuclear aromatic hydrocarbons, and dioxins (Devillers & Pham-Delegue, 2002; Perugini et al., 2011; Giglio et al., 2017; Goretti et al., 2020).

Recent studies have demonstrated that forager bees act as efficient mobile samplers for airborne PM (Negri et al., 2015; Pellecchia & Negri, 2018; Papa et al., 2020 (Chapter 3)). During flight and foraging activity, bee pubescence promotes the accumulation of electrical charge at the body surface owing to air resistance. This charging enhances the attraction of airborne particles, which include not only pollen but also pollutants (Vaknin et al., 2000; Bonmatin et al., 2015). Airborne PM attached to bee bodies can be analysed based on size, morphology, and chemical composition using a scanning electron microscope (SEM) coupled with X-ray spectroscopy (EDX) (Negri et al., 2015; Pellecchia & Negri, 2018). SEM/EDX is a powerful, fast, and non-destructive analysis technique, and determining both the chemical and morphological characteristics of particles typically allows their accurate identification and classification. Single particles can also be counted and their size measured for detailed quantitative assessment. In the present study, we applied this methodology to investigate PM_{10} and $PM_{2.5}$ accumulated on honey bees in an urban area of the Po Valley, which is one of the most important industrial and agricultural areas in Italy and Europe, characterised by a high population density and low air quality (Marcazzan et al., 2001; Pirovano et al., 2015).

The study area includes agricultural fields, a relatively new incinerator plant, and a stretch of the Milano-Bologna motorway. A single fixed monitoring station for the airborne concentrations of gaseous pollutants and PM has already been established, providing daily and annual mean concentrations of PM_{10} and $PM_{2.5}$ particles per cubic metre of air volume,

but no information on the nature and chemical composition of the particles is currently available (Regional Environmental Protection Agency, www.arpae.it).

We aimed to test the use of SEM/EDX for characterising the morphology, chemical composition, and size of PM collected by bees and distinguishing among different emission sources to, ultimately, estimate their relative contributions in the study area. The EDX spectra associated with multiphase aggregations and sub-micrometre PM are also explored.

2.3 Experimental

2.3.1 Study area

A hive was placed in the N-NE peri-urban area of the City of Parma approximately 4 km from the city centre (Figure 2.1 a). The hive was placed on a grassy lot surrounded by cultivated fields approximately 100 m from the A1 motorway, 400 m from the Parma exit, and 400 m from the incinerator plant (Figure 2.1 b). The A1 motorway connects Milan and Naples and is one of the most congested motorways in Italy, experiencing an average traffic load of over 2.5 million vehicles per month.

The local nectar and pollen resources for the bees included several wild plant species (e.g., *Taraxacum officinale*, *Prunus spinosa*, and Brassicaceae) and crops including corn, alfalfa, and rapeseed, and the apiary was surrounded by wheat and alfalfa fields (brown plots in Figure 2.1 b).

Figure 2.1 Location of the hive relative to the city centre of Parma (a) and the incinerator plant and the motorway (b).

In addition to a system that continuously monitors stack emissions from the incinerator (e.g., carbon monoxide and dioxide, nitrogen oxides, hydrogen fluoride, hydrogen chloride, ammonia, and dust), PM_{10}, $PM_{2.5}$, mercury, benzene, toluene, xylene, and ozone are regularly monitored in the area through fixed and mobile monitoring stations (Regional Environmental Protection Agency, www.arpae.it). In this study, airborne PM was monitored from June to October 2017 using honey bees.

2.3.2 Geological outlines

Parma is located in the central Po Valley in a Pliocene/Quaternary alluvial sedimentary plain between the northern Apennines and the Southern Alps (Figure 2.2). The study area includes terraced alluvial fan deposits built up by the hydrographic network of the Taro River and the Parma Stream, both tributaries of the Po River that flows north of Parma. These terrains are distinguished on a morphological, archaeological and pedostratigraphic basis into the Ravenna subsynthem and the Modena Unit (Calabrese & Ceriani, 2009). The Ravenna subsynthem primarily comprises gravels and sandy gravels with local intercalations of sands and silty sands covered by a silty-clay layer of variable thickness. The roof alteration front is moderately thick (0.1-1 m) and the soils show a shallow decarbonated layer. The Modena Unit primarily comprises sands with pebbly lenses and

levels covered by a discontinuous silty layer. The roof alteration front is moderately thick (a few tens of centimetres) with an overall thickness of 5-6 m and (Calabrese & Ceriani, 2009).

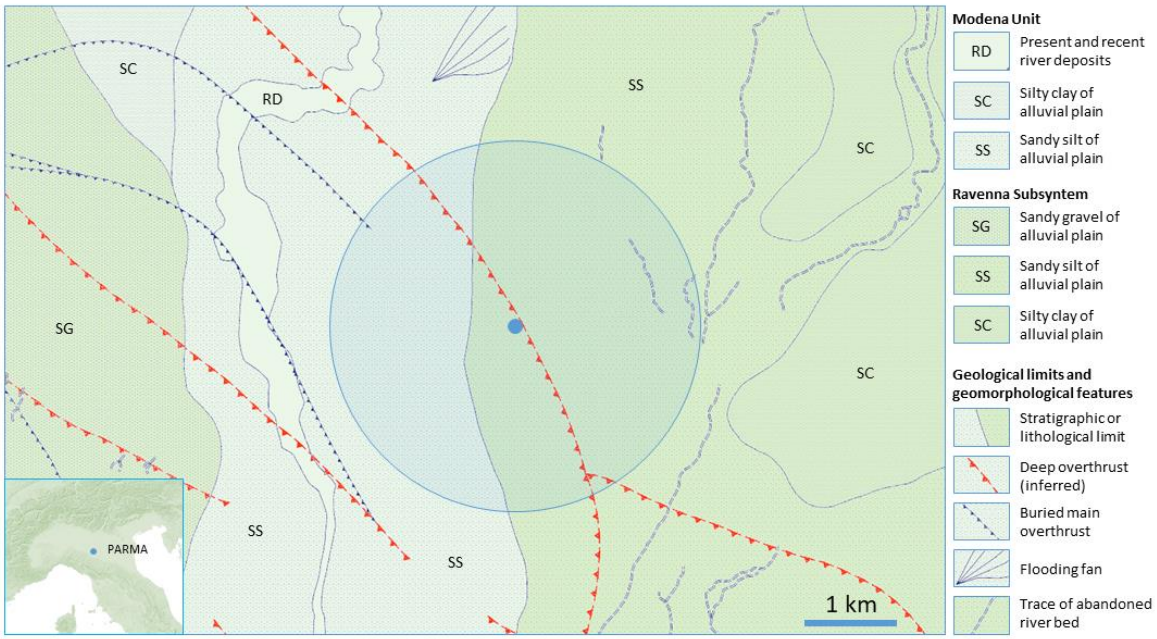

Figure 2.2 Geological map of the area around the hive (small circle). The shaded area represents the average area explored by the worker bees during their foraging activities during warm weather. Based on a map of the Emilia-Romagna Region available at: http://geoportale.regione.emilia-romagna.it/it/mappe/informazioni-geoscientifiche/geologia/carta-geologica-1-50.000.

2.3.3 Sample collection and preparation

The beehive was installed in the study area in February 2017 and worker bees were collected from June to October during warm weather when they are more active and forage across an average area with a radius of about 3 km. Approximately five worker bees were collected on a monthly basis in June, July, August, and October, yielding a total of 20 bees. In September, bees were not sampled owing to the treatments applied by the beekeeper against the ectoparasitic mite *Varroa destructor*.

Negative control bees consisted of newly eclosed individuals from a brood frame kept in a growth chamber. Briefly, a brood frame was selected and placed in an incubator at 36 °C and 60% relative humidity for approximately 16 h. Newly eclosed adults were randomly selected and prepared for SEM/EDX analyses. Once collected, worker bees were immediately placed in soda-glass capped vials, stored on ice to keep them inactive, and rapidly brought to the lab for sample preparation. Preliminary studies have shown that PM on the bees is mostly concentrated along the costal margin of the forewings, medial plane of the head, and inner surface of the hind legs (Negri et al., 2015). In this study, we examined the forewings, which are relatively easy to explore with the SEM probe owing to their flatness and lack of long setae (Pellecchia & Negri, 2018). The bees' wings were cut under a stereoscope with a scalpel and mounted onto SEM stubs using double adhesive carbon tape. Before the SEM/EDX investigation, because of the insulating properties of the samples, the stubs were carbon coated to make them conductive to avoid charging flare during the observations. Moreover, haemolymph (blood) was extracted from the control bees by puncturing the dorsal aorta, following the method standardised by Garrido et al. (2013), to distinguish the potential contribution of the haemolymph (that permeates the wings) to the EDX spectra; haemolymph droplets were set and dehydrated upon stubs under a sterile hood, graphitised, and analysed using SEM/EDX.

2.3.4 SEM-EDX analyses

The SEM/EDX investigation was performed using a Zeiss Gemini 500 field-emission instrument equipped with a Bruker XFlash 6|30 EDX micro-analyser. A panoramic electron backscattered (BSE) image was acquired for each analysed area along with magnified images of some particles representative of the different phases encountered. Each analysed particle was attributed to a phase (or phase aggregate) based on the elements present in the corresponding spectrum as well as the relative amounts and morphologies of the particles

themselves. For instance, different minerals were characterised and distinguished based on elemental compositions; clay minerals generally have a pronounced lamellar habit in addition to a given elemental content; halides have a cubic habit as well as some sulphides that, in turn, feature distinct elemental signals. While this methodology is rapid, cost-effective, and able to reveal nano-sized particles, it has the following limitations: (1) the EDX system is not very sensitive to light elements such as hydrogen and carbon. Therefore, hydrocarbon molecules cannot be efficiently identified and characterised; (2) BSE imaging is sensitive to the average atomic number of the particles. Therefore, heavy particles can most easily be recognised on light organic substrates, including bee wings, while conversely, light particles show poor contrast and tend to be underestimated; (3) even when nanometre-scale image resolutions are obtained under optimal experimental conditions, the spatial resolution of the EDX probe is only few microns. Therefore, for particles smaller than the EDX probe — namely PM with an aerodynamic diameter less than 2-3 μm — the surroundings will always contribute to the resultant spectrum. As such, we could obtain the average composition of the mixture small-particle aggregates; and (4) different mineral species may have the same elements in different proportions, and the only way to distinguish them is to determine the atomic proportions. For example, forsterite (Mg_2SiO_4) can be distinguished from enstatite ($MgSiO_3$) based on their respective Mg/Si ratios of 2:1 and 1:1. Such determinations are straightforward for ideal samples (i.e., with a flat and polished surface and of sufficient size to entirely contain entirely the electron beam interaction volume i.e., < 10 μm^3); however, for non-ideal samples, raw data cannot be properly reduced, that is, intensity data cannot be properly transformed into concentrations. In our case, most particles had an irregular shape, rough surfaces, and were smaller than the EDX probe, meaning that interpretation was sometimes more difficult. The airborne particles on the honey bee wings were also analysed in terms of the number of particles per surface area and their size distribution using the image-processing software

'DigitalMicrograph' (Gatan Inc., Pleasanton, CA, USA). Briefly, 12 SEM-BSE images randomly chosen among the obtained pictures with a homogeneous background and magnifications ranging from 1.14 KX and 25.38 KX were considered. Particles that could be distinguished from the background (i.e., the honey bee wing) based on brightness and contrast were selected and counted, and their morphological parameters were measured. The PM mass was estimated assuming an average particle density of 2.65 g/cm^3 (corresponding to the density of quartz, which is the dominant mineral in soils; Rühlmann, Körschens & Graefe, 2006), and a measured mean circular particle diameter of 0.75 μm.

2.4 Results

2.4.1 Particulate matter analysis

In the negative controls, the electronic scan did not detect any PM contamination (Suppl. Figure 2.11); the experimental bees displayed contamination with inorganic dust typically < 10 μm in diameter. The number of particles/mm^2 identified using the image-processing software varied from 2,724 to 511,121 (mean = 10,819), and images with a higher magnification displayed more particles (Suppl. Figure 2.12). The grain-size distribution of the identified particles is shown in Figure 2.3, which shows an exponential decrease in the number of particles with grain size. The estimated mass of PM per mm^2 was approximately 1.90 ng.

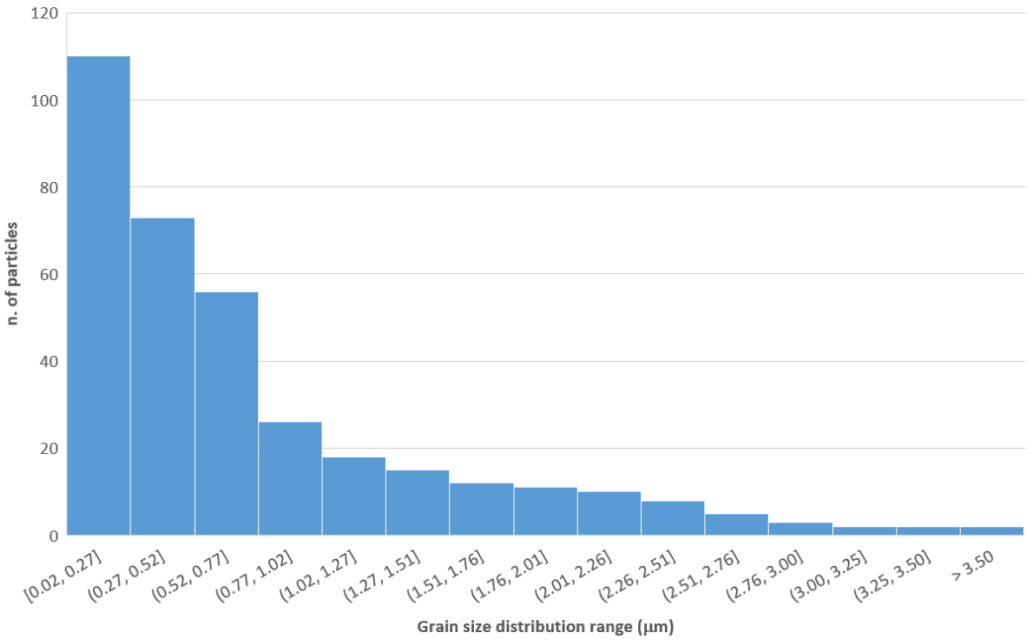

Figure 2.3 Grain-size distribution of PM detected on the honey bee wings obtained via SEM-BSE image processing.

Most of the PM_{10} and $PM_{2.5}$ were identified as quartz, phyllosilicates, calcite, and feldspars. Figure 2.4 presents the crystal morphology and EDX spectra of calcite and clay minerals, whereas some reference spectra for all these mineral phases are provided in supplementary Figure 2.13 and Figure 2.14. Spherical dust PM with a SiO_2 composition was also detected (Figure 2.5 a), the morphology of which suggested anthropogenic origin. Other particles frequently found on bees included Fe-bearing compounds, such as Fe oxides, metallic Fe, and Fe alloys (Figure 2.14). Barium sulphate was present in all samples, generally as a sub-micrometre fraction (Figure 2.5 b). Other metallic particles including Cu, Al, and titanium oxide, were occasionally detected (Suppl. Figure 2.14). Phosphorous was ubiquitous in the studied samples, generally being detected in association with N, Cl, S, and several other elements (see below) and, in one case, having a spectrum consistent with apatite [$Ca_5(PO_4)_3(OH,F,Cl)$].

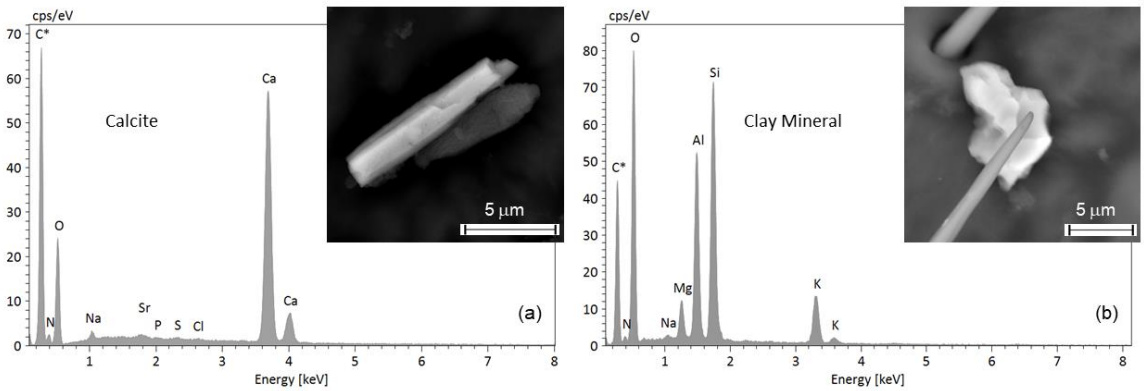

Figure 2.4 Sample 14/10: (a) EDX spectrum of an acicular calcite PM_{10} particle ($CaCO_3$; inset). Small amounts of Na and Sr may be present in calcite. Miner N, P, S, and Cl peaks are attributable to the bee wing; (b) EDX spectrum of a clay mineral particle (inset) consistent with illite $(K(Al,Mg,Fe)_2(Si,Al)_4O_{10}(OH)_2)$.

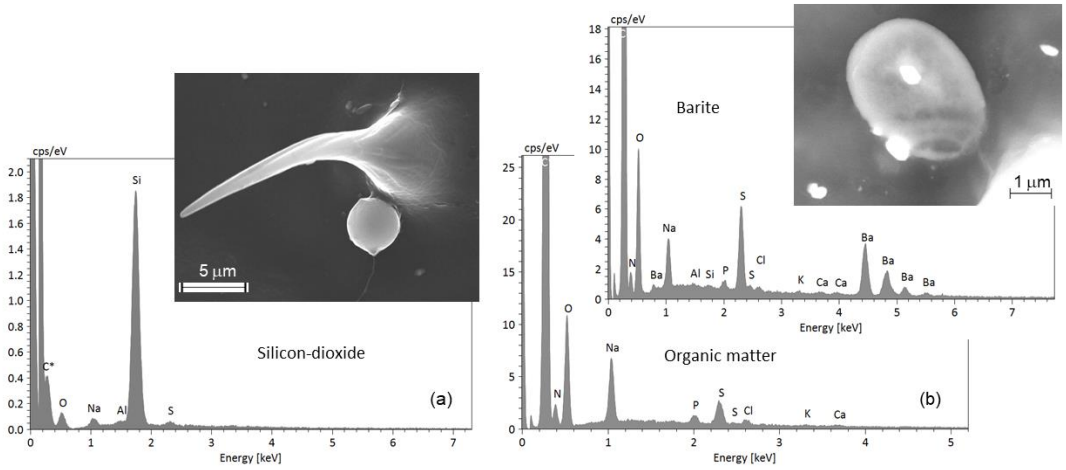

Figure 2.5 Sample 22/06: (a) Spherical SiO_2 particle of possible anthropogenic origin and its EDX spectrum; (b) Sub-microscopic particles of barite (white) distributed on a honey bee wing and a globular particle of possible organic matter with a complex accessory element association in which Na is dominant.

The EDX analysis of sub-micrometre particles was systematically affected by the signal from the bee wings, as outlined in the experimental section. Thus, to account for the contributions of wings to the overall EDX spectra, point analyses were performed directly on the wing membranes. The resulting spectra showed significant N, Si, P, S, Cl, K, ±Al, ±Na, ±Mg, and ±Fe peaks (Figure 2.6 a). These peaks were systematically present for almost all of the analysed particles in proportions that roughly depended on particle

dimension, i.e., the smaller were the particles, the higher were the wing-related peaks (Figure 2.6 b-d). Most of the elements contributing to the spectra of small particles also reflected the EDX spectrum of the insect haemolymph samples (Figure 2.7).

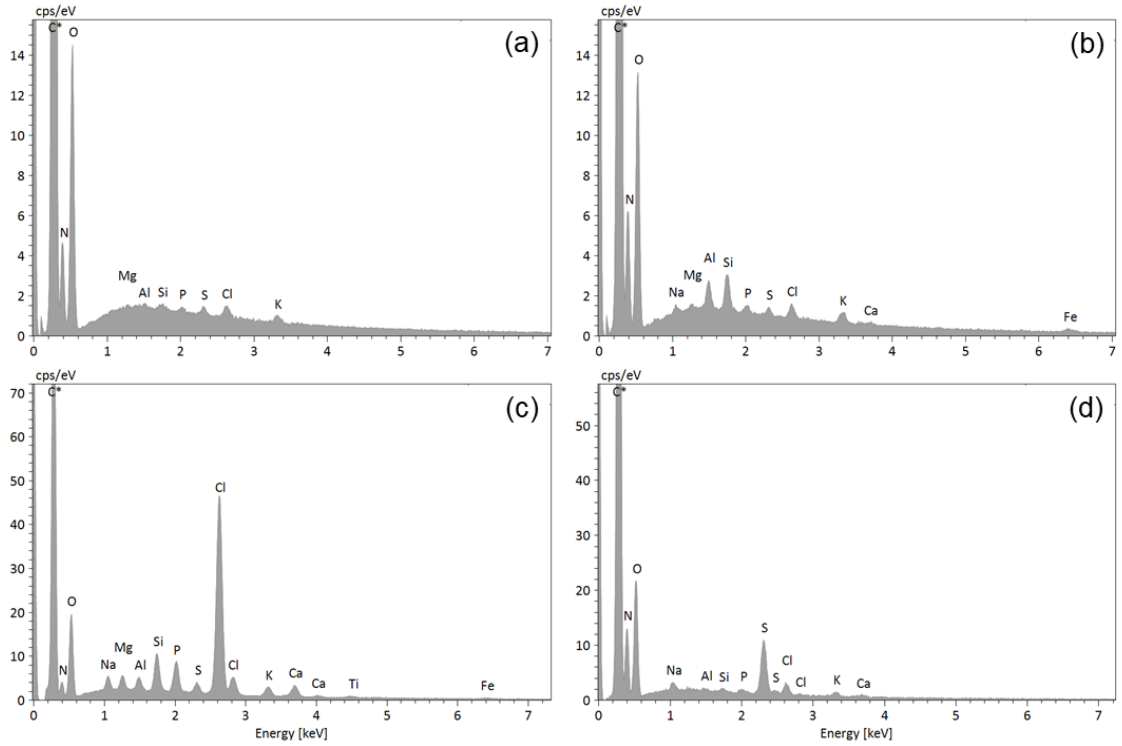

Figure 2.6 EDX spectra of sample 22/06: (a) Representative spectrum of the honey bee wing taken away from visible particles. Note the presence of small Mg, Al, Si, P, S, Cl, and K peaks in addition to the larger C, N, and O peaks; (b) Spectrum of a very small clay mineral particle. Note the increased Mg, Al, Si, and K peaks and the appearance of Na, Ca, and Fe peaks, all of which are elements typical of clay minerals; (c) Spectrum dominated by Cl (after C) possibly relating to a chloride condensed on a clay mineral particle (note the presence of related elements) along with P and S compounds; (d) Spectrum dominated by S and N peaks (after C and O peaks associated with the honey bee wing membrane) possibly indicating NOx- and SOx-derived compounds.

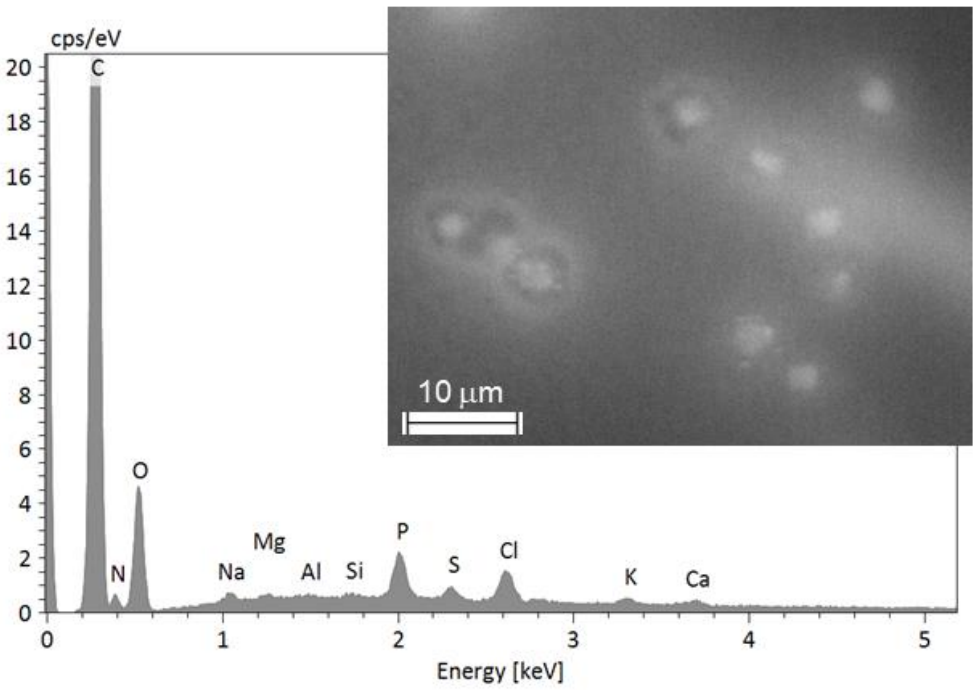

Figure 2.7 Representative EDX spectrum of the haemolymph of the control bees displaying significant levels of N, Na, P, S, Cl, K, and Ca, and trace amounts of Mg, Al, and Si (in addition to abundant C and O). Most of these elements were recurrent in the analyses of all fine particles, although in different proportions. Bright spots are likely insect hemocytes (i.e., insect "blood" cells). The spectrum refers to the ensemble.

2.4.2 Multiphase particles

In many cases, spectral interpretation was complicated by the multiphase nature of the particles, with constituent single phases being smaller than the total analysed volume. In such cases, phase identification can be ambiguous since different proportions or various phases may lead to the same average composition. Thus, compositional analysis can be employed to ensure more accurate spectral interpretation, as shown in Figure 2.8. Herein, the BSE images and elemental distributions show that the PM_{10} particles comprise at least three different major phases and contribute to the whole spectrum. The upper left particle primarily contains Si, Al, K, and Fe, likely being a clay mineral such as illite, with sub-microscopic inclusions of Fe oxides; the lower right particles primarily contain Na, S, Cl, and Ca, although Na and Ca are present in much greater abundance suggesting these elements may be combined with C to form secondary oxalates. In other cases, the different

phases were easily distinguished by the BSE imaging, as in Figure 2.9 where clay minerals associated with organic matter are shown. The two different materials yielded different EDX spectra. For example, the P, S, and Na peaks were much higher in the organic matter spectrum than in the clay mineral one, suggesting that P, S, and Na were more highly concentrated in the former, and the small peaks in the clay mineral spectrum were spurious. Analogously, the small Si and Al peaks in the organic matter spectrum are considered to be spurious peaks originating from the clay minerals.

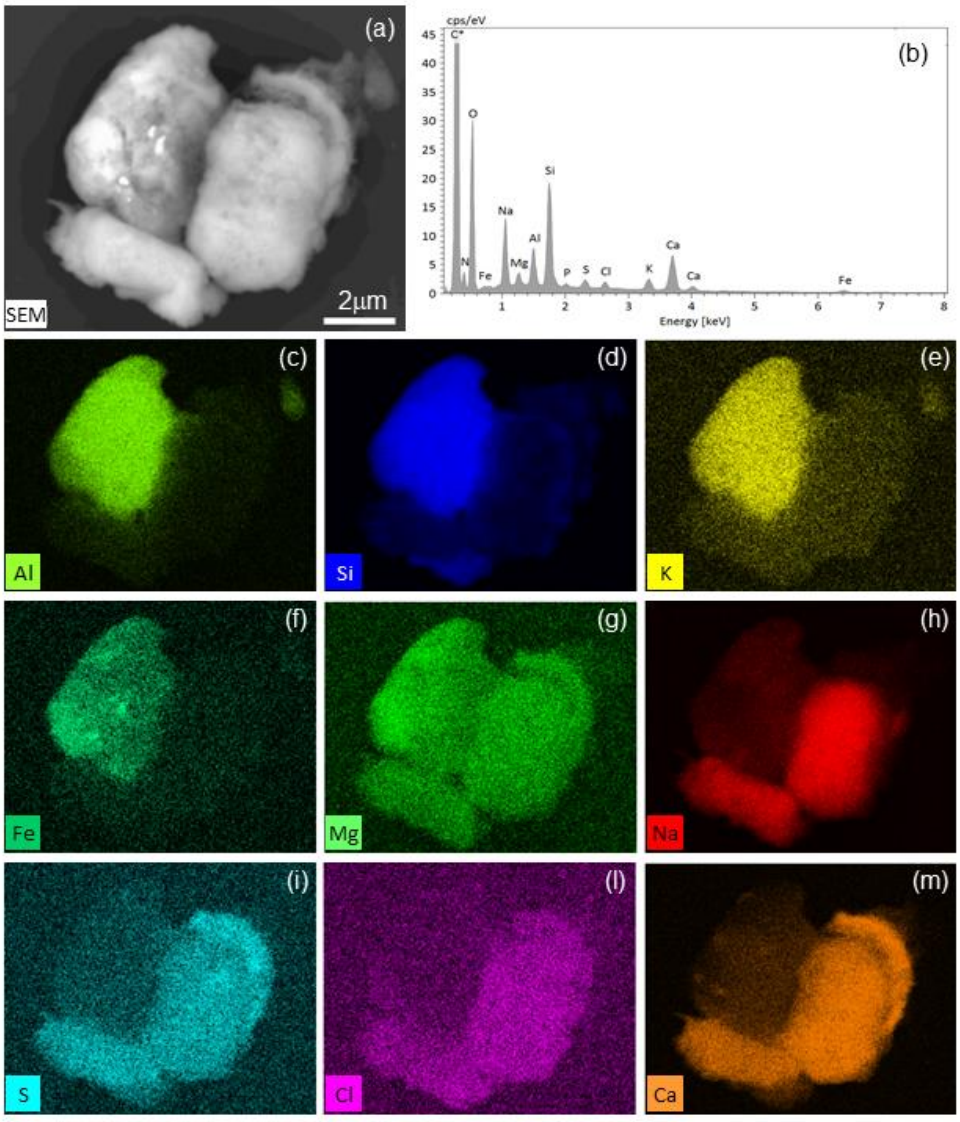

Figure 2.8 Elemental mapping of compound PM_{10} particles (sample 14/10): (a) SEM-BSE image showing at least three different particles and some brighter inclusions within the particle in the upper left; (b) averaged EDX spectrum; (c)-(m) single element maps. Note that Al, Si, K, and Fe (c-f, respectively) are concentrated

in the upper left of the particle, whereas Na, S, Cl, and Ca (h-m, respectively), are concentrated in the particles in the lower right; Mg (g) is present along with P (map not shown). Fe (f) is concentrated in the inclusion within the upper left particle (arrows). Finally, Na (h) is not present in the curved particle in the upper right, whereas S (i) and Ca (m) are abundant (arrows).

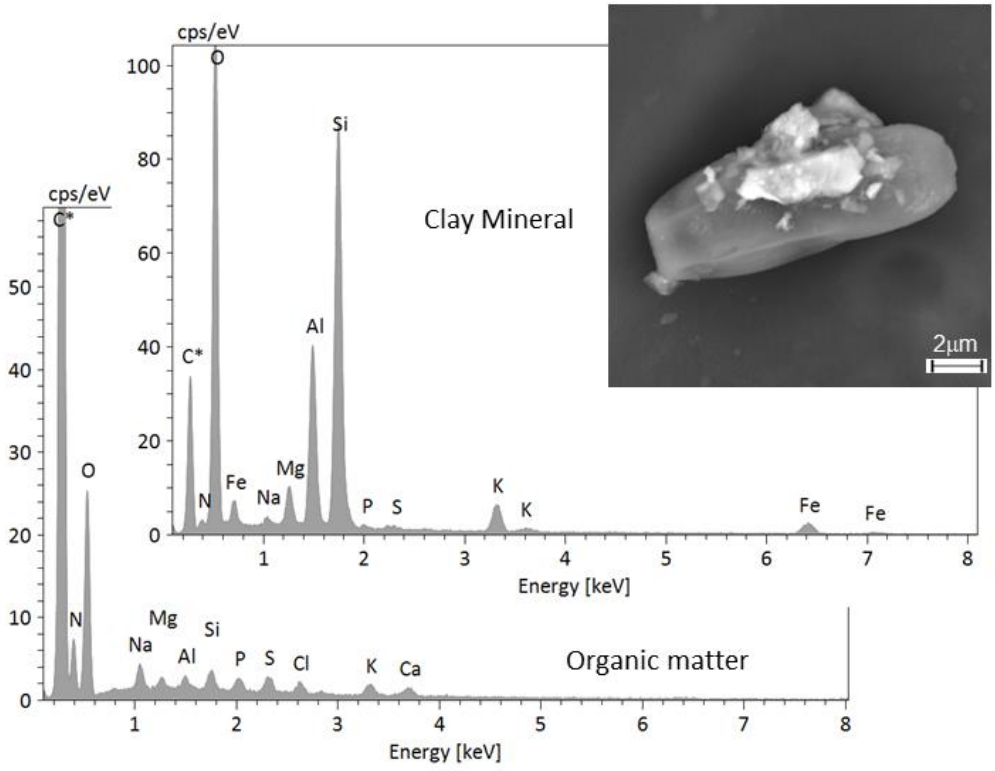

Figure 2.9 EDX spectra of a complex particle composed of clay minerals (upper spectrum, from the small bright particles in the inset) attached to an organic particle (lower spectrum, from the large dark particle in the inset).

2.4.3 Mineral phases distribution over time

Quartz was as abundant as calcite and clay minerals, and more abundant than feldspar (Fig. 10). Clay minerals and calcite were more abundant on the bees collected in June and October, accounting for approximately 75% of the acquired spectra. In June, the ratio between clay minerals and calcite was 1.3:1; conversely, in October, calcite was more than twice as abundant as clay. In July and August, the percentage of clay minerals and calcite was lower than in June and October, decreasing to approximately 56% and 36%, respectively (Figure 2.10). Fe-bearing PM appeared rarely on bees collected in June (2%),

more commonly on those collected in July (13%), and peaked on those collected in August (50%). In October, Fe compounds comprised approximately 12% of the total obtained spectra (Figure 2.10). A relatively small number of particles containing barium sulphate was present on the bees collected across all months.

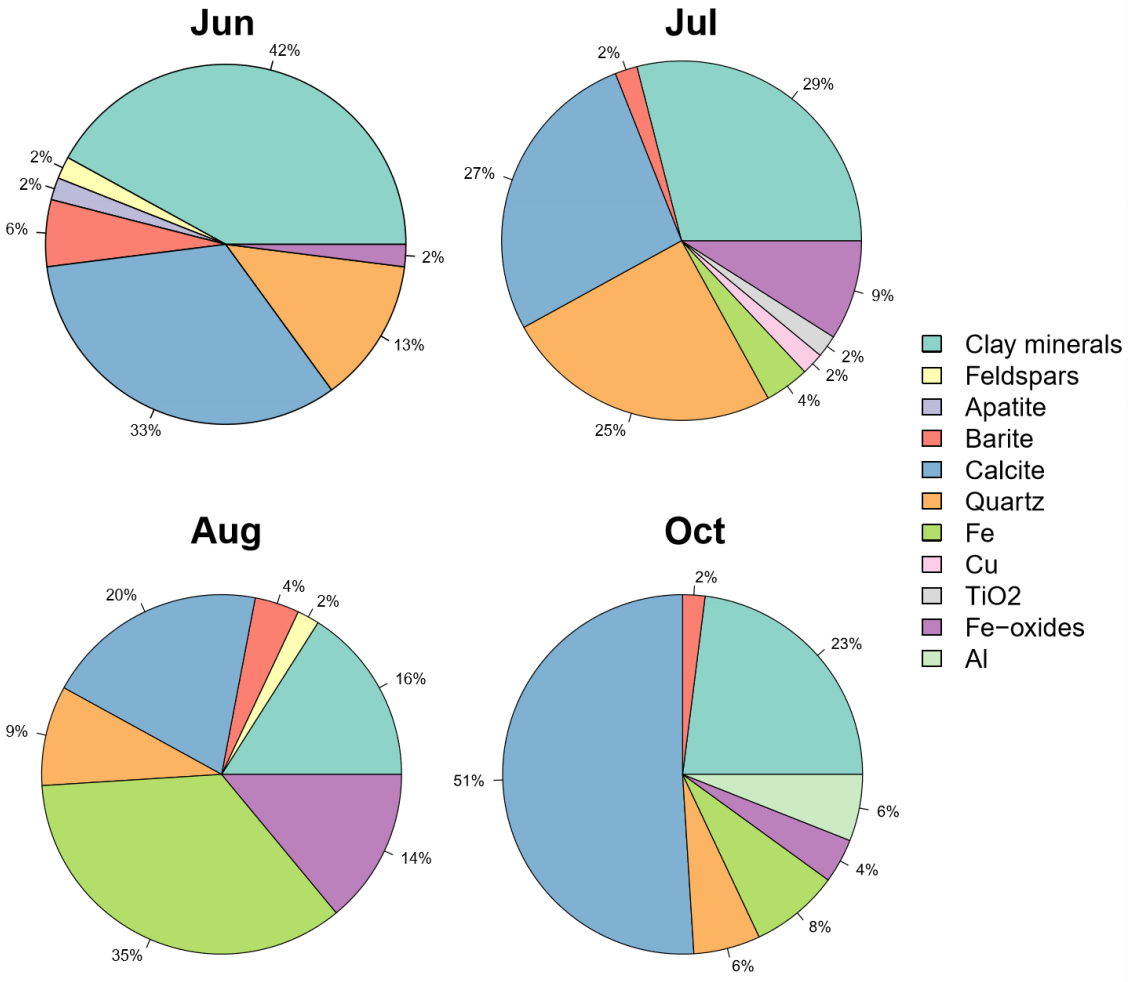

Figure 2.10 Pie charts representing the mineral abundances in the coarse PM fraction observed on honey bee wings. For consistency, only samples with a statistically significant number of analysed particles are reported: (a) sample 22/06 (52 spectra attributed); (b) sample 20/07 (48 spectra); (c) sample 10/08 (55 spectra); and (d) sample 14/10 (49 spectra).

2.5 Discussion

All the investigated honey bee samples from the monitoring station were remarkably "dirty", i.e., the bees had accumulated large amounts of airborne PM, while the control

bees did not display any PM contamination. For the contaminated bees, the density of particles ranged from a few thousand to several hundreds of thousands per mm^2; however, this difference was primarily attributable to differing image magnifications rather than actual differences in PM concentrations. In general, low-magnification images tended to underestimate fine and ultrafine particles, while high-magnification images obscured coarser particles. Ultrafine particles ($PM_{0.1}$) did not contribute much to the overall PM mass, although they contributed considerably to the total number of particles (Donaldson et al., 2001; Kurth et al., 2014).

Most of PM accumulated on bees could be interpreted as naturally derived minerals, such as quartz, phyllosilicates, calcite, and feldspars from the surrounding alluvial deposits and agricultural soils. Calcite and clay minerals were found in all samples and, along with quartz, are by far the most abundant mineral phases in the silty clays and sandy silts that comprise the alluvial deposits of the Taro River and the Parma Stream. These waterways originate in the numerous Flysch formations of the Apennines that feed the alluvial deposits of the Po Valley on the southern side of the Po River. Agricultural activities, especially those involving the harvesting and sowing of wheat and alfalfa near the hive, may have contributed to the spread of minerals from the soils. However, the abundance of clay minerals and calcite was highly variable over time. This suggests the influence of further human activities, such as municipal waste incineration. Calcite is indeed one of the most common phases found on incinerator bottom ash, but further work is needed to assess the specific contributions of waste-treatment process including the removal and disposal of ash. The incinerator plant could also be responsible for the presence of airborne quartz PM, as SiO_2 is often abundant in bottom ash (Alam et al., 2019; Tang et al., 2020). In the studied samples, quartz was typically more abundant than feldspar, although both are prevalent in sedimentary lithic rocks, particularly in silts and sands. A possible explanation

is that feldspars are much more sensitive to weathering than quartz, and therefore, degrade to clay minerals more rapidly (Klein & Philpotts, 2016).

Other mineral phases frequently found were Fe compounds including Fe oxides, metallic Fe, and Fe alloys. Fe oxides (and Fe hydroxides) can be very abundant in nature, especially in association with mafic and ultramafic rocks, lateritic horizons, and the alteration of sulphide ores; however, these compounds are not abundant in the outcrops in the study area, which are largely Flysch rock. Metallic Fe is rare and may reach the Earth's surface via siderite meteorites in small quantities. Similarly, natural Fe alloys, in particular Fe-Ni alloys, may have an extra-terrestrial origin, and therefore, are very rare. In contrast, metallic Fe and Fe alloys derived from anthropogenic activities can be very abundant in the environment, being present in various manufactured goods (Gonet & Maher, 2019). For example, materials containing Fe are commonly used in the automotive industry (Carrero, Arana & Madariaga, 2014; Gonet & Maher, 2019). Thus, the Fe compounds identified in the study area may originate from the wearing of the mechanical parts of vehicles travelling on the adjacent A1 motorway. Other occasionally detected metallic particles, such as Cu and Al particles, may have similar origins, as they are otherwise considered rare (Cu) or absent (Al) in nature but are widely used in electric circuitry (Cu) and in the lighter chassis and engine parts of vehicles (Al). In July and August, tourism-related road traffic is particularly high due to the summer holiday season, often resulting in frequent traffic jams. In 2017, between the end of July and the first two weeks of August, during the "summer exodus", light vehicle traffic on the motorway increased by more than 50%, and the average daily number of light and heavy vehicles taking the nearby exit was 11,280 and 3,460, respectively (Autostrade per l'Italia S.p.A., traffic report). Thus, during this peak traffic period, bees collected on August 10 would have been exposed to increased levels of metal-bearing PM (relative to bees collected on July 20).

Another mineral phase frequently found on the bee wings was barite, a Ba sulphate. Barite is not rare in nature but is concentrated in hydrothermal deposits; therefore, it must be rare in the study area. Barite is, however, commonly used as a filler in various manufactured objects including vehicle tires and brakes. In particular, barite is the major chemical phase of break-pad material and is used as a filler to improve thermal and noise properties as well as wear resistance (Österle et al., 2001; Neis et al., 2017; Menapace et al., 2018). In this study, barite was present in all samples, and always as part of the < 1 μm size fraction. This is in agreement with previous studies demonstrating that, when abraded from brakes and tyres, the grain size of barite is significantly reduced to the nanometre scale (Österle et al., 2001; Pellecchia & Negri, 2018; Papa et al., 2020 (Chapter 3)).

Round, non-crystalline SiO_2 dust found on the bee wings could be linked to high-temperature combustion, such as that occurring at the nearby incinerator plant. According to the European Waste Incineration Directive, incinerator combustion must be conducted at above 850 °C to ensure the proper breakdown of toxic organic substances such as dioxins (Directive 2000/76/EC). Under such conditions, silicate matter may melt, and rapid post-combustion cooling can result in the formation of spherical PM (Kutchko & Kim, 2006; Alam et al., 2019).

An anthropogenic origin is also suggested for Ti oxide. Titanium dioxide, occurring as rutile, is not rare in nature and may concentrate in the heavy fraction of sediments. Yet, synthetic TiO_2 is widely used as a filler and whitening agent in various manufactured objects, such as plastics and paints, and is abundant in vehicle components.

Phosphorous was a minor but common element in the studied samples, generally associated with other elements as N, Cl, S. In one case, the observed spectrum was consistent with apatite [$Ca_5(PO_4)_3(OH,F,Cl)$]. Apatite, one of the main constituents of bones (Hughes & Rakovan, 2002), is an accessory mineral in many types of rocks, and can occur at relatively

high concentrations in igneous and marine sedimentary rocks. Apatite is not, therefore, expected to be naturally abundant in the study area. Given the prevalence of phosphate-based fertilisers, the observed apatite may have had a secondary origin stemming from reactions between phosphates and Ca-compounds (Moore et al., 2004; Arai & Sparks, 2007; Shen et al., 2011). For example, such nutrients are needed in large quantities by Medicago sativa, a widespread crop in the study area, as low nutrient availability reduces the yield and persistence of this perennial plant (Berg et al., 2005).

We hypothesised that the background N, Si, P, S, Cl, K, ±Al, ±Na, ±Mg, and ±Fe peaks obtained for the measured smaller particles (i.e., < 1 μm in diameter) were signals from the honey bee wings components, including the cuticle and the haemolymph. The cuticle is primarily composed of chitin (a long-chain polymer with the composition $(C_8H_{13}O_5N)n$) microfibers fixed in a protein matrix, e.g., hydrophobic proteins, with alanine ($C_3H_7NO_2$) as the predominant amino acid (Micas et al., 2016; Falcon et al., 2019) and resilin, an elastomeric protein with proline ($C_5H_9NO_2$) and glycerine ($C_2H_5NO_2$) as principal amino acids (Ma et al., 2015). Insect haemolymph comprises water, inorganic salts (mostly Na, Cl, K, Mg, and Ca), and organic compounds (carbohydrates, proteins, and lipids). Trehalose ($C_{12}H_{22}O_{11}$) and glucose ($C_6H_{12}O_6$) are the major circulating carbohydrates, and fatty acids, diglycerides, triglycerides, and phospholipids are major lipids in the haemolymph (Mikulecky & Bounias, 1997). While C, H, and O are major constituents of all these lipids, P is a minor constituent of phospholipids. Key proteins in adult bee haemolymph are transferrin, an Fe(III) transporter; apolipophorin, a lipid transporter; and vitellogenin, a nutrient-storage protein (Chan, Howes & Foster, 2006). P and S are minor constituents of these organic compounds. Therefore, C, H, O, and to a lesser extent, N, are major elements in honey bee wings, which is consistent with the EDX spectral features observed for small particles (PM_1). All other background elements, with the possible

exception of Si and Al, are minor elements in the aforementioned wing components and consistently appeared in the spectra at very low concentrations.

In many cases, the spectra generated for very fine particles were dominated by Cl, S, or N peaks. At least in some cases, these elements could represent chlorides, SOx, and NOx as well as ammonia stemming from vehicle exhaust gas and incinerator emissions. These compounds may condense either directly onto honey bee wings or on fine airborne PM, such as clay minerals, that acts as condensation nuclei before accumulating on bees. This might explain the recurrent association of the background peaks with Na, Mg, Al, Si, and K. In other cases, background peaks were associated with Fe or Ba, suggesting that fine particles of iron or barite, respectively, may have acted as condensation nuclei. Detailed results and implications relating to fine and ultrafine particles are reported elsewhere (Papa et al., 2020 (Chapter 3)).

P, K, and N are also major constituents of fertilisers (Gowariker et al., 2008), and Cl, P, S, and N (and Br and F) may be present in pesticides used in beekeeping and/or applied to crops (Ravoet, Reybroeck & de Graaf, 2015). These substances may contaminate the bodies directly when bees visit inflorescences during foraging or, in a manner similar to vehicle exhaust gas and incinerator emissions, may be present in the atmosphere as aerosols and condense either directly onto bee wings or suspended fine mineral particles later collected by the bees. However, as our discussion demonstrates, the precise identification and provenance of fine particles continue to pose challenges.

2.6 Conclusion

Our results provide evidence of the presence of specific inhalable and respirable airborne PM (i.e., dust able to pass beyond the larynx and ciliated airways, respectively) in the study area. The honey bees analysed were highly contaminated with PM_{10} and $PM_{2.5}$ primarily

comprising quartz, calcite, clay minerals, Fe-bearing PM including iron oxides/hydroxides, metallic iron, Fe alloys, and barite.

Our data suggest that people living in the area are subjected to chronic (continuous/repeated) exposure to specific airborne PM emitted by vehicular traffic, local agricultural operations, and waste incineration, and exposure levels may vary rapidly based on recurrent local activities. For example, the increase in natural mineral compounds (e.g., clay minerals, calcite, and quartz) was closely linked to cultivation cycles, while metal-bearing PM abundance increased in conjunction with periods of elevated local road traffic.

In view of the recent COVID-19 outbreak occurring in Italy and centred in the Po Valley, it is important to verify the possible association between the outbreak of respiratory viruses and exposure to specific components of airborne PM. More particle identification and classification data are needed, therefore, alongside improved information on viral viability on specific airborne PM components.

2.7 Acknowledgements

We thank Dr. Alice Dondè and Dr. Antonia Desiante for their support in data collection.

2.8 Supplementary

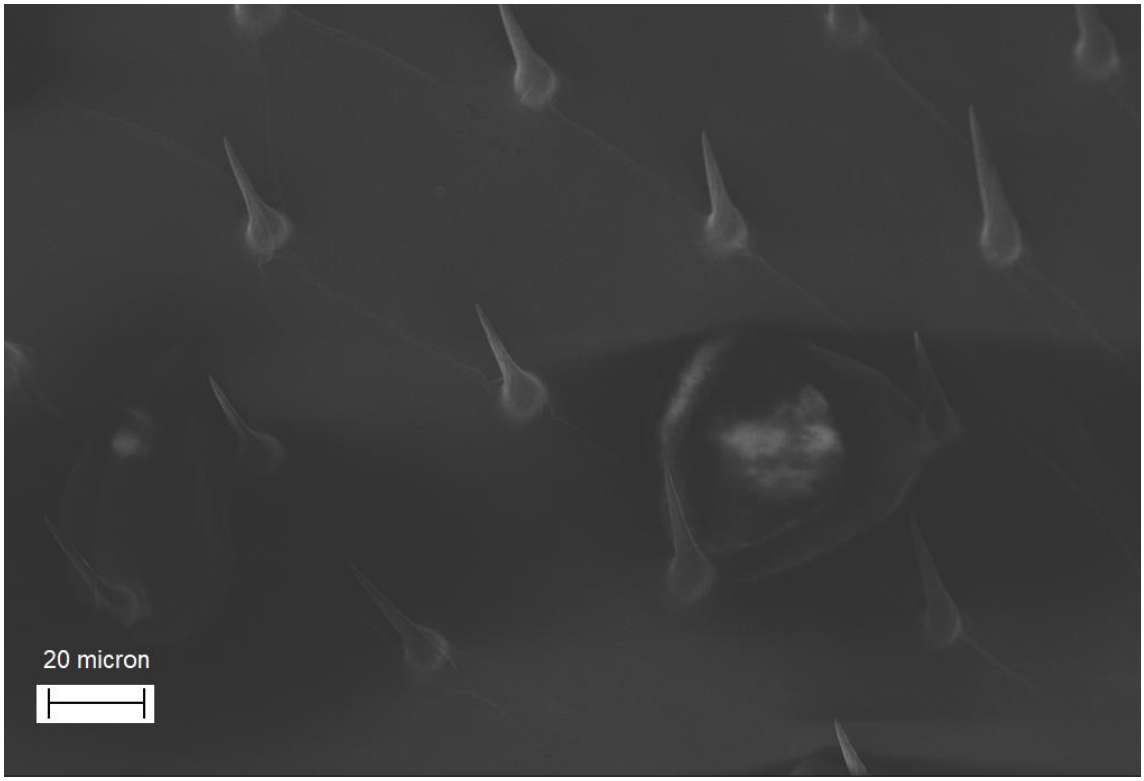

Figure 2.11 SEM micrograph of a wing from a newly eclosed adult (control bee); bar = 20 µm.

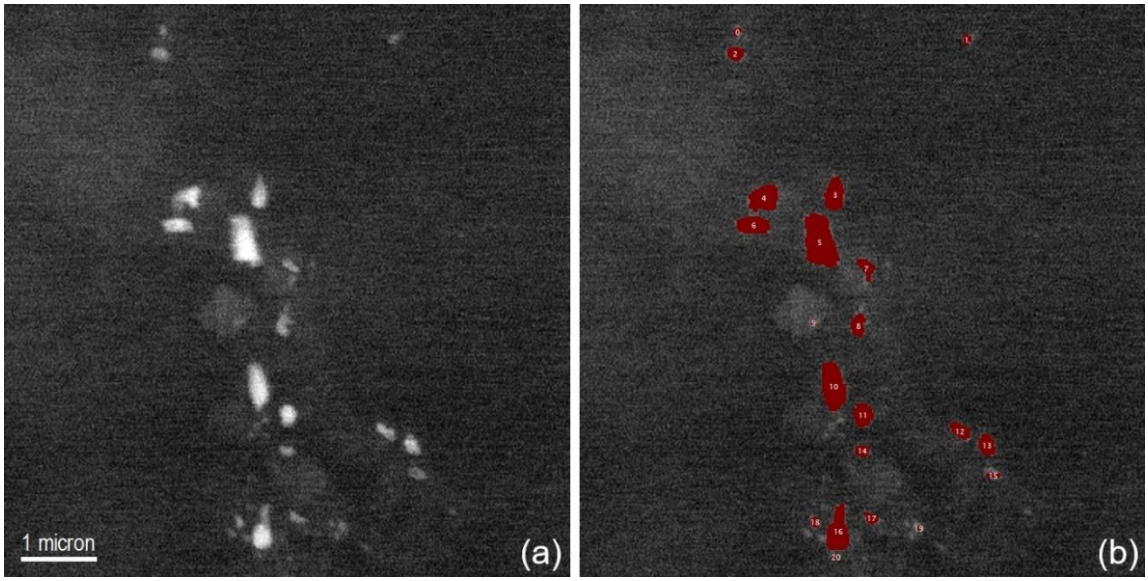

Figure 2.12 (a) SEM-BSE images (13.11 KX) of mineral particles (bright features) on a honey bee wing (dark background) along with low atomic mass materials. (b) particles that were selected and measured (red areas).

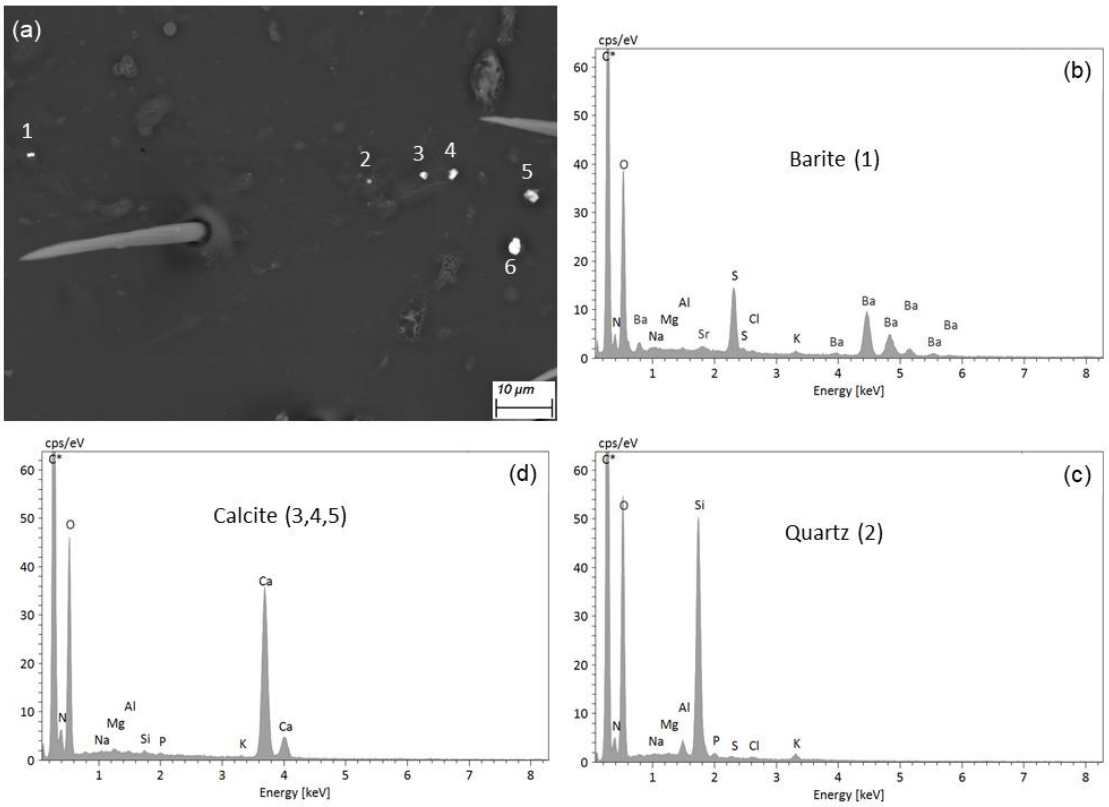

Figure 2.13 (a) SEM-BSE image of a honey bee wing (sample 10/08) showing several mineral particles (numbered brighter features) selected for EDX analysis: particle 1 is barite ($BaSO_4$), the spectrum of which is shown in (b); particle 2 is quartz (SiO_2), the spectrum of which is shown in (c); particles 3-5 are calcite ($CaCO_3$) (d); particle 6 is an iron oxide (spectrum shown elsewhere). Minor N, Na, Mg, Al, Si, S, Cl, and K peaks not accounted for in the chemical formulae stem from the supporting wing or contaminants (see text for explanation), with the following exceptions: Sr may be present in barite and Mg may be present in calcite.

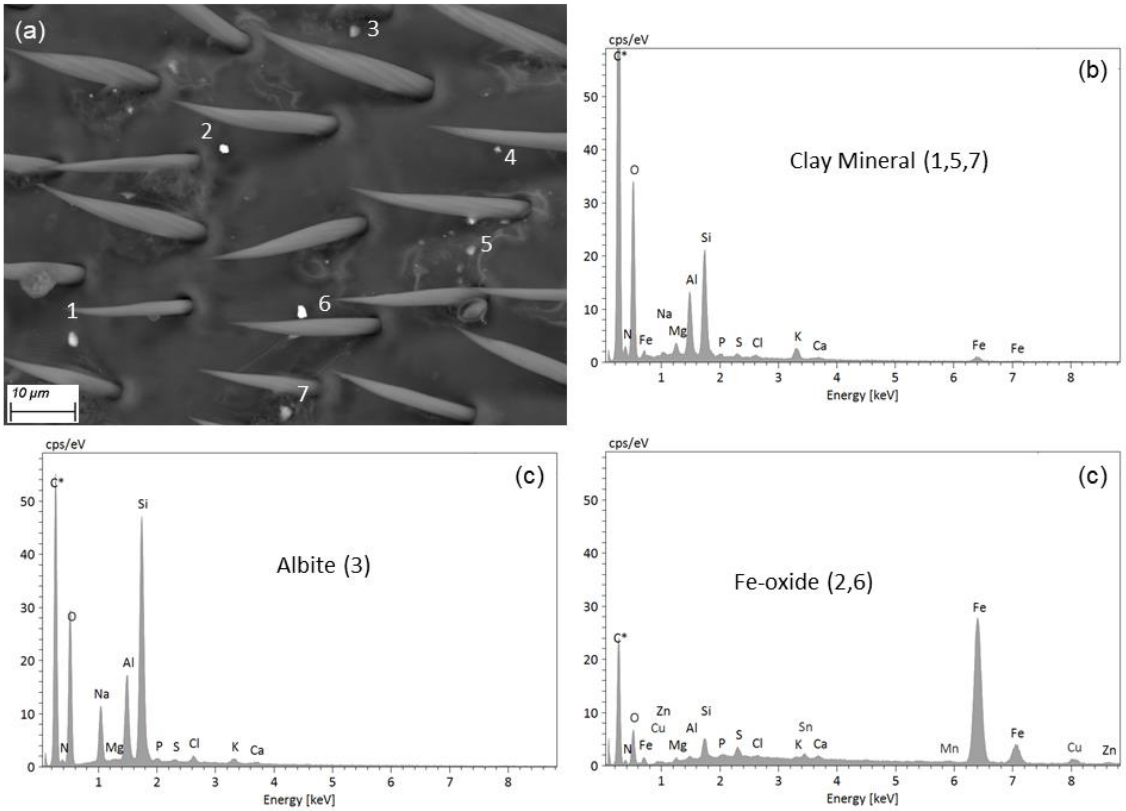

Figure 2.14 (a) SEM-BSE image of a honey bee wing (sample 10/08) showing several mineral particles (numbered brighter features) selected for EDX analysis. Particles n. 1, 5 and 7 are clay minerals (largely aluminum-silicates with K, Na, Ca, Mg, and Fe present in variable proportions); a representative spectrum is shown in (b). Particles 2 and 6 are Fe oxides; a representative spectrum is shown in (c). Particle 3 is albite (NaAlSi3O8) (d). Particle 4 is calcite (spectrum reported elsewhere). Minor N, P, S, and Cl peaks stem from the supporting wing; K and Ca may be present in albite; Mg, Mn, Cu; and Zn may be present in Fe oxides; and the Si in (c) may stem from a quartz particle attached to the Fe oxide. Judging from the small intensity of the O peak in (c), it is very probable that the particle could be indeed metallic iron with just a thin oxidized surface.

Chapter 3 Vehicle-derived ultrafine particulate contaminating bees and bee products

Published in *Science of the Total Environment*

Short Communication; https://doi.org/10.1016/j.scitotenv.2020.141700

Giulia Papa[a], Giancarlo Capitani[b], Ettore Capri[c], Marco Pellecchia[d], Ilaria Negri[a*]

[a] DIPROVES – Università Cattolica del Sacro Cuore, Piacenza, Italy

[b] DISAT – Università Milano Bicocca, Milano, Italy

[c] DISTAS – Università Cattolica del Sacro Cuore, Piacenza Italy

[d] KOINE' – Consulenze Ambientali, Montechiarugolo (Parma), Italy

*Corresponding author: ilaria.negri@unicatt.it

Article history:

Received 17 June 2020

Received in revised form 28 July 2020

Accepted 13 August 2020

Available online 14 August 2020

GRAPHICAL ABSTRACT

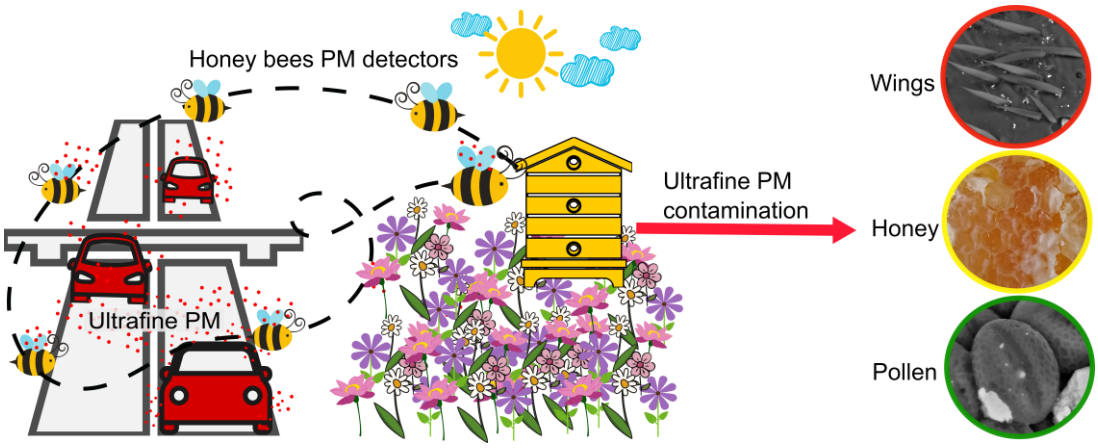

3.1 Abstract

Despite adverse health effects, ultrafine particulate matter (UFP), i.e., PM less than 0.1 μm in diameter, is an emerging pollutant not subject to regulation. UFP may cause both lung inflammation and cardiopulmonary disease and may enter the brain directly via the olfactory bulb, affecting the nervous system. In highly urbanized environments, diesel and gasoline vehicles are among the major sources of UFP including combustion-generated solid particle pollutant and metal-based particles. Metal-based UFP are of much concern, as they may promote inflammation and DNA damage via oxidative stress with generation of free radicals and reactive oxygen species (ROS).

We used the honey bee as an alternative sampling system of UFP in an area of the Po Valley (Northern Italy), which is subject to intense traffic. Worker bees are widely recognised as efficient samplers of air pollutants, including airborne PM. During flight and foraging activity, pubescence of the bees promotes the accumulation of electrical charge on the body's surface, enhancing attraction to air pollutants.

Bees living near the main Italian highway, the Autostrada A1, displayed a contamination of nanosized Fe-oxides/hydroxides and baryte. Sources of Fe-bearing and baryte ultrafine particles are primarily the vehicles speeding on the motorway.

Pollen collected by forager bees and honey produced by the bee colony displayed contamination by nanosized Fe-oxides/hydroxides and baryte. Such a contamination exposes pollinators and humans to UFP ingestion, endangering the safety of food produced at traffic-influenced sites.

Given the global spread of traffic, our findings suggest that exposure and environmental impact of ultrafine Fe-oxides/hydroxides and baryte are potentially ubiquitous, although usually overlooked in environmental policy discussions.

3.2 Introduction

Vehicular traffic is responsible for the emission of a significant amount of airborne particulate matter (PM), a complex mixture of airborne chemical components, commonly classified by a particle size up to 10 μm (PM_{10}). PM toxicity depends on morphology, chemical composition, and dimension of the dust, with ultrafine PM (UFP; PM less than 0.1 μm in diameter) able to penetrate deeply into the lungs and enter blood circulation. UFP may cause both lung inflammation and cardiopulmonary disease and may enter the brain directly via the olfactory bulb, affecting the nervous system (Brook et al., 2010; Maher et al., 2016; Bencsik, Lestaevel & Guseva Canu, 2018). Metal-based particles are of much concern, as they may promote inflammation and DNA damage via oxidative stress caused by generation of free radicals and reactive oxygen species (ROS) (Dashtipour et al., 2015; Soltani et al., 2018; Jan et al., 2019). Neurological disorders such as Alzheimer's and Parkinson's disease are associated to metal-based UFP exposure (Maher et al., 2016). Despite the known adverse health effects to humans at a low-level dose exposure (Lanphear, 2017), UFP is not subject to regulations, while limits for the protection of human health are available for PM_{10} and $PM_{2.5}$ (Directive 2008/50/EC of the European Parliament and of the Council of 21st May 2008 on ambient air quality and cleaner air for Europe). Such limits are expressed as mass per unit volume of atmospheric air with no specific indication on the chemical nature of the particles.

In highly urbanized environments, vehicular traffic is a steady source of ultrafine metal-based particles (Liati et al., 2018). Relatively few studies investigate the chemical and physical-structural characteristics of such PM while the great majority of them deals with particle counting (Liati et al., 2018). The honey bee is a well-known indicator of environmental pollution (Perugini et al., 2011; van der Steen, de Kraker & Grotenhuis, 2012; Zarić et al., 2018a,b). Recently, it has been demonstrated that each single forager bee

acts as an efficient mobile sampler of airborne PM (Negri et al., 2015; Pellecchia & Negri, 2018). During the flight and foraging activity, the pubescence of the bees promotes accumulation of electrical charges on the surface of the body due to friction with the air (Vaknin et al., 2000). The charges enhance attraction of airborne particles, including pollen for pollination and pollutants (Vaknin et al., 2000; Bonmatin et al., 2015). Airborne PM attached to the bee's body is typically up to 10 μm in diameter and can be analysed by size, morphology, and chemical composition using a scanning electron microscope (SEM) coupled with energy dispersive X-ray fluorescence (EDX) (Negri et al., 2015; Pellecchia & Negri, 2018). SEM/EDX is a powerful, fast, and non-destructive technique, and the information given by the morphology and composition of particles leads to particle identification and classification (Negri et al., 2015; Pellecchia & Negri, 2018).

In the present paper, honeybees were used as an alternative sampling system of UFP in the peri-urban area of the City of Parma (Po Valley, Northern Italy). The Po Valley is one of the most important industrial and agricultural areas in Italy and Europe, characterized by a high population density and a low level of air quality (Marcazzan et al., 2001). According to source apportionment studies, PM_{10} and $PM_{2.5}$ in the Po Valley in the warm season mainly originate from traffic and agriculture (Marcazzan et al., 2001; Pietrogrande et al., 2016; Pozzer et al., 2019). In the City of Parma, the fixed monitoring network of airborne pollutants consists of a few stations of the Regional Environmental Protection Agency (ARPAE) (http://www.arpae.it/), located in different domains (e.g., urban trafficked sites, rural and industrial areas). Higher concentrations of $PM_{2.5}$ are usually displayed in colder months than in warmer months; however, annual mean values are always below the limit set by the Directive 2008/50/EC (i.e., an annual mean value of 20 $\mu g/m^3$ based on a 3-year average). Mean values of approximately 40 $\mu g/m^3$ were displayed in the winter months of 2017 with a peak concentration in February, and approximately 15 $\mu g/m^3$ in the warmer

months (http://www.arpae.it/). However, no data are available on the nature and chemical composition of the particles. In this work, SEM/EDX analysis of UFP collected by forager bees provided information on the nature, morphology, and mineralogical composition of the ultrafine fraction of PM present in the area. Analysis performed on honey and bee pollen demonstrated the potential for UFP to enter the food chain and to expose pollinators to UFP ingestion.

3.3 Material and methods

3.3.1 Area of investigation

In February 2017, a beehive for PM monitoring was placed in a lawn in the peri-urban area of the City of Parma. Parma is located in the middle of the Po Valley (Northern Italy), an alluvial sedimentary plain of Pliocene and quaternary age, which lies between the Northern Apennine and the Southern Alps. Alluvial deposits of the area include silty clays and sandy silts from the Taro River and the Parma stream, which originate from numerous Flysch formations of the Apennine that feed the alluvial deposits of the Po Valley in this southern side of the Po River (http://geoportale.regione.emilia-romagna.it).

The hive was surrounded by about 35 hectares of uncultivated and cultivated lands of Medicago sativa, placed at approximately 150 m south of the main Italian highway, the Autostrada A1, and approximately 800 m away from the highway exit of the City. The monitoring period lasted 4 months, from May to August 2017, during which foragers had access to nectar/pollen resources from wild plants (e.g., *Taraxacum officinale*, *Prunus spinosa*, *Brassicaceae*) and crops (e.g., *Zea mays*, *Medicago sativa*), nearby the highway. During the monitoring period, the highway was subject to the passage of approximately 11 million vehicles (approximately 75% light vehicles and 25% heavy vehicles) and the daily average number of light and heavy vehicles taking the nearby exit was 11,280 and 3,460, respectively (Autostrade per l'Italia, personal communication).

3.3.2 Bee, honey, and pollen samples

Ten forager bees, with and without pollen grains, were collected monthly from May to August with a sweeping net while entering and exiting the hive, for four sampling sessions. Forewings and hindlegs with pollen grains from each forager bee were cut and mounted onto SEM stubs using double adhesive carbon tape for SEM/EDX, as previously described by Negri et al. (2015) and Pellecchia and Negri (2018).

Negative control bees consisted of newly eclosed individuals from a brood frame kept in a growth chamber. Briefly, a brood frame was selected and placed in an incubator at 36°C and 60% relative humidity for approximately 16 h. Newly eclosed adults were randomly selected and prepared for SEM/EDX analyses.

A honey frame full of fresh honey was collected in August from the hive and the honey was prepared for a SEM/EDX analysis for the inorganic sediment contained in the sugar matrix, following a specifically modified protocol for melissopalynological analysis (Von Der Ohe et al., 2004). Briefly, 100 g of honey was dissolved in 100 mL of hot ultrapure Milli-Q water (40°C), then put into four clean 50-mL falcon tubes and centrifuged at 3000 rpm for 15 minutes. After the supernatant liquid was removed, 20 mL of hot Milli-Q water was added and centrifuged at 8500 rpm for 15 minutes. After a second supernatant removal, another 20 mL of hot Milli-Q water was added and the solution was mixed in two falcon tubes, and then centrifuged for 15 minutes at 8500 rpm. For complete removal of honey sugars, three further steps of centrifugation with 15 mL of hot Milli-Q water were conducted. Ten microliters of the obtained sediment were then put onto SEM stubs and left to dry under a laminar flow hood. Additionally, three blank stubs were prepared with ultra-pure Milli-Q water. Any laboratory metalware was avoided, and a laminar flow hood was used in order to minimize external contamination.

3.3.3 Sem/EDX analyses

Samples (bee forewings, pollen, and honey sediment) mounted on stubs were carbon-coated. SEM/EDX measurements were performed with a Zeiss Gemini 500 field emission instrument (nominal spatial resolution of 3.5 nm), equipped with a Bruker XFlash 6|30 EDX micro-analyser. A panoramic electron backscattered (BSE) image was taken for each analysed area, along with UFP zoomed images. Secondary electron (SE) and backscattered electron (BSE) images and EDX point analyses were acquired to obtain the chemical composition, morphology, surface characteristics, and size of the particles. EDX spectra were interpreted according to a mineralogical perspective, considering the mineral content of the surrounding geological formations, as previously described by Pellecchia and Negri (2018).

3.4 Results and discussion

While all negative controls did not display any PM contamination (Suppl. Figure 3.4), the wings of the bees from the monitoring station showed a contamination of inorganic dust typically less than 10 µm. While PM up to 5 µm were mostly of natural origin (i.e., soil-derived clay minerals), UFP was exclusively made of Fe-oxides/hydroxides (occasionally with traces of Cu and/or Ti) and baryte, a barium sulphate (Figure 3.1, Figure 3.2). Additionally, bee pollen collected from the hindlegs of insects (Figure 3.1, Figure 3.2) and honey produced by the bee colony showed a contamination of ultrafine Fe-oxides and baryte (Figure 3.3).

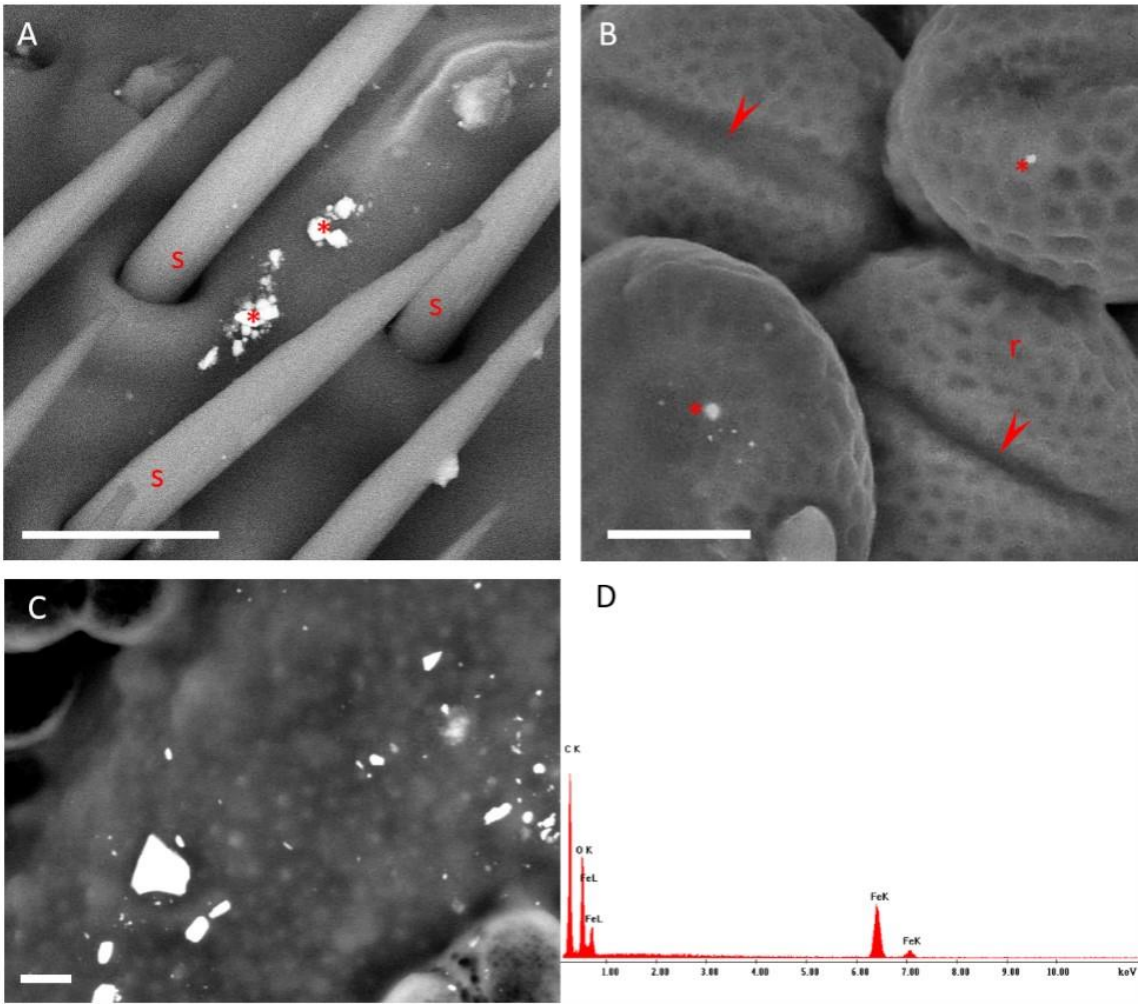

Figure 3.1 Backscattered electron micrographs (BSE) of bee forewing and bee pollen contaminated by fine and ultrafine Fe oxides/hydroxides (bright spots). (A) UFP on the wing and its setae (s). Asterisks, fine dusts (PM ≤1.3 µm). (B) UFP stuck to a pollen grain of a Brassicacea. Asterisks, larger particles (PM ≤1.2 µm). r, reticulate ornamentation of the pollens; arrowheads, pollen apertures. (C) Detail of a pollen grain contaminated by fine and ultrafine PM. (D) Edx spectrum of iron PM. A-B bars = 10 µm; C bar = 1 µm.

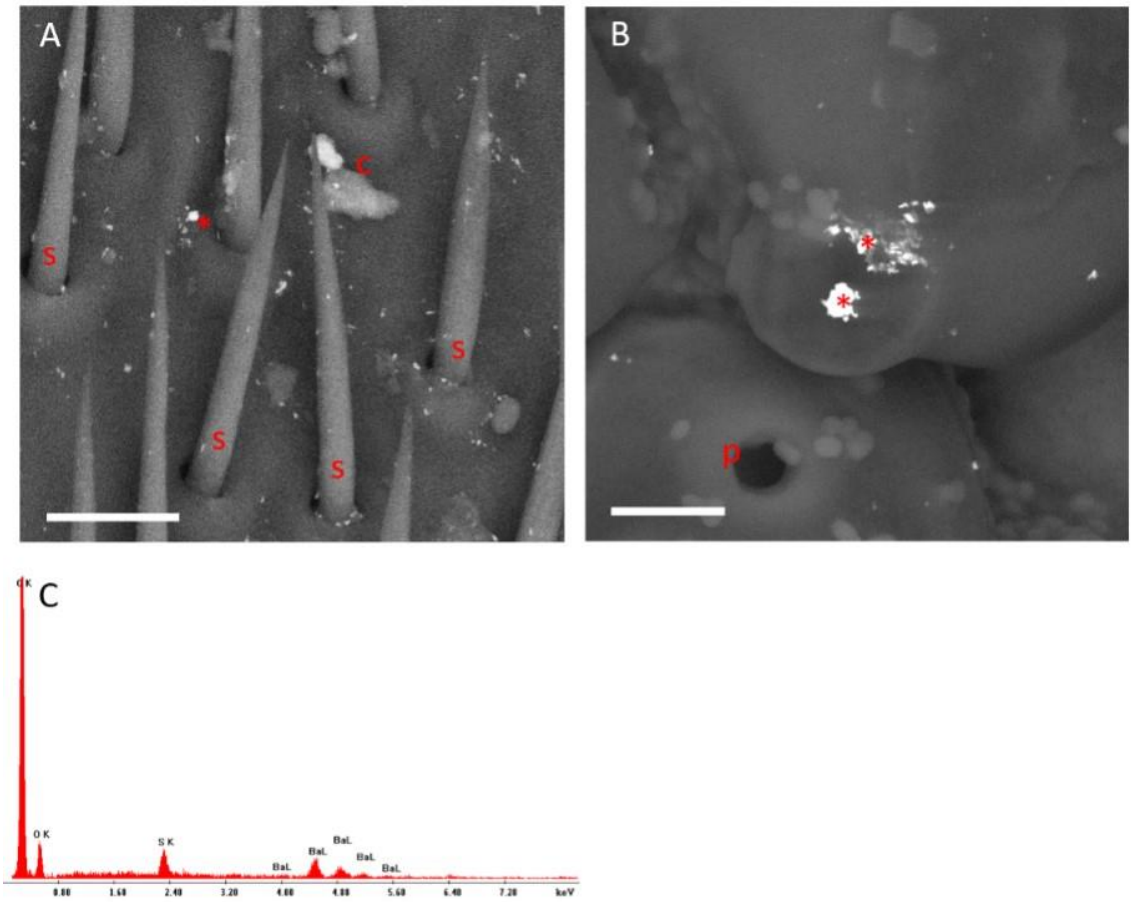

Figure 3.2. Backscattered electron micrographs of a honey bee forewing and bee pollen contaminated by UFP of baryte (bright spots). (A) UFP on the wing and its setae (s). A fine PM (0.9 µm) of iron oxide/hydroxide is visible (asterisk); c, clay mineral (6 µm). (B) UFP stuck to corn pollen. Larger baryte fragments are present as single PM or as clusters (asterisks); (p) circular pore of the corn pollen. (C) EDX spectrum of baryte PM. Bars = 10 µm.

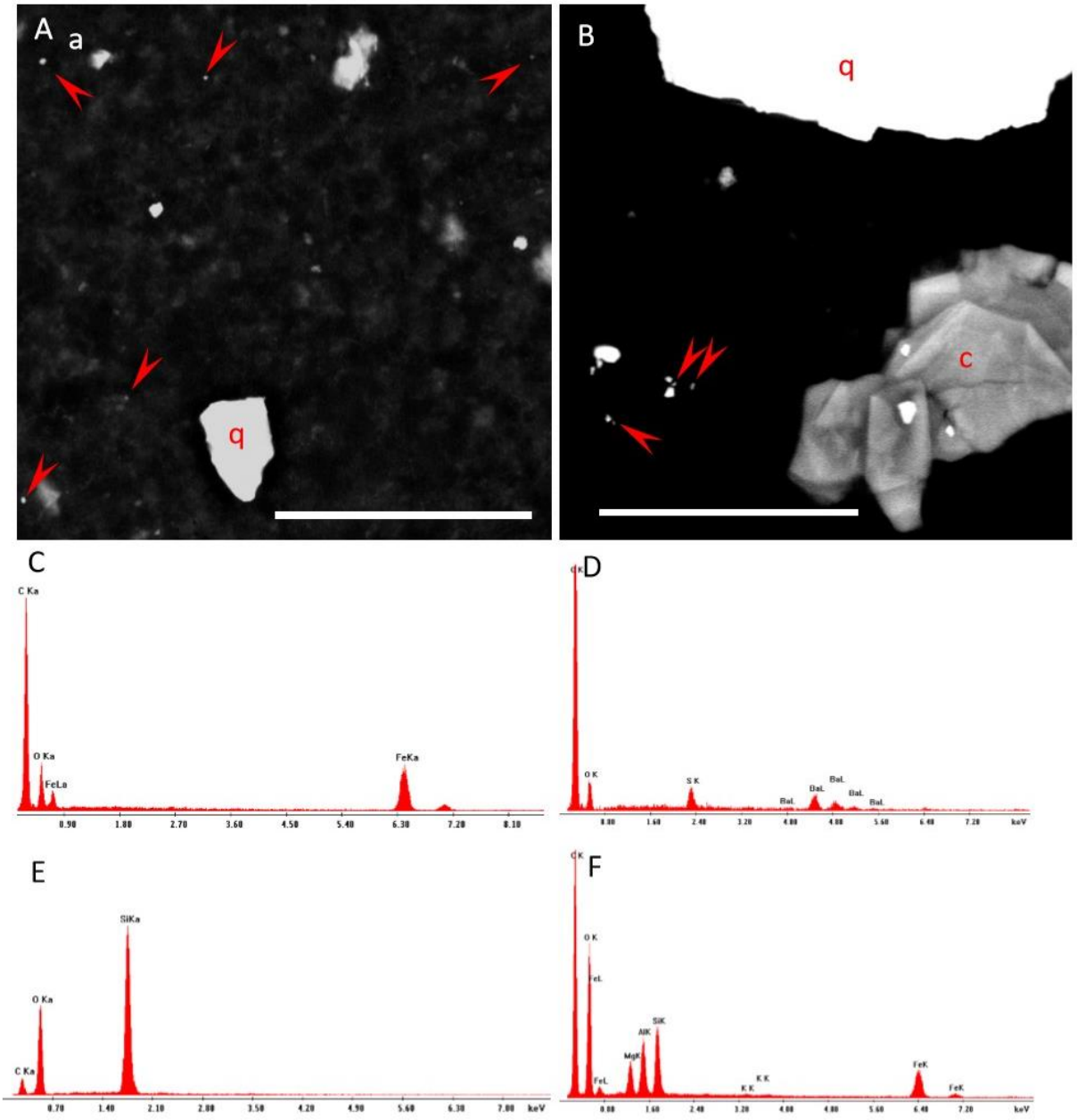

Figure 3.3. (A-B) Backscattered electron micrographs of inorganic sediment contained in honey: (A) fine and ultrafine (arrowheads) PM of Fe oxides/hydroxides; q = quartz fragment; (B) fine and ultrafine (arrowheads) fragments of baryte; c = clay mineral; q = quartz; Bars = 10 μm. (C) EDX spectrum of Fe oxide/hydroxide. (D) EDX spectrum of baryte. (E) EDX spectrum of quartz. (F) EDX spectrum of clay mineral.

Natural Fe-oxides are associated with mafic and ultramafic rocks, lateritic horizons, and the alteration of sulphide ores, whereas baryte usually concentrates in hydrothermal deposits. Therefore, both minerals are not expected to be abundant in the sediments cropping out in the studied area, which is supplied by the Flysch rock that crops out in the high valleys of

the Taro River and Parma Stream. Nonetheless, materials containing iron belong to major components that are used in the automotive industry, and both baryte and iron are common constituents of the braking systems of vehicles (Kukutschová et al., 2011; Carrero, Arana & Madariaga, 2014; Adamiec, Jarosz-Krzemińska & Wieszała, 2016; Gonet & Maher, 2019). In particular, brake discs are made of cast iron, and Fe-oxides are used as abrasives in brake lining materials (Österle et al., 2001; Gonet & Maher, 2019). Baryte is the major constituent of brake pads (Neis et al., 2017; Menapace et al., 2018) and Ba is used as a tracer element for brake dust at major roads (Gietl et al., 2010).

Ultrafine PM of Fe-oxides and baryte can be emitted from vehicular braking systems (Österle et al., 2001; Yang et al., 2016; Pellecchia & Negri, 2018; Gonet & Maher, 2019). The formation of nanosized baryte fragments has been demonstrated in braking simulation tests, and Ba-containing nanoparticles and other metal oxides are dominant in road dust (Österle et al., 2001; Labrada-Delgado et al., 2012; Yang et al., 2016).

Although emissions of Fe-oxides from braking systems is expected to be very high in areas close to motorway exits, we cannot exclude the fact that some UFP may originate from additives in the lubricating oil and from abrasion of engine parts (Liati et al., 2018). Further work involving for example hives located far from the motorway exits is needed to demonstrate a possible contribution from engine wear to the environmental contamination.

Given the global spread of traffic, our findings suggest that exposure and environmental impact of ultrafine Fe-oxides/hydroxides and baryte are potentially ubiquitous, although usually overlooked in environmental policy discussions.

3.5 Conclusion

By using the honeybee as an alternative natural and inexpensive sampling system of UFP, we demonstrate that areas subject to intense traffic are contaminated by metal-based dust,

primarily originating from vehicular traffic. Additionally, honey and pollen displayed contamination by the PM; thus, demonstrating the potential for UFP to enter the food chain and to expose pollinators to UFP ingestion.

Given the global spread of traffic, the exposure to ultrafine Fe-oxides/hydroxides and baryte is potentially ubiquitous. In the absence of mitigating actions for pollutants, such as plant barriers and "buffer" green zones, citizens living nearby major roads are chronically exposed to a well-defined spectrum of UFP, known to induce specific health issues. Further work is needed to evaluate specifically the exposure levels of local inhabitants. Toxicological studies on long-term low-dose exposure via inhalation and ingestion routes of UFP of Fe-oxides/hydroxides and baryte are urgently needed.

Honey and pollen are key elements of the bee diet; thus, pollinators may be exposed to UFP via the oral route. Specific ecotoxicological studies should therefore highlight any potential risk for the health of bees that are important providers of provisioning and regulating ecosystem services.

3.6 Acknowledgments

This project has been funded with a support from the ECORESILIENTE project of Università Cattolica (E.C. and I.N.). G.P. was partially supported by the Doctoral School on the Agro-Food System (Agrisystem) of the Università Cattolica del Sacro Cuore (Italy). Special thanks to Liceo Ulivi of Parma and Comune di Parma for supporting beekeeping activity during the educational project "Che aria tira". We thank Dr. Antonia Desiante for her support in data collection, and Dr. Paolo Gentile (Università Milano Bicocca, Italy) for SEM/EDX analysis and help in EDX spectra interpretation.

3.7 Supplementary

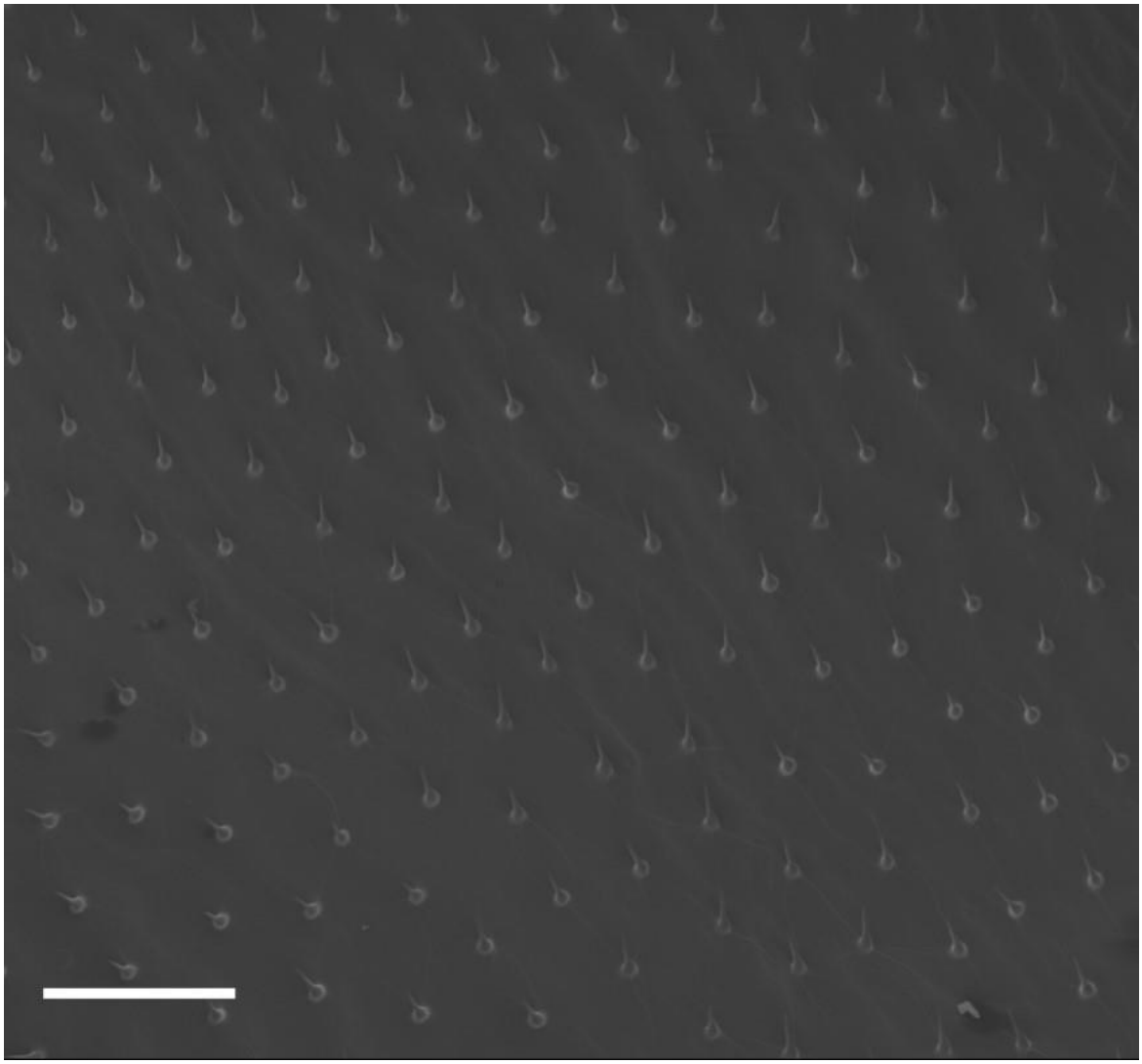

Figure 3.4 SEM micrograph of a clean wing from a newly enclosed adult (control bee); bar = 100 µm.

Chapter 4 Acute and chronic effects of Titanium dioxide (TiO_2) PM_1 on honey bee gut microbiota under laboratory conditions

Submitted for publication

Papa G.[1], Di Prisco G.[2,3,4], Spini G.[5], Puglisi E.[5]*, Negri I.[1]

[1] Department of Sustainable Crop Production – DIPROVES, Università Cattolica del Sacro Cuore Via Emilia Parmense 84, 29122 Piacenza, Italy

[2] Institute for Sustainable Plant Protection, National Research Council, Piazzale Enrico Fermi 1, 80055 Portici, Naples, Italy

[3] CREA Research Centre for Agriculture and Environment, Via di Corticella 133, 40128 Bologna, Italy

[4] Department of Agricultural Sciences – University of Napoli Federico II, Via Università 100, 80055 Portici, Italy.

[5] Department for Sustainable Food Process – DISTAS, Università Cattolica del Sacro Cuore, Via Emilia Parmense 84, 29122 Piacenza, Italy

*Corresponding author: edoardo.puglisi@unicatt.it

4.1 Abstract

Apis mellifera is an important provider of ecosystem services, and during flight and foraging behaviour is exposed to environmental pollutants including airborne particulate matter (PM). While exposure to insecticides, antibiotics, and herbicides may compromise bee health through alterations of the gut microbial community, no data are available on the impacts of PM on the bee microbiota.

Here we tested the effects of ultrapure Titanium dioxide (TiO_2) submicrometric PM (i.e., PM_1, less than 1 µm in diameter) on the gut microbiota of adult bees. TiO_2 PM_1 is widely used as a filler and whitening agent in a range of manufactured objects, and ultrapure TiO_2 PM_1 is also a common food additive, even if it has been classified by the International Agency for Research on Cancer (IARC) as a possible human carcinogen in Group 2B.

Due to its ubiquitous use, honey bees may be severely exposed to TiO_2 ingestion through contaminated honey and pollen. Here, we demonstrated that acute and chronic oral administration of ultrapure TiO_2 PM_1 to adult bees alters the bee microbial community; therefore, airborne PM may represent a further risk factor for the honey bee health, promoting sublethal effects against the gut microbiota.

4.2 Introduction

Honey bees (*Apis mellifera* Linnaeus) are important providers of ecosystem services, both regulating, through pollination of a wide range of crops and uncultivated plants, and provisioning, for the delivery of honey, pollen, propolis and other products to humans. Moreover, the honey bee is an important bioindicator of environmental contamination, and both the insect and its products are used for the detection of environmental pollutants (Devillers & Pham-Delegue, 2002; Satta et al., 2012; Negri et al., 2015; Goretti et al., 2020; Papa et al., 2020 (Chapter 3)).

In the last decade, one of the major problems plaguing honey bees is a phenomenon named Colony Collapse Disorder (CCD) which causes loss of colonies worldwide (vanEngelsdorp & Meixner, 2010; Dainat, VanEngelsdorp & Neumann, 2012; Brodschneider et al., 2016). The multifactorial origin of CCD is widely acknowledged, and environmental stressors such as pesticides, heavy metals, or airborne particulate matter (PM) pollutants may play a key role in driving the bees' decline (Feldhaar & Otti, 2020).

While the effects of pesticides and heavy metals on bees are widely recognised, till now very few data are available on the effects of PM on bees' health. These studies include lethal and sublethal effects (e.g., behaviour, gene expression, and cellular alterations) of the exposure to lead and cadmium oxides and TiO_2 nanoparticles (Özkan et al., 2014; Dabour et al., 2019; Ferrara et al., 2019; AL Naggar et al., 2020).

In polluted environments, airborne PM is known to stuck to the body of the bee and can be also ingested through contaminated pollen and honey that represent the food sources of the bee colony (Negri et al., 2015; Pellecchia & Negri, 2018; Papa et al., 2020 (Chapter 3)). If ingested, dusts can come into contact with the gut microbiome lining the intestinal epithelium posing a hazard to the bacterial community. Recent evidence suggests that environmental stressors can indirectly compromise bee health through gut microbiota disruption (Raymann & Moran, 2018). The honey bee harbours a simple and distinct gut community, thought to be the result of a long-lasting evolutionary relationship (Raymann & Moran, 2018). While no evidence has been reported until now on the impacts of PM on the bee health, alterations of the gut microbial community composition were demonstrated in bees exposed to antibiotics (Raymann, Shaffer & Moran, 2017), glyphosate (Motta et al., 2020), insecticides (Liu et al., 2020; Zhu et al., 2020) and sublethal doses of cadmium and selenite (Rothman et al., 2019).

The gut of worker bees is dominated by nine clusters of bacterial species comprising between 95% and 99.9% of total diversity in almost all individuals, based on investigations carried out on 16S rDNA (Moran et al., 2012; Sabree, Hansen & Moran, 2012; Corby-Harris, Maes & Anderson, 2014) and on total DNA metagenomics of intestinal samples (Engel, Martinson & Moran, 2012). The two omnipresent Gram-negative species are *Snodgrassella alvi* and *Gilliamella apicola*, both members of Phylum Proteobacteria (Kwong & Moran, 2013). Among Gram-positive bacteria, two groups of species in the Firmicutes phylum are ubiquitous and abundant, referred to as the *Lactobacillus* Firm-4 and *Lactobacillus* Firm-5 clades (Martinson et al., 2011). Although often less abundant, the cluster of the species *Bifidobacterium asteroides* (Bottacini et al., 2012) is also found in most adult worker bees. Less numerous and even less prevalent are the Proteobacteria species *Frischella perrara* (Engel, Kwong & Moran, 2013), *Bartonella apis* (Kešnerová, Moritz & Engel, 2016), *Parasaccharibacter apium* (Corby-Harris, Maes & Anderson, 2014) and a group of Gluconobacteria species designated Alpha2.1. These species have narrow niches in the intestines of bees (e.g., *F. perrara*) or are generalists, i.e., they are also found in the hive environment (for example, *P. apium*, *Lactobacillus kunkeei* and the Alpha2.1 group), which may explain their relatively lower frequency in bee gut detections. While other bacteria may occasionally be present, these nine species groups represent bacterial lineages that appear to be specifically adapted to life alongside their hosts, bees. This gut microbiota organization is well described by Kwong & Moran (2016).

The newly hatched larvae are free of bacteria that start colonizing the gut thanks to interactions with worker bees and the hive environment (Vojvodic, Rehan & Anderson, 2013; Hroncova et al., 2015). During the metamorphosis of the larvae to pupae and finally, into adult bees, the lining of the intestine is renewed: the newly emerged adult bees have

very few bacteria in the intestine and are readily colonized by the typical intestinal microbial community (Powell et al., 2014).

Titanium dioxide (TiO_2) is a naturally occurring metal oxide. As rutile, TiO_2 is not rare in nature and may concentrate in the heavy fraction of sediments. Synthetic TiO_2 in form of sub-micrometric PM, i.e., PM_1, less than 1 μm in diameter, is widely used as a filler and whitening agent in a range of manufactured objects, such as plastics, paints, paper, printing inks, textiles, catalysts, floor and roofing materials, and vehicles components. TiO_2 is also a common ingredient in cosmetics, pharmaceuticals, sunscreen and as a food additive. While TiO_2 used for non-food applications has surface coatings of alumina and silica, to reduce photoactivity, and organic surface treatments, conferring hydrophobic properties, TiO_2 as a food additive is ultrapure, and PM size ranges from 400 μm to 30 nm (Bettini et al., 2017; Younes et al., 2019).

The potential ecological and human health impact of exposure to TiO_2 is of growing concern. Indeed, inhalation and intra-tracheally administration of PM of TiO_2, including nano-meter sized particles, induces lung cancer in rats (Baan, 2007). TiO_2 has indeed been classified by the International Agency for Research on Cancer (IARC) as a possible human carcinogen in Group 2B (IARC, 2010). New evidence suggests that oral exposure to nanosized TiO_2 promotes chronic intestinal inflammation and carcinogenesis in rats (Bettini et al., 2017), as well as dysbiosis of gut microbiota (Chen et al., 2019).

Trace element analyses already demonstrated that Titanium can be detected in honey, pollen and bees, especially in high density urban and residential/suburban areas (Omode & Ademukola, 2008; Ribeiro et al., 2014; Solayman et al., 2016; Smith et al., 2019). Titanium can be only found in combined form and the most widespread chemical form both from natural and anthropogenic sources is TiO_2. Therefore, honey bees may be severely exposed

to TiO_2 ingestion through contaminated honey and pollen, and in severely polluted areas, PM_1 of TiO_2 can be detected in pollen grains and honey (Negri, personal communication).

The toxicity of TiO_2 PM_1 at nano-scale has been already studied in honey bee with histological and immunohistochemical approaches (Ferrara et al., 2019) shedding light on the negative effects at high doses. However, in-depth studies on the effects on the gut environment of the TiO_2 ingested by bees are still lacking, and no studies on specific impacts on the bee's gut microbiota are available. Here we wanted to fill this gap by studying the effect of TiO_2 on honey bees gut microbiota in the experimental context of controlled oral administration, providing evidence that ingestion of PM_1 of TiO_2 can alter the bee microbial community. Sub-lethal doses were employed, while acute and chronic exposures were assessed at 24 and 96 h post-emergency for acute and chronic experiments respectively.

4.3 Results

4.3.1 SEM-EDX

Scanning electron microscope (SEM) coupled with X-ray (EDX) analyses were used to assess the morphology, chemical composition and size of TiO_2 particles delivered to the bees.

SEM analyses showed that the TiO_2 stock powder had a sub-micrometre size <1 µm (between 800 and 200 nm) and an ellipsoidal/spherical shape (Figure 4.1 A). Moreover, EDX analyses and compositional mapping confirm the purity of TiO_2 rutile (Figure 4.1 B-E).

SEM-EDX analyses demonstrated the absence of TiO_2 in haemolymph collected from the acute, chronic and control samples (Suppl. Figure 4.8 A and B). In the haemolymph, EDX

spectra (Suppl. Figure 4.8 B) showed the presence of many elements e.g., Mg, Ca, Na, S, P, K, Cl (Chan, Howes & Foster, 2006).

SEM observation performed on chronic and control gut highlighted the presence of many lanceolate crystals likely due to precipitation of salts. EDX analysis confirmed their chemical composition as K_2SO_4 (Figure 4.2 A-D). In the rectum of treated bees, TiO_2 was found both associated (Figure 4.2 E and F) and not associated (Figure 4.2 G-L) with K_2SO_4 crystals.

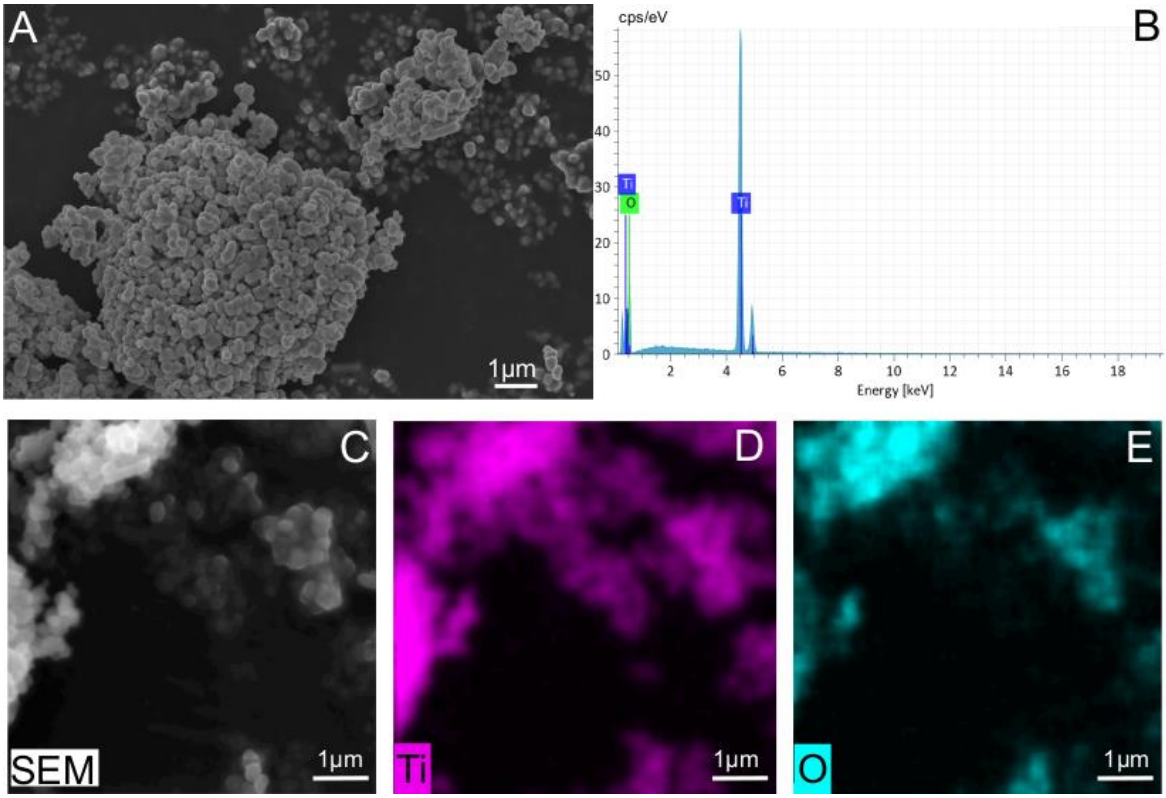

Figure 4.1 Control sample of TiO_2 rutile powder and elemental mapping. (A) SEM image showing the morphology and size and (B) EDX spectrum showing the purity of the TiO_2 powder. C) SEM-BSE image and the D) Titanium and E) Oxygen element maps.

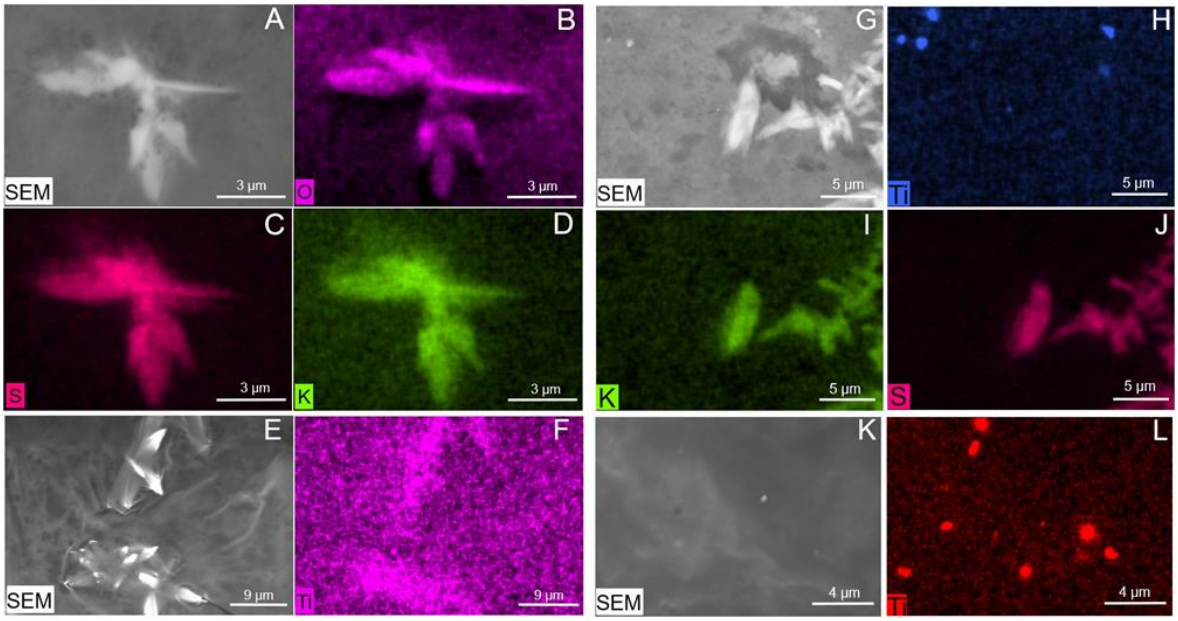

Figure 4.2 Elemental mapping of the rectum in control (A-D) and chronical samples (E-L). (A, E, G, K) SEM-BSE images; (B-D) element analysis highlighting the presence of K_2SO_4 crystals in the control sample; (F) Titanium dioxide associated with K_2SO_4 crystals; (H-L) Titanium dioxide not associated with K_2SO_4 crystals.

4.3.2 Bacterial diversity in the studied honey bees

The gut bacterial diversity was assessed by means of Illumina HTS of bacterial 16S amplicons covering the V3-V4 regions. A total of 537,641 sequences were produced, filtered and downscaled to 216,000 (i.e., 12,000 per each sample) after elimination of homopolymers, sequences not aligning to the target region, chimaeras, non-bacterial sequences and rarefaction to the least populated sample. After this downscaling, one out of 18 samples (a replicate of the 100X acute test) was eliminated because it had a lower number of sequences. The resulting Good's index of coverage of the rarefied samples was 94.7 ± 1.2 %, indicating that the vast majority of bees gut bacterial diversity was covered by the sequencing.

The structure of honey bee gut bacterial community was investigated at OTUs level, testing with a CCA model if the treatment (control vs chronic vs acute) and the dose had significant effects on the bacterial gut communities of the studied bees. Results (Figure 4.3)

indicated that the bees from the acute and the chronic experiments, being sampled at different life stages, hosted very different gut microbiota. Within each exposure time, it was found that samples were clearly grouped among doses for chronic exposure, but not for the acute. Similar outcomes were obtained by Principal Component Analyses (Suppl. Figure 4.9).

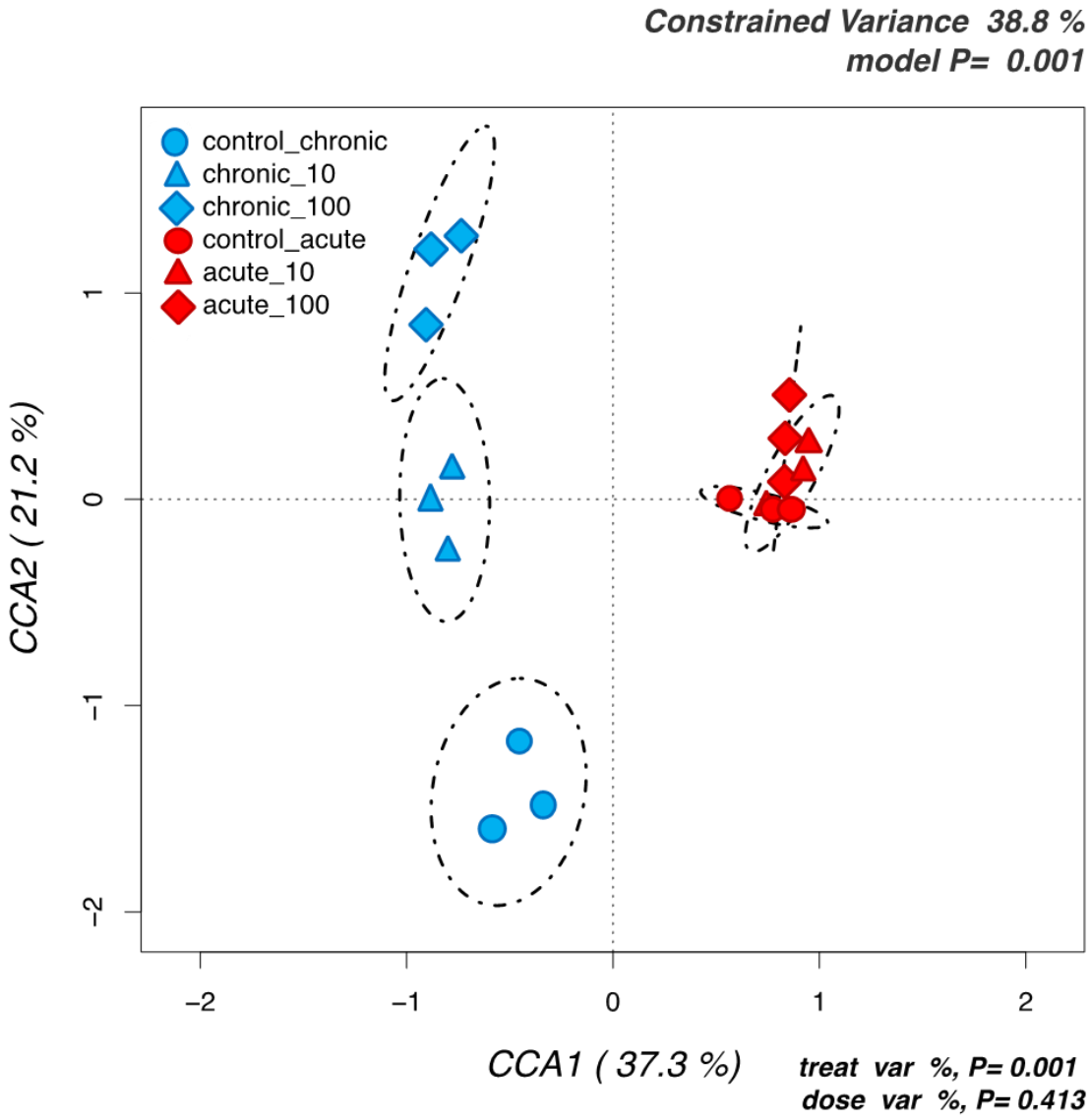

Figure 4.3 Hypothesis-driven canonical correspondence analysis (CCA) of honey bees gut microbiota testing the significance of the treatment and dose effects on the abundances of all analysed OTUs. Samples are labelled according to the 6 groups studied.

Differences among samples were also reflected by α-diversity analyses on the total number of OTUs identified in each treatment, which highlighted a clear trend: bees exposed to both chronic and acute TiO_2 PM displayed a higher diversity as compared to their relative controls. The difference was significant according to LSD test between the chronic control and the two acute treatments (Figure 4.4).

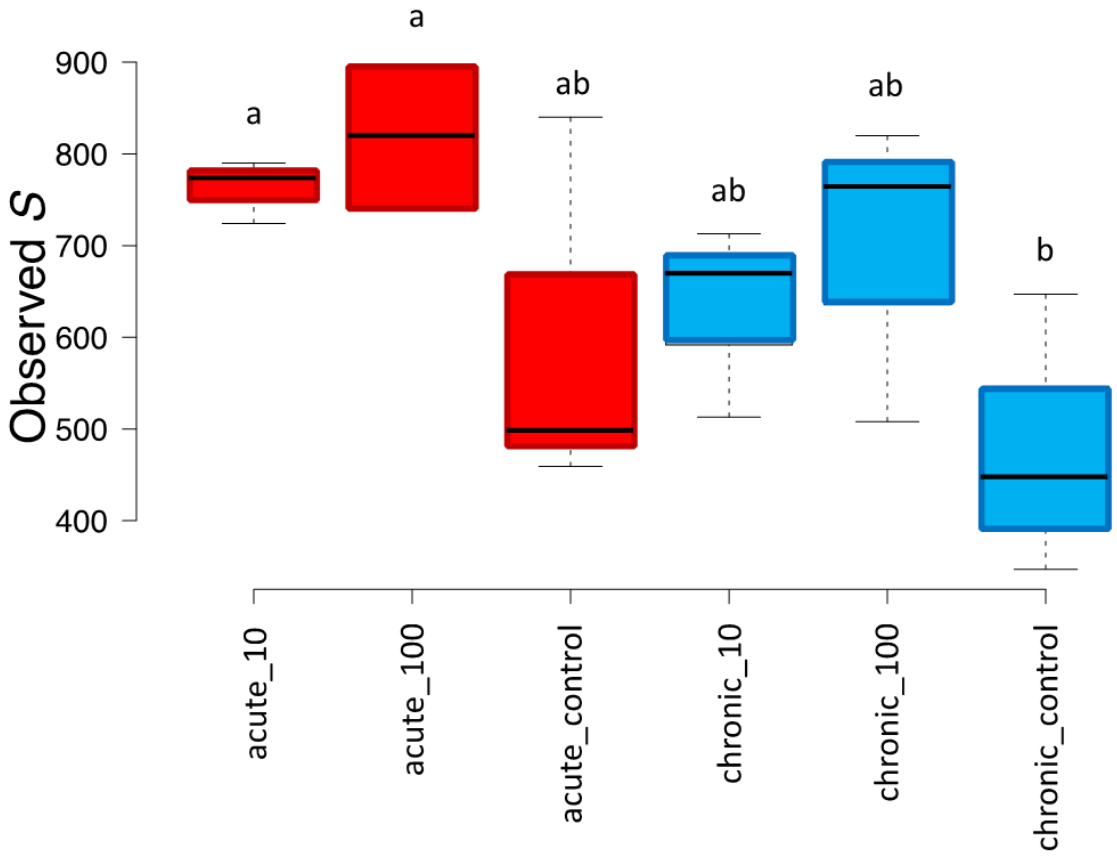

Figure 4.4 Number of observed OTUs (S) for the chronic and acute treatments and their respective controls. Significant differences are highlighted with different letters according to Tukey's HSD test for comparison of means.

The distinct bacterial community structures induced by TiO_2 PM exposure were also highlighted by hierarchical clustering of sequences classified at the genus level (Figure 4.5): in agreement with the CCA results, chronic and acute experiments were grouped in two main separate clusters sharing less than 70% of similarity. The two controls for each treatment representing adults sampled at two different life stages were also grouped

separately one from the other. *Gilliamella* was the dominant genus in the acute experiments (24h), with relative percentages reaching more than 80% of total abundance in a number of acute treatments at both 10X and 100X, followed by *Lactobacillus* and *Acetobacter*. A very different composition was identified in 96h bees of the chronic exposure experiment (Figure 4.5): here the dominant genus was *Lactobacillus*, which decreased in the TiO_2 exposed bees. The latter was however enriched in *Bifidobacterium*, reaching relative concentration between 5 to 12% in a number of chronically exposed bees. A particular feature was detected in two treated replicates at 10X and 100X, with *Acetobacter* covering the vast majority (i.e., >98%) of the observed diversity at the genus level.

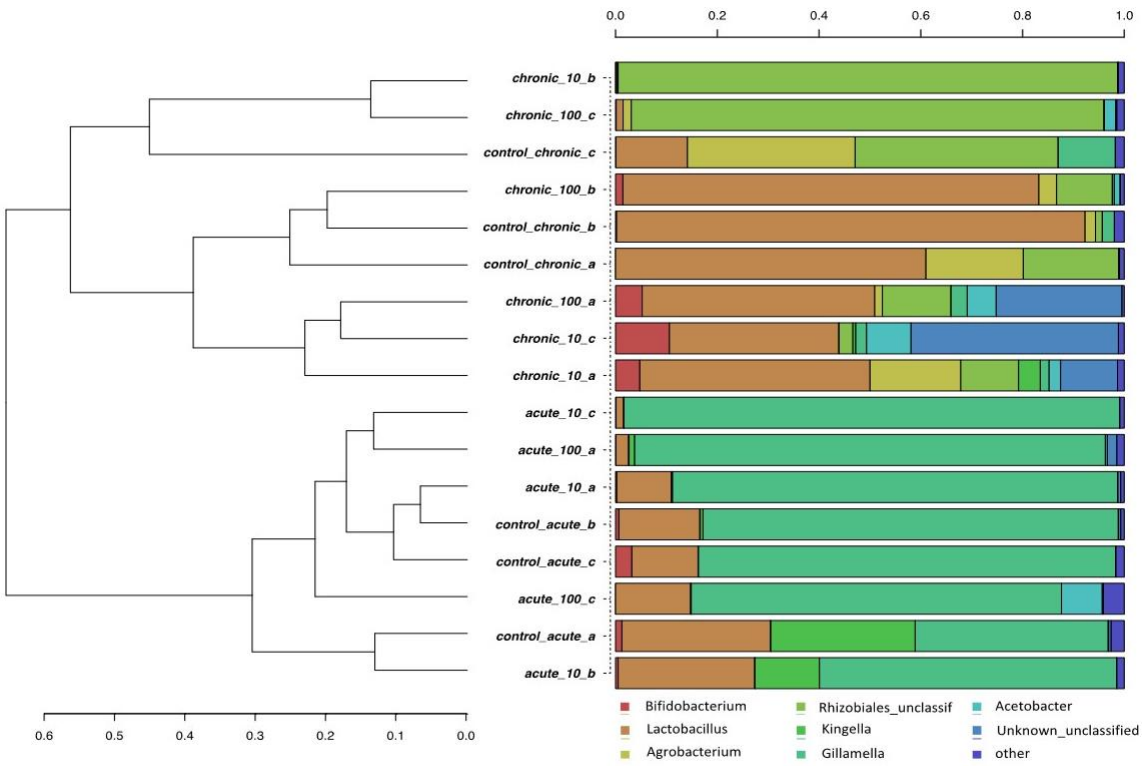

Figure 4.5 Hierarchical clustering of sequences classified at the genus level for both chronic and acute treatments. Bars of different colours indicated the relative percentage of the genera identified in the honey bees gut. Only genera participating with >1% in at least one sample are shown, while taxa with lower participations were added to the "other" group. Similar samples were clustered using the average linkage algorithm.

4.3.3 Distinctive features in the gut microbiota of honey bees acutely exposed to TiO_2

After defining that the two bee groups from the acute and the chronic exposure experiments had very different gut bacterial compositions (Figure 4.3 and Figure 4.5), separate analyses were carried out on the two groups, focusing on the relative presence of the most abundant OTUs classified at the species level.

In the acute exposure experiments, *G. apicola* was the most abundant species with an average of ca 70% of the total bacterial community, followed by *Lactobacillus apis*, *S. alvi*, *Lactobacillus kimbladii* and *Acetobacter tropicalis* (Figure 4.6 a). The clustering did not show clear discrimination between control and treated bees, but a Metastats model on the same OTUs revealed a number of significant differences (Figure 4.6 b). Specifically, a significant reduction with increasing acute doses of TiO_2 was found for *L. kimbladii*. The same trend was detected for *L. apis* and *S. alvi*, but with no statistical significance.

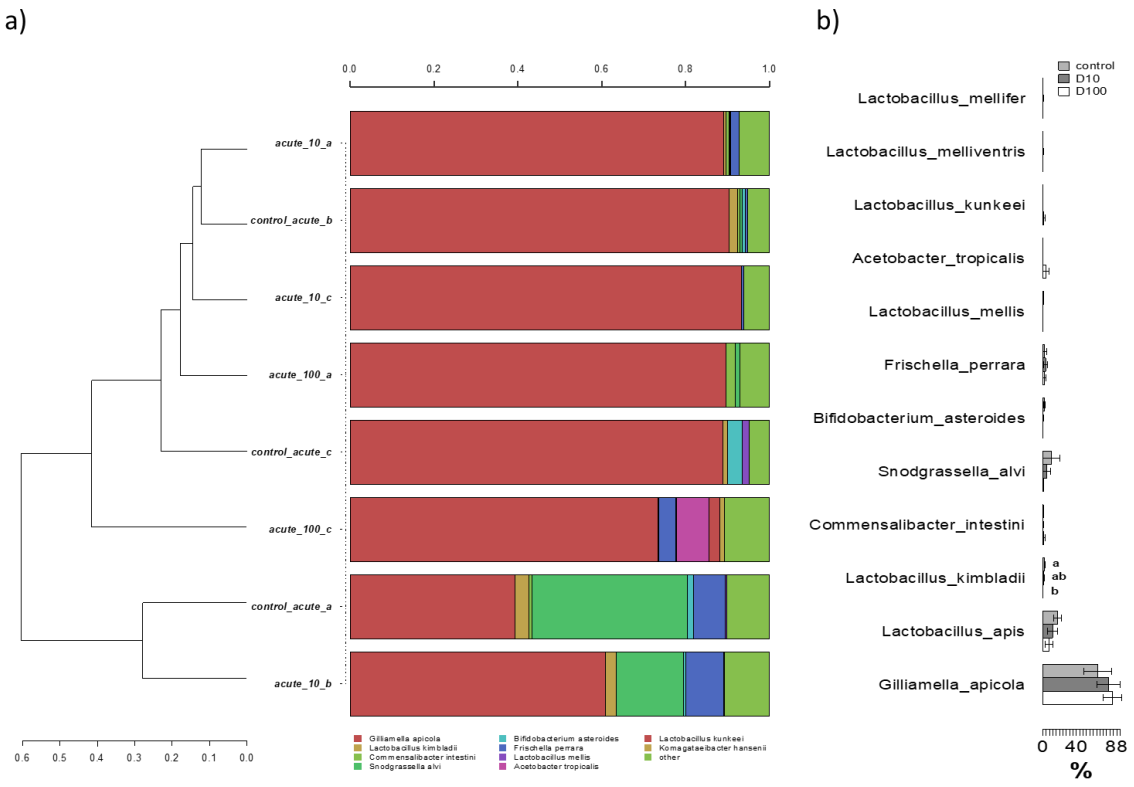

Figure 4.6 a) Hierarchical clustering of sequences of OTUs participating with >1% in at least one sample for the acute exposure experiment. Rare OTUs with lower participation were added to the "other" group; b) Metastats model showing differences among treatments for the most abundant OTUs. Significant differences are highlighted with different letters according to Tukey's HSD test for comparison of means.

4.3.4 Distinctive features in the gut microbiota of honey bees chronically exposed to TiO_2

A stronger differentiation between control and TiO_2 exposed bees was found in the chronic experiments. Here, the composition at the species level was very different, reflecting the age differences between this and the previous group of bees. *G. apicola* was still present, but with much lower relative abundances (<2%). On the contrary, a strong increase in abundances was found for *B. apis*, *L. apis*, *L. kimbladii*, *Commensalibacter intestini*, and *Bartonella* spp. (Figure 4.7 a). Much higher was also the number of species displaying significant differences between treatments and controls (Figure 4.7 b), thus highlighting significant effects of chronic TiO_2 exposure on the honey bees gut microbiota. Specifically,

L. apis, *Lactobacillus melliventris* and *Bartonella* spp. were significantly reduced by the exposure to TiO_2, in most cases with a dose dependent effect. On the contrary, *Bombella intestini* was found to be significantly enriched only in the X100 treatment.

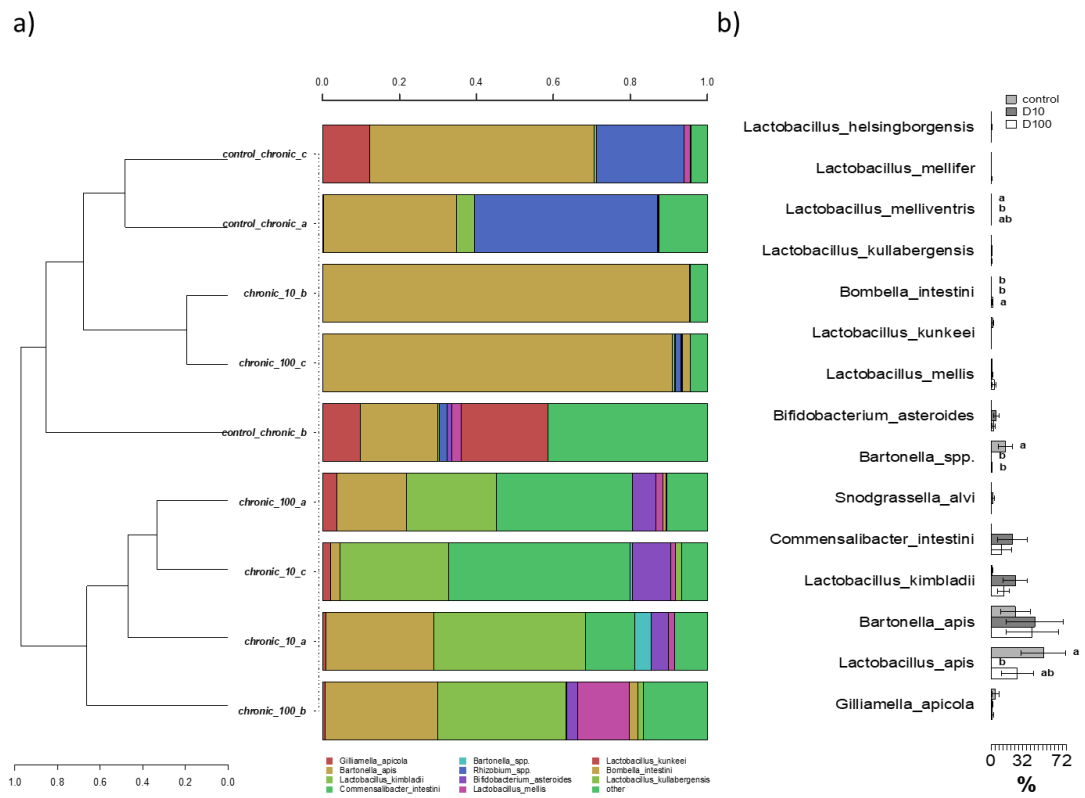

Figure 4.7 a) Hierarchical clustering of sequences of OTUs participating with >1% in at least one sample for the chronic exposure experiment. Rare OTUs with lower participation were added to the "other" group; b) Metastats model showing differences among treatments for the most abundant OTUs. Significant differences are highlighted with different letters according to Tukey's HSD test for comparison of means.

4.4 Discussion

In the present study, we explored the potential effects of acute and chronic oral administration of pure TiO_2 rutile on honey bee gut microbiota. The particles used were PM_1; ranging from 800 to 200 nm as characterized by SEM-EDX analysis. In a preliminary assay, we fed newly emerged worker bees with four different concentrations of TiO_2 in 1M sucrose solution, including 100 ng/µL and 10 ng/µL as test doses, after the rejection of the two higher doses 104 ng/µL and 103 ng/µL. Newly emerged worker bees were orally

exposed to the selected doses of TiO_2 in an acute (single treatment, sampling at 24 h) and a chronic application (treatments repeated every 24 h, sampling at 96h). In both assays, we obtained no mortality for the entire trials. This is partly in contrast with similar experiments on the honey bee, that however applied higher doses than the one tested here: TiO_2 resulted highly toxic at 1000 ng/µL (Ferrara et al., 2019), while in another study the LC50 at 96 hours resulted in 5.9 ng/µL (Özkan et al., 2014). Nevertheless, TiO_2 showed high mortality at a very high dose of 2400 ng/µL) in cutworm (*Spodoptera litura*) (Chakravarthy, 2012).

Unfortunately, the studies by Özkan et al., (2014) and Ferrara et al., (2019) do not provide a specific characterization of the size, morphology and purity of TiO_2 dust delivered to the bees. In our research, TiO_2 dust were carefully characterised by SEM/EDX, demonstrating the absence of contaminants or coatings and the dimensions greater than 200 nm. Such size might also explain the absence of TiO_2 PM in the haemolymph since particles might not be able to cross the barrier of the gut epithelium. However, a more in-depth study involving the analysis of the gut epithelium should be carried out to exclude the presence of TiO_2 PM from the epithelial cells or cytological abnormalities.

An indirect impact of TiO_2 on haemolymph has been thoroughly investigated in other organisms. In *Mytilus galloprovincialis*, TiO_2 has been shown to affect several immune parameters in both circulating haemocytes and haemolymph serum, resulting in immunomodulation (Barmo et al., 2013; Corsi et al., 2014; Auguste et al., 2019). In larvae of *Galleria mellonella* (Lepidoptera: Pyralidae), exposure with dietary TiO_2 nanoparticles (NPs) has dose-dependent toxic effects and can enhance the stress-resistant capacity with a significant increase in the total protein amount and content of malondialdehyde (MDA) and glutathione S-transferase activity at 100, 500 and 1000 ppm (Zorlu, Nurullahoğlu & Altuntaş, 2018). In our experiments, SEM-EDX reveals the typical haemolymph elements spectrum (Mg, Ca, Na, S, P, K, Cl) of the honey bee (Mikulecky & Bounias, 1997).

The analyses of bacterial community composition allowed by HTS of 16S amplicons clearly show that the acute and chronic exposed bees populations had hosted very different bacterial gut populations (Figure 4.5, Figure 4.6 and Figure 4.7). This is expected since analyses were carried out after 1 dpe (day post-emergence) for the acute experiment and at 4 dpe for the chronic experiment. The β-diversity analyses here carried out by means of unconstrained (PCA and hierarchical clustering, Figure 4.5 and Suppl. Figure 4.9) and constrained (CCA, Figure 4.3) analyses showed a clear distinction in bacterial community structure between the chronic and the acute experiments, and in the chronic experiments among controls and treated bees. These results are in line with several studies on other chemical stressors (Raymann, Shaffer & Moran, 2017; Rothman et al., 2019; Liu et al., 2020; Motta et al., 2020; Zhu et al., 2020), thus confirming that also PM modulates the honey bees gut bacterial community.

The results obtained in the unexposed controls are quite in agreement with previous evidence and showed the typical community of adult worker bee microbiota that is dominated by *Lactobacillus*, *Bifidobacterium*, *Gilliamella*, *Snodgrassella*. The presence of *Bartonella* and *Commensalibacter* in 4 dpe bees from the chronic experiment is in agreement with the characteristic gut microbial community of the so-called "winter bees", i.e., the last generations of workers characterised by overwintering individuals with an extended lifespan to ensure colony survival until spring (Kešnerová et al., 2020). The variability occurring in control bees is in agreement with other studies, where it has been demonstrated that, while many of the phylotypes are consistently present in adult worker bees, their relative abundance can vary across individuals (Kešnerová et al., 2020; Lamei et al., 2020), and representative of these two genera can be found also in early stages of development (Dong et al., 2019; Rothman et al., 2019).

In the treated populations, the two tested doses of TiO_2 had significant impacts on the gut bacterial communities, with more differences between exposed and control bees in the chronic as compared to the acute exposure. As far as we know, this is the first study where the effects of TiO_2 particles where specifically studied on bees gut microbiota, but they can be compared with a number of studies that previously assessed the detrimental impacts of airborne PM on the bees physiology (Özkan et al., 2014; Ferrara et al., 2019). Regarding α-diversity indexes, we found a dose-dependent increase in diversity, (Figure 4.3), while the opposite was found for the neonicotinoid insecticide Thiacloprid (Liu et al., 2020), polystyrene particles at µm levels (Wang et al., 2021), and antibiotics (Raymann, Shaffer & Moran, 2017). It must be highlighted that in these cited works a significant mortality was detected, whereas in our study sub-lethal doses were tested and no mortality registered. It can thus be speculated that the microbiota responded to the sub-lethal stressors by increasing the diversity, as postulated by the ecological theory of the intermediate disturbance hypothesis firstly proposed by Connell in 1978.

Concerning the changes in species abundances, we found that in the acute test only one species, *L. kimbladii*, was significantly reduced by the highest dose of TiO_2 applied (Figure 4.6). Firstly described in 2014 by Olofsson (2014) and colleagues, this species was more recently proposed as a possible probiotic (Mårtensson et al., 2016; Duong et al., 2020). Interestingly, *L. kimbladii* was instead found at higher abundances in the 96 h bees from the chronic exposure, with values higher than the control in the two treated theses (Figure 4.7). This change may point to an adaptation in time of the microbial community, with a probiotic species becoming more abundant to counteract the chronic effects of a chemical stressor, as previously shown for *Bifidobacterium* species in bees exposed to the insecticide Nitenpyram (Zhu et al., 2020).

While in the acute experiment only *L. kimbladii* was significantly inhibited by the TiO_2 particles (Figure 4.6), in the chronic exposure three species were inhibited: *L. apis*, *L. melliventris* and *Bartonella* spp. (Figure 4.7). *L. apis* is one of the most studied components of the bees gut microbiome, whose functions as probiotics were demonstrated by processes such as the attenuation of immune dysregulation (Daisley et al., 2020) and the inhibition of *Paenibacillus larvae* and other pathogens (Lamei et al., 2019); the induction of resistance towards bacterial infection was also demonstrated for *L. melliventris*, which was accordingly proposed as a bee probiotic (Hyrsl et al., 2017). Finally, the reduction of species belonging to *Bartonella* was also found in bees parasitized by *Varroa* (Hubert et al., 2015), but this genus was also found to be increased after exposure to glyphosate (Motta et al., 2020). The only taxon whose relative presence was significantly increased by chronic TiO_2 exposure was *B. intestinii*, an acetic acid bacterium (AAB) firstly isolated in honey bees in 2017 by Yun and colleagues (Yun et al., 2017). This species, together with other AAB, may play a role in the regulation of the innate immune system homeostasis (Crotti et al., 2010) and may thus represent an adaptation of the gut bacterial community to counteract the stressors sub-lethal effects.

Titanium oxide nanoparticles are known to exert a toxic effect on several bacteria, with proposed modes of action related to both chemical and physical interactions with the cells envelopes (Baysal, Saygin & Ustabasi, 2018), and alterations in human gut bacterial communities are often found including detrimental effects, as recently reviewed by Lamas et al. (2020). Here we provide for the first time modulation of the honey bees gut microbiota induced by both acute and chronic exposure to TiO_2 PM_1, with stronger effects in the latter case. The effects we report are related to doses that are probably higher than the ones that can be found under field conditions and can be considered sub-lethal since no mortality was observed among all treated bees, and an increase in bacterial diversity was

even found. On the other side, some negative effects related to the decrease in the relative percentages of some beneficial lactobacilli were however observed, and for this reason the role of airborne particulate as a further risk factor for *Apis mellifera* health in addition to other chemical stressors should be further explored.

4.5 Materials and methods

4.5.1 Honey bees

Experiments were conducted during October 2018 with *Apis mellifera ligustica* colonies maintained in the experimental apiary of the University of Napoli "Federico II", Department of Agricultural Sciences. Brood frames with capped cells from two colonies were selected and kept in a climatic chamber at 36°C and 60% relative humidity for approximately 16 hours. Newly emerged workers were randomly selected and used for the bioassays.

4.5.2 Preparation of TiO_2 feeding solution

Titanium dioxide rutile (TiO_2) powder was acquired from 2B Minerals S.r.l. (Modena, Italy). Suspensions were prepared by dissolving 0.5g TiO_2 in 50 mL distilled H_2O, vortexed for ~20 seconds and sonicated for 15 minutes to increase dispersion and ensure the maximum distribution of particles in water (Özkan et al., 2014). A 1M sucrose solution was then prepared with TiO_2 suspensions.

Preliminary palatability tests on bees were carried out with the following dilutions: 104 ng/µL, 103 ng/µL, 100 ng/µL, 10 ng/µL. The last two concentrations were chosen for the experiments following rejection of the more concentrated solutions by the bees.

4.5.3 Chronic and acute exposure

Two groups of 30 newly eclosed bees were randomly collected from the combs. The bees were fed ad libitum with 1 µL of 10 ng/µL and 100 ng/µL TiO_2 solutions (1M sucrose),

respectively (hereinafter CH10- and CH100-bees), and then placed into plastic cages containing 1.5 mL of the same solution to which they were previously fed. Control bees consisted of 30 individuals fed ad libitum with an untreated sucrose solution (1M).

The solution was changed every 24 hours. During the experiments, all caged bees were kept in a climatic chamber at 36°C and 60% relative humidity. After 96 hours the bees were anesthetized with CO_2 for ~30 seconds and the whole gut dissected as previously described (Carreck et al., 2013). Guts were stored in absolute ethanol and immediately refrigerated at -80°C for the subsequent microbiological analysis. Experiments were conducted in triplicate (i.e., 3 replicates each made by three guts pooled together). Bees survival was recorded each day.

The experimental design of acute exposure was the same as in chronic exposure except for the duration of the experiment that in acute exposure lasted only 24 hours instead of 96, and bees were fed only once with 10 ng/µL or 100 ng/µL TiO_2 solutions (hereinafter AC10- and AC100-bees).

4.5.4 TiO_2 detection in the gut

To assess morphology, average size and chemical purity of TiO_2 powder, few µgrams were mounted onto stubs and analysed through a Scanning Electron Microscope (SEM) provided with X-ray spectroscopy (EDX) (Zeiss Gemini SEM 500 - Bruker Quanta X-Flash 6131). Secondary Electrons (SE), BackScattered Electrons (BSE) images, and EDX point analyses, were acquired as previously described (Negri et al., 2015; Pellecchia & Negri, 2018).

The presence of TiO_2 in the haemolymph and gut of chronic bees was investigated by SEM-EDX. Haemolymph from 4 randomly selected CH10- and CH100-bees plus 4 randomly selected control bees was sampled from the dorsal aorta, following the method

standardized by Garrido and colleagues (Garrido et al., 2013). The bee gut (rectum with excrements) from CH10- and CH100-bees plus control bees (n=4 randomly selected, for each concentration and control) were mounted onto stub and dried in a sterilized oven at 20°C for 40 minutes. Samples were carbon coated and analyzed with SEM/EDX.

4.5.5 Microbiota analysis

4.5.5.1 DNA extraction

DNA was extracted from gut samples collected for microbiological analyses. For each dose – acute and chronical – n. 3 groups of three guts were analysed. From these samples, the total microbial DNA was extracted using the Fast DNA SPIN Kit for Soil (MP Biomedicals, USA) with the following modifications: each sample was homogenized in the FastPrep for 40 seconds at speed setting of 6.5 twice, keeping it in ice between the two homogenisation steps, while the final centrifugation was carried out at 14,000 x g for 15 minutes, and the final resuspension of the Binding Matrix was carried out in 50 µL of nuclease-free water.

The DNA extractions were checked with electrophoresis on a 1% agarose gel, and then quantified using a QuBit fluorometer (Invitrogen, United Kingdom).

4.5.5.2 DNA amplification

The V3-V4 region of the bacterial 16S rRNA gene (between 480bp and 490bp) was amplified by PCR using the universal primers 343f (5'-TACGGRAGGCAGCAG-3'), and 802r (5'-TACNVGGGTWTCTAATCC-3') (Połka et al., 2015). A two-step PCR protocol was implemented in order to reduce the possibility of generating non-specific primer annealing, as detailed in Berry et al. (2011). The PCR reaction mix comprised of 20.5 µL of MegaMix (Microzone Limited, United Kingdom), 1.25 µL of each primer (10µM), and 2 µL (1ng/µL concentration) of DNA template. Thermal cycling conditions were as follows: Step 1: an initial denaturation at 94 °C for 5 min, followed by 25 cycles at 94 °C for 30 s,

50 °C for 30 s, 72 °C for 30 s, followed by a final extension at 72 °C for 10 min. Step 2: initial hold at 95 °C for 5 min, followed by 10 cycles of 95°C for 30 s, 50 °C for 30 s, and 30 °C for 30 s; then, a final extension at 72 °C for 10 min. At the second step, each sample was amplified using a dedicated forward primer with a 9- base extension at the 5' end, which acts as a tag, in order to make simultaneous analyses of all samples in a single sequencing run possible The DNA amplifications were checked with electrophoresis on a 1% agarose gel, and then quantified using a QuBit fluorometer (Invitrogen, United Kingdom). PCR products generated from the second step were multiplexed as a single pool using equivalent molecular weights (20 ng). The pool was then purified using the solid phase reversible immobilization (SPRI) method with Agencourt AMPure XP kit (REF A63880, Beckman Coulter, Milan, Italy), then sequenced by Fasteris S.A. (Geneva, Switzerland). The TruSeq DNA sample preparation kit (REF 15026486, Illumina Inc, San Diego, CA) was used for amplicon library preparation, whereas the sequencing was carried out with the MiSeq Illumina instrument (Illumina Inc., San Diego, CA) generating 300 bp paired-end reads.

4.5.5.3 Sequence data preparation and statistical analyses

High-throughput sequencing data filtering, multiplexing and preparation for concomitant statistical analyses were carried out as previously detailed (Vasileiadis et al., 2015). In summary, paired-reads were assembled to reconstruct the full V3-V4 amplicons using the "pandaseq" script (Masella et al., 2012) with a maximum of 2 allowed mismatches and at least 30 bp of overlap between the read pairs. was then carried out with the Fastx-toolkit was then employed for samples demultiplexing (http://hannonlab.cshl.edu/fastx_toolkit/).

Mothur v.1.32.1 (Schloss et al., 2009) was applied in order to remove sequences with large homopolymers (≥10), sequences that did not align within the targeted V3-V4 region, chimeric sequences (Edgar et al., 2011) and sequences not classified as bacterial after

alignment against the Mothur version of the RDP training data set. Mothur and R (http://www.R-proje ct.org/) were employed to analyze the resulting high-quality sequences following the operational taxonomic unit (OTU) and the taxonomy-based approach. For the OTU approach, sequences were first aligned against the SILVA reference aligned database for bacteria (Pruesse et al., 2007) using the NAST algorithm and a kmer approach (DeSantis et al., 2006; Schloss, 2010), and then clustered at the 3% distance using the average linkage algorithm. OTUs having a sum of their abundances across all samples of than 0.1% of the total were grouped into a single "rare OTUs" group. For taxonomy based analyses, sequences were classified into taxa using an amended version of the Greengenes database (McDonald et al., 2012).

Mothur and R were also employed for statistical analyses on OTU and taxonomy matrixes using hierarchical clustering with the average linkage algorithm at different taxonomic levels, Principal component analysis (PCA) for unconstrained samples grouping, Canonical correspondence analyses (CCA) to assess the significance of different treatments on the analysed diversity. Features that were significantly different between treatments were identified with Metastats (McDonald et al., 2012).

Sequence data were submitted to the National Centre for Biotechnology Information Sequence Read Archive (BioProject accession number PRJNA693145).

4.6 Acknowledgments

GP was partially supported by the Doctoral School on the Agro-Food System (Agrisystem) of the Università Cattolica del Sacro Cuore (Italy). We thank Tiziano Catelani and Paolo Gentile for advices on the SEM-EDX analyses and Francesco Pennacchio for the permission to use the Entomology laboratory at the Federico II University of Naples (Italy).

4.7 Supplementary

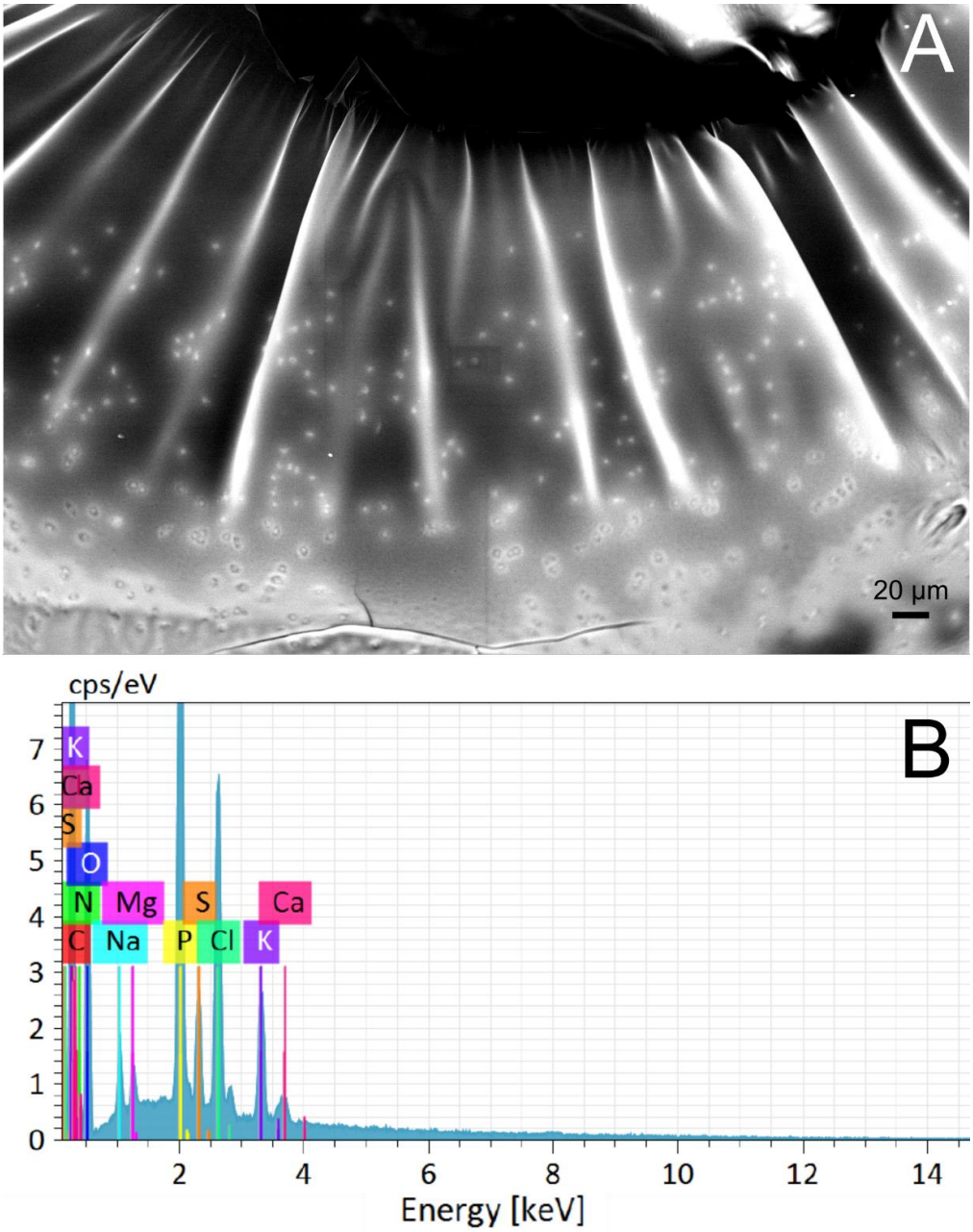

Figure 4.8 Haemolymph control drop. A) SEM image of haemolymph with haemocytes (light spots). B) EDX spectrum showing the absence of TiO_2 in haemolymph.

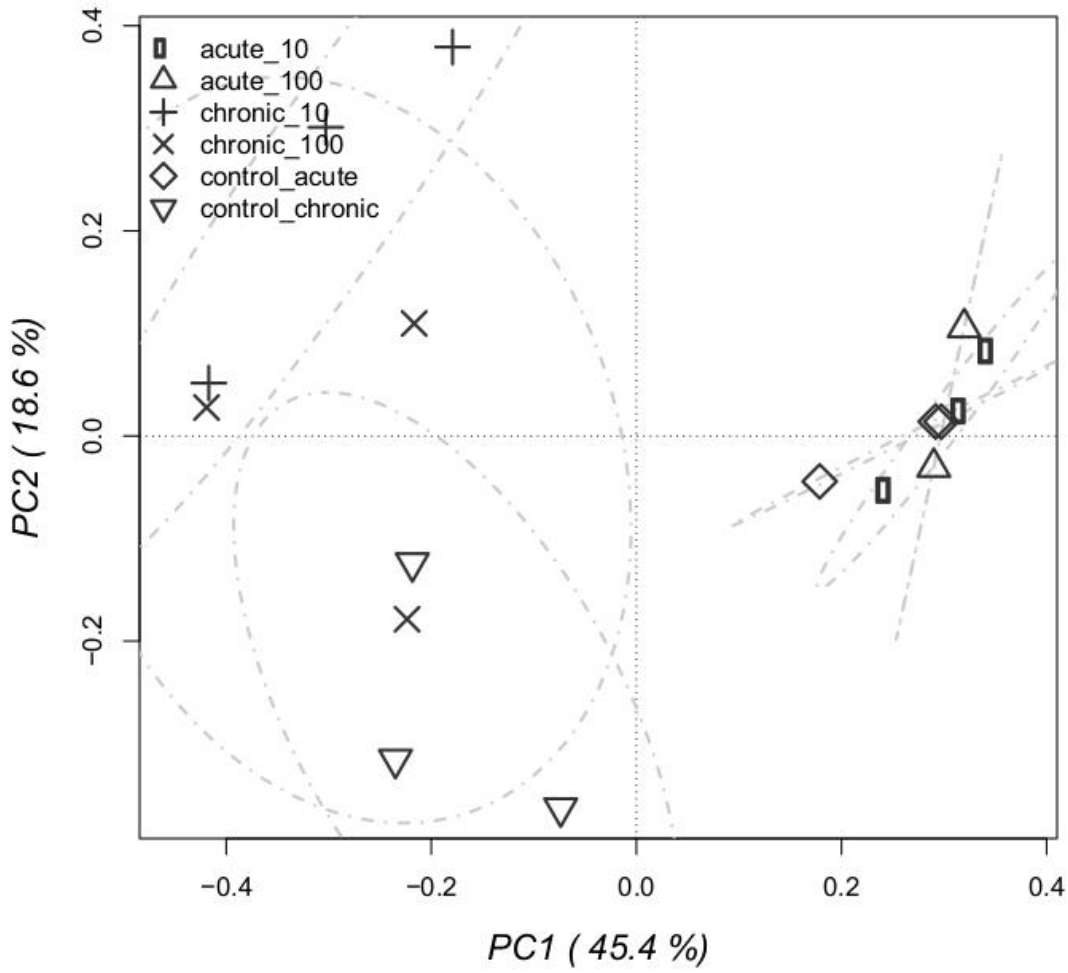

Figure 4.9 Principal component analysis (PCA) on the total measured OTUs highlighting possible groupings of honey bee gut bacterial communities according to the treatment or the dose.

Chapter 5 General conclusions

Here, we confirmed the use of *Apis mellifera* as an alternative, efficient and inexpensive sampling system of airborne PM, able to collect the main PM pollutants emitted from different sources. We applied this methodology to investigate PM_{10}, $PM_{2.5}$ and ultrafine PM accumulated on honey bees in an urban area of the Po Valley, one of the most important industrial and agricultural areas in Italy and Europe, characterized by a high population density and low air quality. The study area included agricultural fields, a relatively new incinerator plant and a portion of the 'A1 Milano-Bologna', one of the most trafficked motorways in Italy (Chapter 2 and Chapter 3). A single fixed monitoring station for the airborne concentration of PM is in place in the target area and provides the daily and annual mean concentrations of PM_{10} and $PM_{2.5}$ particles per cubic meter of air volume. However, no information on the nature and chemical composition of the particles and ultrafine PM is collected (Regional Environmental Protection Agency, www.arpae.it).

Our results suggest that people living in the area are subjected to chronic exposure, i.e., the continuous/repeated contact with specific airborne PM_{10} and $PM_{2.5}$ emitted by vehicular traffic, local agricultural operations and the incineration of waste, and that exposure levels may vary rapidly based on recurrent local activities (Chapter 2). Furthermore, we used the honeybee as an alternative sampling system of nanosized PM, since bees typically collect dust of size <10 μm, easing the identification and analysis of the ultrafine fraction. This approach allowed us to demonstrate that areas subject to intense traffic are contaminated by metal-based dust, primarily originating from vehicular traffic.

Simple preventing measures, such as properly isolated loading and unloading premises, would suffice as containment measures to substantially reduce the fugitive emission load. Additionally, previous research showed that wall-plant species, when adequately positioned nearby roads and highways, can significantly reduce the PM deposition (Paull et al., 2020).

Specifically, *Chlorophytum comosus variegatus*, *Philodendron xanadu*, *Nematanthus glabra* and *Spathiphyllum wallisii* proved particularly effective in accumulating PM and should be a first choice in high PM pollution environments (Paull et al., 2020).

Honey and pollen showed PM contamination, supporting the possibility for nanosized PM to enter the bee food chain (Chapter 3). Based on the knowledge that insecticides have an effect on navigation and orientation, olfaction and gustation, learning and memory, and behaviour and thermoregulation (Belzunces, Tchamitchian & Brunet, 2012), it is possible that also contamination of airborne PM through contact and ingestion can have an effect on the bee health. Therefore, in this study, the sub-lethal effects of oral exposure of pollutant PM were tested on adult bees (Chapter 4). We selected Titanium dioxide (TiO_2) PM_1 which is commonly used as a filler and whitening agent in a range of manufactured objects. Importantly, TiO_2 as ultrapure PM_1 is a common food additive, even if it has been classified by the International Agency for Research on Cancer (IARC) as a possible human carcinogen in Group 2B. First, we characterized the PM chemically, morphologically and by size using SEM-EDX. Second, we fed adult bees with acute and chronical doses under controlled conditions. Finally, we applied microscopical and molecular analyses to assess the effects of the dosage. Our results showed for the first time a modulation of the honey bees gut microbiome induced by both acute and chronic exposure to TiO_2 PM_1, with stronger effects in the latter case. Although no increase in mortality was observed among all treated bees, we recorded a reduction in the total number of bacterial species, and a general decrease in the relative percentages of beneficial species (e.g., lactobacilli). Airborne particulate can represent a further risk factor for the bee health in addition to other chemical stressors previously studied.

The analytical framework developed in this thesis could be applied to frequent airborne PM contaminants other than TiO_2. It would be particularly interesting to test, for example,

baryte, Fe-oxides/hydroxides and silicon dioxide that are potentially ubiquitous in the environment, although usually overlooked in environmental policy discussions. Secondary effects of ultrafine particles possibly compromising the role of bees in regulating and provisioning ecosystem services (as demonstrated for TiO_2), should also be investigated.

Bibliography

Abou-Shaara HF. 2014. The foraging behaviour of honey bees, *Apis mellifera*: A review. *Veterinarni Medicina* 59:1–10. DOI: 10.17221/7240-VETMED.

Adamiec E, Jarosz-Krzemińska E, Wieszała R. 2016. Heavy metals from non-exhaust vehicle emissions in urban and motorway road dusts. *Environmental Monitoring and Assessment* 188:1–11. DOI: 10.1007/s10661-016-5377-1.

Alam Q, Schollbach K, van Hoek C, van der Laan S, de Wolf T, Brouwers HJH. 2019. In-depth mineralogical quantification of MSWI bottom ash phases and their association with potentially toxic elements. *Waste Management* 87:1–12. DOI: 10.1016/j.wasman.2019.01.031.

Arai Y, Sparks DL. 2007. Phosphate Reaction Dynamics in Soils and Soil Components: A Multiscale Approach. In: 135–179. DOI: 10.1016/S0065-2113(06)94003-6.

Auguste M, Balbi T, Montagna M, Fabbri R, Sendra M, Blasco J, Canesi L. 2019. In vivo immunomodulatory and antioxidant properties of nanoceria (nCeO2) in the marine mussel *Mytilus galloprovincialis*. *Comparative Biochemistry and Physiology Part C: Toxicology & Pharmacology* 219:95–102. DOI: 10.1016/j.cbpc.2019.02.006.

Baan RA. 2007. Carcinogenic Hazards from Inhaled Carbon Black, Titanium Dioxide, and Talc not Containing Asbestos or Asbestiform Fibers: Recent Evaluations by an IARC Monographs Working Group. *Inhalation Toxicology* 19:213–228. DOI: 10.1080/08958370701497903.

Bargańska Ż, Ślebioda M, Namieśnik J. 2016. Honey bees and their products: Bioindicators of environmental contamination. *Critical Reviews in Environmental Science and Technology* 46:235–248. DOI: 10.1080/10643389.2015.1078220.

Barmo C, Ciacci C, Canonico B, Fabbri R, Cortese K, Balbi T, Marcomini A, Pojana G, Gallo G, Canesi L. 2013. In vivo effects of n-TiO_2 on digestive gland and immune function of the marine bivalve *Mytilus galloprovincialis*. *Aquatic Toxicology* 132–133:9–18. DOI: 10.1016/j.aquatox.2013.01.014.

Baysal A, Saygin H, Ustabasi GS. 2018. Interaction of $PM_{2.5}$ airborne particulates with ZnO and TiO_2 nanoparticles and their effect on bacteria. *Environmental Monitoring and Assessment* 190:34. DOI: 10.1007/s10661-017-6408-2.

Belzunces LP, Tchamitchian S, Brunet JL. 2012. Neural effects of insecticides in the honey bee. *Apidologie* 43:348–370. DOI: 10.1007/s13592-012-0134-0.

Bencsik A, Lestaevel P, Guseva Canu I. 2018. Nano- and neurotoxicology: An emerging discipline. *Progress in Neurobiology* 160:45–63. DOI: 10.1016/j.pneurobio.2017.10.003.

Berg WK, Cunningham SM, Brouder SM, Joern BC, Johnson KD, Santini J, Volenec JJ. 2005. Influence of Phosphorus and Potassium on Alfalfa Yield and Yield Components. *Crop Science* 45:cropsci2005.0297. DOI: 10.2135/cropsci2005.0297.

Berry D, Ben Mahfoudh K, Wagner M, Loy A. 2011. Barcoded Primers Used in Multiplex Amplicon Pyrosequencing Bias Amplification. *Applied and Environmental Microbiology* 77:7846–7849. DOI: 10.1128/AEM.05220-11.

Bettini S, Boutet-Robinet E, Cartier C, Coméra C, Gaultier E, Dupuy J, Naud N, Taché S, Grysan P, Reguer S, Thieriet N, Réfrégiers M, Thiaudière D, Cravedi JP, Carrière M, Audinot JN, Pierre FH, Guzylack-Piriou L, Houdeau E. 2017. Food-grade TiO_2 impairs intestinal and systemic immune homeostasis, initiates preneoplastic lesions and promotes aberrant crypt development in the rat colon. *Scientific Reports* 7:1–13. DOI: 10.1038/srep40373.

Bommuraj V, Chen Y, Klein H, Sperling R, Barel S, Shimshoni JA. 2019. Pesticide and trace

element residues in honey and beeswax combs from Israel in association with human risk assessment and honey adulteration. *Food Chemistry* 299:125123. DOI: 10.1016/j.foodchem.2019.125123.

Bomphrey RJ, Lawson NJ, Taylor GK, Thomas ALR. 2006. Application of digital particle image velocimetry to insect aerodynamics: measurement of the leading-edge vortex and near wake of a Hawkmoth. *Experiments in Fluids* 40:546–554. DOI: 10.1007/s00348-005-0094-5.

Bomphrey RJ, Taylor GK, Thomas ALR. 2009. Smoke visualization of free-flying bumblebees indicates independent leading-edge vortices on each wing pair. *Experiments in Fluids* 46:811–821. DOI: 10.1007/s00348-009-0631-8.

Bonmatin J-M, Giorio C, Girolami V, Goulson D, Kreutzweiser DP, Krupke C, Liess M, Long E, Marzaro M, Mitchell EAD, Noome DA, Simon-Delso N, Tapparo A. 2015. Environmental fate and exposure; neonicotinoids and fipronil. *Environmental Science and Pollution Research* 22:35–67. DOI: 10.1007/s11356-014-3332-7.

Bortolotti L, Marcazzan GL. 2017. *I prodotti dell'alveare*. Edagricole.

Bottacini F, Milani C, Turroni F, Sánchez B, Foroni E, Duranti S, Serafini F, Viappiani A, Strati F, Ferrarini A, Delledonne M, Henrissat B, Coutinho P, Fitzgerald GF, Margolles A, van Sinderen D, Ventura M. 2012. *Bifidobacterium asteroides* PRL2011 Genome Analysis Reveals Clues for Colonization of the Insect Gut. *PLoS ONE* 7:e44229. DOI: 10.1371/journal.pone.0044229.

Brodschneider R, Gray A, van der Zee R, Adjlane N, Brusbardis V, Charrière J-D, Chlebo R, Coffey MF, Crailsheim K, Dahle B, Danihlík J, Danneels E, de Graaf DC, Dražić MM, Fedoriak M, Forsythe I, Golubovski M, Gregorc A, Grzęda U, Hubbuck I, İvgin Tunca R, Kauko L, Kilpinen O, Kretavicius J, Kristiansen P, Martikkala M, Martín-Hernández R,

Mutinelli F, Peterson M, Otten C, Ozkirim A, Raudmets A, Simon-Delso N, Soroker V, Topolska G, Vallon J, Vejsnæs F, Woehl S. 2016. Preliminary analysis of loss rates of honey bee colonies during winter 2015/16 from the COLOSS survey. *Journal of Apicultural Research* 55:375–378. DOI: 10.1080/00218839.2016.1260240.

Bromenshenk JJ, Carlson SR, Simpson JC, Thomas JM. 1985. Pollution Monitoring of Puget Sound with Honey Bees. *Science* 227:632–634. DOI: 10.1126/science.227.4687.632.

Brook RD, Rajagopalan S, Pope CA, Brook JR, Bhatnagar A, Diez-Roux A V., Holguin F, Hong Y, Luepker R V., Mittleman MA, Peters A, Siscovick D, Smith SC, Whitsel L, Kaufman JD. 2010. Particulate matter air pollution and cardiovascular disease: An update to the scientific statement from the american heart association. *Circulation* 121:2331–2378. DOI: 10.1161/CIR.0b013e3181dbece1.

Brown JS, Gordon T, Price O, Asgharian B. 2013. Thoracic and respirable particle definitions for human health risk assessment. *Particle and Fibre Toxicology* 10:12. DOI: 10.1186/1743-8977-10-12.

Calabrese L, Ceriani A. 2009. *Note illustrative della carta geologica d'Italia alla scala 1 :50.000 : Foglio 181 : Parma Nord*. Firenze.

Carreck NL, Andree M, Brent CS, Cox-Foster D, Dade HA, Ellis JD, Hatjina F, van Englesdorp D. 2013. Standard methods for *Apis mellifera* anatomy and dissection. *Journal of Apicultural Research* 52:1–40. DOI: 10.3896/IBRA.1.52.4.03.

Carrero JA, Arana G, Madariaga JM. 2014. Chapter 6. Use of Raman spectroscopy and scanning electron microscopy for the detection and analysis of road transport pollution. In: *Spectroscopic Properties of Inorganic and Organometallic Compounds*. 178–210. DOI: 10.1039/9781782621485-00178.

Chakravarthy AK. 2012. DNA-tagged nano gold: A new tool for the control of the armyworm,

Spodoptera litura Fab. (Lepidoptera: Noctuidae). *African Journal of Biotechnology* 11. DOI: 10.5897/AJB11.883.

Chan QWT, Howes CG, Foster LJ. 2006. Quantitative Comparison of Caste Differences in Honeybee Hemolymph. *Molecular & Cellular Proteomics* 5:2252–2262. DOI: 10.1074/mcp.M600197-MCP200.

Chemistry N, Tonelli D, Gattavecchia E, Ghini S, Porrini C, Celli G, Botanico I. 1990. Honey bees and their products as indicators of environmental radioactive pollution A network of about 200 bee hives located far from the towns in different regions. 141.

Chen Z, Han S, Zhou D, Zhou S, Jia G. 2019. Effects of oral exposure to titanium dioxide nanoparticles on gut microbiota and gut-associated metabolism: In vivo. *Nanoscale* 11:22398–22412. DOI: 10.1039/c9nr07580a.

Christmann S. 2020. Pollinator protection strategies must be feasible for all nations. *Nature Ecology and Evolution* 4:896–897. DOI: 10.1038/s41559-020-1210-x.

Connell JH. 1978. Diversity in Tropical Rain Forests and Coral Reefs. *Science* 199:1302–1310. DOI: 10.1126/science.199.4335.1302.

Contessi A. 2009. *Le api: biologia, allevamento, prodotti*. Edagricole.

Corby-Harris V, Maes P, Anderson KE. 2014. The bacterial communities associated with honey bee (*Apis mellifera*) foragers. *PLoS ONE* 9. DOI: 10.1371/journal.pone.0095056.

Corsi I, Cherr GN, Lenihan HS, Labille J, Hassellov M, Canesi L, Dondero F, Frenzilli G, Hristozov D, Puntes V, Della Torre C, Pinsino A, Libralato G, Marcomini A, Sabbioni E, Matranga V. 2014. Common Strategies and Technologies for the Ecosafety Assessment and Design of Nanomaterials Entering the Marine Environment. *ACS Nano* 8:9694–9709. DOI: 10.1021/nn504684k.

Crotti E, Rizzi A, Chouaia B, Ricci I, Favia G, Alma A, Sacchi L, Bourtzis K, Mandrioli M, Cherif A, Bandi C, Daffonchio D. 2010. Acetic Acid Bacteria, Newly Emerging Symbionts of Insects. *Applied and Environmental Microbiology* 76:6963–6970. DOI: 10.1128/AEM.01336-10.

Dabour K, Al Naggar Y, Masry S, Naiem E, Giesy JP. 2019. Cellular alterations in midgut cells of honey bee workers (*Apis millefera* L.) exposed to sublethal concentrations of CdO or PbO nanoparticles or their binary mixture. *Science of the Total Environment* 651:1356–1367. DOI: 10.1016/j.scitotenv.2018.09.311.

Daily GC. 1997. *Nature's services: Societal dependence on natural ecosystems. Island Press, Washington, DC. 392 pp. ISBN 1-55963-475-8 (hbk), 1 55963 476 6 (soft cover).* Washington, DC: Island Press.

Dainat B, VanEngelsdorp D, Neumann P. 2012. Colony collapse disorder in Europe. *Environmental Microbiology Reports* 4:123–125. DOI: 10.1111/j.1758-2229.2011.00312.x.

Daisley BA, Pitek AP, Chmiel JA, Al KF, Chernyshova AM, Faragalla KM, Burton JP, Thompson GJ, Reid G. 2020. Novel probiotic approach to counter *Paenibacillus larvae* infection in honey bees. *The ISME Journal* 14:476–491. DOI: 10.1038/s41396-019-0541-6.

Dashtipour K, Liu M, Kani C, Dalaie P, Obenaus A, Simmons D, Gatto NM, Zarifi M. 2015. Iron accumulation is not homogenous among patients with Parkinson's disease. *Parkinson's Disease* 2015. DOI: 10.1155/2015/324843.

DeSantis TZ, Hugenholtz P, Keller K, Brodie EL, Larsen N, Piceno YM, Phan R, Andersen GL. 2006. NAST: a multiple sequence alignment server for comparative analysis of 16S rRNA genes. *Nucleic Acids Research* 34:W394–W399. DOI: 10.1093/nar/gkl244.

Devillers J, Pham-Delegue M-H. 2002. *Honey Bees: Estimating the Environmental Impact of Chemicals*. London: Taylor & Francis.

Donaldson K, Stone V, Clouter A, Renwick L, MacNee W. 2001. Ultrafine particles. *Occupational and Environmental Medicine* 58:211–216. DOI: 10.1136/oem.58.3.211.

Dong Z-X, Li H-Y, Chen Y-F, Wang F, Deng X-Y, Lin L-B, Zhang Q-L, Li J-L, Guo J. 2019. Colonization of the gut microbiota of honey bee (*Apis mellifera*) workers at different developmental stages. *Microbiological Research* 231:126370. DOI: 10.1016/j.micres.2019.126370.

van Doremalen N, Bushmaker T, Morris DH, Holbrook MG, Gamble A, Williamson BN, Tamin A, Harcourt JL, Thornburg NJ, Gerber SI, Lloyd-Smith JO, de Wit E, Munster VJ. 2020. Aerosol and Surface Stability of SARS-CoV-2 as Compared with SARS-CoV-1. *New England Journal of Medicine*:NEJMc2004973. DOI: 10.1056/NEJMc2004973.

Duong BTT, Lien NTK, Thu HT, Hoa NT, Lanh PT, Yun B-R, Yoo M-S, Cho YS, Van Quyen D. 2020. Investigation of the gut microbiome of *Apis cerana* honeybees from Vietnam. *Biotechnology Letters* 42:2309–2317. DOI: 10.1007/s10529-020-02948-4.

Edgar RC, Haas BJ, Clemente JC, Quince C, Knight R. 2011. UCHIME improves sensitivity and speed of chimera detection. *Bioinformatics* 27:2194–2200. DOI: 10.1093/bioinformatics/btr381.

Engel MS. 1999. The Taxonomy of Recent and Fossil Honey Bees (Hymenoptera: Apidae; *Apis*). *Journal of Hymenoptera research.* 8:165–196.

Engel P, Kwong WK, Moran NA. 2013. *Frischella perrara* gen. nov., sp. nov., a gammaproteobacterium isolated from the gut of the honeybee, *Apis mellifera*. *International Journal of Systematic and Evolutionary Microbiology* 63:3646–3651. DOI: 10.1099/ijs.0.049569-0.

Engel P, Martinson VG, Moran NA. 2012. Functional diversity within the simple gut microbiota of the honey bee. *Proceedings of the National Academy of Sciences of the United States of America* 109:11002–11007. DOI: 10.1073/pnas.1202970109.

Falcon T, Pinheiro DG, Ferreira-Caliman MJ, Turatti ICC, Abreu FCP de, Galaschi-Teixeira JS, Martins JR, Elias-Neto M, Soares MPM, Laure MB, Figueiredo VLC, Lopes NP, Simões ZLP, Garófalo CA, Bitondi MMG. 2019. Exploring integument transcriptomes, cuticle ultrastructure, and cuticular hydrocarbons profiles in eusocial and solitary bee species displaying heterochronic adult cuticle maturation. *PLOS ONE* 14:e0213796. DOI: 10.1371/journal.pone.0213796.

Feldhaar H, Otti O. 2020. Pollutants and Their Interaction with Diseases of. *Insects* 11:1–20.

Ferrara G, Salvaggio A, Pecoraro R, Scalisi EM, Presti AM, Impellizzeri G, Brundo MV. 2019. Toxicity assessment of nano-TiO_2 in *Apis mellifera* L., 1758: histological and immunohistochemical assays. *Microscopy Research and Technique* 83:332–337. DOI: 10.1002/jemt.23418.

von Frisch K. 1967. *The dance language and orientation of bees*. Harvard University Press.

Garrido PM, Martin ML, Negri P, Eguaras MJ. 2013. A standardized method to extract and store haemolymph from *Apis mellifera* and the ectoparasite *Varroa destructor* for protein analysis. *Journal of Apicultural Research* 52:67–68. DOI: 10.3896/IBRA.1.52.2.13.

Ghisalberti EL. 1979. Propolis: A Review. *Bee World* 60:59–84. DOI: 10.1080/0005772X.1979.11097738.

Gietl JK, Lawrence R, Thorpe AJ, Harrison RM. 2010. Identification of brake wear particles and derivation of a quantitative tracer for brake dust at a major road. *Atmospheric Environment* 44:141–146. DOI: 10.1016/j.atmosenv.2009.10.016.

Giglio A, Ammendola A, Battistella S, Naccarato A, Pallavicini A, Simeon E, Tagarelli A, Giulianini PG. 2017. *Apis mellifera ligustica*, Spinola 1806 as bioindicator for detecting environmental contamination: a preliminary study of heavy metal pollution in Trieste, Italy. *Environmental Science and Pollution Research* 24:659–665. DOI: 10.1007/s11356-016-7862-z.

Gonet T, Maher BA. 2019. Airborne, Vehicle-Derived Fe-Bearing Nanoparticles in the Urban Environment: A Review. *Environmental Science and Technology* 53:9970–9991. DOI: 10.1021/acs.est.9b01505.

Goretti E, Pallottini M, Rossi R, La Porta G, Gardi T, Cenci Goga BT, Elia AC, Galletti M, Moroni B, Petroselli C, Selvaggi R, Cappelletti D. 2020. Heavy metal bioaccumulation in honey bee matrix, an indicator to assess the contamination level in terrestrial environments. *Environmental Pollution* 256:113388. DOI: 10.1016/j.envpol.2019.113388.

Gowariker V, Krishnamurthy VN, Gowariker S, Dhanorkar M, Paranjape K. 2008. *The Fertilizer Encyclopedia*. Hoboken, NJ, USA: John Wiley & Sons, Inc. DOI: 10.1002/9780470431771.

Hagler JR, Mueller S, Teuber LR, Machtley SA, Van Deynze A. 2011. Foraging Range of Honey Bees, *Apis mellifera* , in Alfalfa Seed Production Fields. *Journal of Insect Science* 11:1–12. DOI: 10.1673/031.011.14401.

Harrison RM. 2020. Airborne particulate matter. *Philosophical Transactions of the Royal Society A: Mathematical, Physical and Engineering Sciences* 378:20190319. DOI: 10.1098/rsta.2019.0319.

Harrison RM, Shi JP, Xi S, Khan A, Mark D, Kinnersley R, Yin J. 2000. Measurement of number, mass and size distribution of particles in the atmosphere. *Philosophical Transactions of the Royal Society A: Mathematical, Physical and Engineering Sciences*

358:2567–2580. DOI: 10.1098/rsta.2000.0669.

Hroncova Z, Havlik J, Killer J, Doskocil I, Tyl J, Kamler M, Titera D, Hakl J, Mrazek J, Bunesova V, Rada V. 2015. Variation in honey bee gut microbial diversity affected by ontogenetic stage, age and geographic location. *PLoS ONE* 10:1–17. DOI: 10.1371/journal.pone.0118707.

Hubert J, Erban T, Kamler M, Kopecky J, Nesvorna M, Hejdankova S, Titera D, Tyl J, Zurek L. 2015. Bacteria detected in the honeybee parasitic mite *Varroa destructor* collected from beehive winter debris. *Journal of Applied Microbiology* 119:640–654. DOI: 10.1111/jam.12899.

Hughes JM, Rakovan J. 2002. The Crystal Structure of Apatite, $Ca_5(PO_4)_3(F,OH,Cl)$. *Reviews in Mineralogy and Geochemistry* 48:1–12. DOI: 10.2138/rmg.2002.48.1.

Hyrsl P, Dobes P, Vojtek L, Hroncova Z, Tyl J, Killer J. 2017. Plant alkaloid sanguinarine and novel potential probiotic strains *Lactobacillus apis*, *Lactobacillus melliventris* and *Gilliamella apicola* promote resistance of honey bees to nematobacterial infection. *Bulletin of Insectology* 70:31–38.

Jan R, Roy R, Bhor R, Pai K, Satsangi PG. 2019. Toxicological screening of airborne particulate matter in atmosphere of Pune: Reactive oxygen species and cellular toxicity. *Environmental Pollution* 261:113724. DOI: 10.1016/j.envpol.2019.113724.

Juda-Rezler K, Reizer M, Oudinet J-P. 2011. Determination and analysis of PM_{10} source apportionment during episodes of air pollution in Central Eastern European urban areas: The case of wintertime 2006. *Atmospheric Environment* 45:6557–6566. DOI: 10.1016/j.atmosenv.2011.08.020.

Kelly FJ, Fussell JC. 2012. Size, source and chemical composition as determinants of toxicity attributable to ambient particulate matter. *Atmospheric Environment* 60:504–526. DOI:

10.1016/j.atmosenv.2012.06.039.

Kešnerová L, Emery O, Troilo M, Liberti J, Erkosar B, Engel P. 2020. Gut microbiota structure differs between honeybees in winter and summer. *The ISME Journal* 14:801–814. DOI: 10.1038/s41396-019-0568-8.

Kešnerová L, Moritz R, Engel P. 2016. *Bartonella apis* sp. nov., a honey bee gut symbiont of the class Alphaproteobacteria. *International Journal of Systematic and Evolutionary Microbiology* 66:414–421. DOI: 10.1099/ijsem.0.000736.

Kim KH, Kabir E, Kabir S. 2015. A review on the human health impact of airborne particulate matter. *Environment International* 74:136–143. DOI: 10.1016/j.envint.2014.10.005.

Klein C, Philpotts A. 2016. *Earth Materials: Introduction to Mineralogy and Petrology*.

Klein AM, Vaissière BE, Cane JH, Steffan-Dewenter I, Cunningham SA, Kremen C, Tscharntke T. 2007. Importance of pollinators in changing landscapes for world crops. *Proceedings of the Royal Society B: Biological Sciences* 274:303–313. DOI: 10.1098/rspb.2006.3721.

Kremen C, Williams NM, Aizen MA, Gemmill-Herren B, LeBuhn G, Minckley R, Packer L, Potts SG, Roulston T, Steffan-Dewenter I, Vázquez DP, Winfree R, Adams L, Crone EE, Greenleaf SS, Keitt TH, Klein AM, Regetz J, Ricketts TH. 2007. Pollination and other ecosystem services produced by mobile organisms: A conceptual framework for the effects of land-use change. *Ecology Letters* 10:299–314. DOI: 10.1111/j.1461-0248.2007.01018.x.

Kukutschová J, Moravec P, Tomášek V, Matějka V, Smolík J, Schwarz J, Seidlerová J, Šafářová K, Filip P. 2011. On airborne nano/micro-sized wear particles released from low-metallic automotive brakes. *Environmental Pollution* 159:998–1006. DOI: 10.1016/j.envpol.2010.11.036.

Kurth LM, McCawley M, Hendryx M, Lusk S. 2014. Atmospheric particulate matter size distribution and concentration in West Virginia coal mining and non-mining areas. *Journal of Exposure Science & Environmental Epidemiology* 24:405–411. DOI: 10.1038/jes.2014.2.

Kutchko BG, Kim AG. 2006. Fly ash characterization by SEM – EDS. 85:2537–2544. DOI: 10.1016/j.fuel.2006.05.016.

Kwong WK, Moran NA. 2013. Cultivation and characterization of the gut symbionts of honey bees and bumble bees: Description of *Snodgrassella alvi* gen. nov., sp. nov., a member of the family Neisseriaceae of the betaproteobacteria, and *Gilliamella apicola* gen. nov., sp. nov., a memb. *International Journal of Systematic and Evolutionary Microbiology* 63:2008–2018. DOI: 10.1099/ijs.0.044875-0.

Kwong WK, Moran NA. 2016. Gut microbial communities of social bees. *Nature Reviews Microbiology* 14:374–384. DOI: 10.1038/nrmicro.2016.43.

Labrada-Delgado G, Aragon-Pina A, Campos-Ramos A, Castro-Romero T, Amador-Munoz O, Villalobos-Pietrini R. 2012. Chemical and morphological characterization of $PM_{2.5}$ collected during MILAGRO campaign using scanning electron microscopy. *Atmospheric Pollution Research* 3:289–300. DOI: 10.5094/APR.2012.032.

Lamas B, Martins Breyner N, Houdeau E. 2020. Impacts of foodborne inorganic nanoparticles on the gut microbiota-immune axis: potential consequences for host health. *Particle and Fibre Toxicology* 17:19. DOI: 10.1186/s12989-020-00349-z.

Lamei S, Stephan JG, Nilson B, Sieuwerts S, Riesbeck K, de Miranda JR, Forsgren E. 2020. Feeding Honeybee Colonies with Honeybee-Specific Lactic Acid Bacteria (Hbs-LAB) Does Not Affect Colony-Level Hbs-LAB Composition or *Paenibacillus larvae* Spore Levels, Although American Foulbrood Affected Colonies Harbor a More Diverse Hbs-

LAB Community. *Microbial Ecology* 79:743–755. DOI: 10.1007/s00248-019-01434-3.

Lamei S, Stephan JG, Riesbeck K, Vasquez A, Olofsson T, Nilson B, de Miranda JR, Forsgren E. 2019. The secretome of honey bee-specific lactic acid bacteria inhibits *Paenibacillus larvae* growth. *Journal of Apicultural Research* 58:405–412. DOI: 10.1080/00218839.2019.1572096.

Lanphear BP. 2017. Low-level toxicity of chemicals: No acceptable levels? *PLoS Biology* 15:1–8. DOI: 10.1371/journal.pbio.2003066.

Leita L, Muhlbachova G, Cesco S, Barbattini R, Mondini C. 1996. Investigation of the use of honey bees and honey bee products to assess heavy metals contamination. *Environmental Monitoring and Assessment* 43:1–9. DOI: 10.1007/BF00399566.

Liati A, Schreiber D, Arroyo Rojas Dasilva Y, Dimopoulos Eggenschwiler P. 2018. Ultrafine particle emissions from modern Gasoline and Diesel vehicles: An electron microscopic perspective. *Environmental Pollution* 239:661–669. DOI: 10.1016/j.envpol.2018.04.081.

Liati A, Schreiber D, Lugovyy D, Gramstat S, Dimopoulos Eggenschwiler P. 2019. Airborne particulate matter emissions from vehicle brakes in micro- and nano-scales: Morphology and chemistry by electron microscopy. *Atmospheric Environment* 212:281–289. DOI: 10.1016/j.atmosenv.2019.05.037.

Liu YJ, Qiao NH, Diao QY, Jing Z, Vukanti R, Dai PL, Ge Y. 2020. Thiacloprid exposure perturbs the gut microbiota and reduces the survival status in honeybees. *Journal of Hazardous Materials* 389:121818. DOI: 10.1016/j.jhazmat.2019.121818.

Ma Y, Ning JG, Ren HL, Zhang PF, Zhao HY. 2015. The function of resilin in honeybee wings. *Journal of Experimental Biology* 218:2136–2142. DOI: 10.1242/jeb.117325.

Mackensen O. 1951. Viability and sex determination in the honey bee (*Apis mellifera* L.).

Genetics 36:500–509.

Maher BA, Ahmed IAM, Karloukovski V, MacLaren DA, Foulds PG, Allsop D, Mann DMA, Torres-Jardón R, Calderon-Garciduenas L. 2016. Magnetite pollution nanoparticles in the human brain. *Proceedings of the National Academy of Sciences* 113:10797–10801. DOI: 10.1073/pnas.1605941113.

Manisalidis I, Stavropoulou E, Stavropoulos A, Bezirtzoglou E. 2020. Environmental and Health Impacts of Air Pollution: A Review. *Frontiers in Public Health* 8:1–13. DOI: 10.3389/fpubh.2020.00014.

Marcazzan GM, Vaccaro S, Valli G, Vecchi R. 2001. Characterisation of PM_{10} and $PM_{2.5}$ particulate matter in the ambient air of Milan (Italy). *Atmospheric Environment* 35:4639–4650. DOI: 10.1016/S1352-2310(01)00124-8.

Markert BA, Breure AM, Zechmeister HG. 2003. *Bioindicators and Biomonitors*. Elsevier.

Mårtensson A, Greiff L, Lamei SS, Lindstedt M, Olofsson TC, Vasquez A, Cervin A. 2016. Effects of a honeybee lactic acid bacterial microbiome on human nasal symptoms, commensals, and biomarkers. *International Forum of Allergy & Rhinology* 6:956–963. DOI: 10.1002/alr.21762.

Martinson VG, Danforth BN, Minckley RL, Rueppell O, Tingek S, Moran NA. 2011. A simple and distinctive microbiota associated with honey bees and bumble bees. *Molecular Ecology* 20:619–628. DOI: 10.1111/j.1365-294X.2010.04959.x.

Masella AP, Bartram AK, Truszkowski JM, Brown DG, Neufeld JD. 2012. PANDAseq: paired-end assembler for illumina sequences. *BMC Bioinformatics* 13:31. DOI: 10.1186/1471-2105-13-31.

McDonald D, Price MN, Goodrich J, Nawrocki EP, DeSantis TZ, Probst A, Andersen GL,

Knight R, Hugenholtz P. 2012. An improved Greengenes taxonomy with explicit ranks for ecological and evolutionary analyses of bacteria and archaea. *The ISME Journal* 6:610–618. DOI: 10.1038/ismej.2011.139.

Menapace C, Leonardi M, Matějka V, Gialanella S, Straffelini G. 2018. Dry sliding behavior and friction layer formation in copper-free barite containing friction materials. *Wear* 398–399:191–200. DOI: 10.1016/j.wear.2017.12.008.

Micas AFD, Ferreira GA, Laure HJ, Rosa JC, Bitondi MMG. 2016. Proteins of the integumentary system of the honeybee, *Apis mellifera*. *Archives of Insect Biochemistry and Physiology* 93:3–24. DOI: 10.1002/arch.21336.

Michener CD. 2007. *The bees of the world*. The Johns Hopkins University Press.

Mikulecky M, Bounias M. 1997. Worker honeybee hemolymph lipid composition and synodic lunar cycle periodicities. *Brazilian Journal of Medical and Biological Research* 30:275–279. DOI: 10.1590/S0100-879X1997000200018.

Millennium Ecosystem Assessment. 2005. *Ecosystems and Human Well-being: Synthesis.* Washington, Dc: Island Press/Center for Resource Economics.

Moore RC, Sanchez C, Holt K, Zhang P, Xu H, Choppin GR. 2004. Formation of hydroxyapatite in soils using calcium citrate and sodium phosphate for control of strontium migration. *Radiochimica Acta* 92. DOI: 10.1524/ract.92.9.719.55000.

Moran NA, Hansen AK, Powell JE, Sabree ZL. 2012. Distinctive gut microbiota of honey bees assessed using deep sampling from individual worker bees. *PLoS ONE* 7:1–10. DOI: 10.1371/journal.pone.0036393.

Motta EVS, Mak M, De Jong TK, Powell JE, O'Donnell A, Suhr KJ, Riddington IM, Moran NA. 2020. Oral or topical exposure to glyphosate in herbicide formulation impacts the gut

microbiota and survival rates of honey bees. *Applied and Environmental Microbiology* 86:1–21. DOI: 10.1128/AEM.01150-20.

AL Naggar Y, Dabour K, Masry S, Sadek A, Naiem E, Giesy JP. 2020. Sublethal effects of chronic exposure to CdO or PbO nanoparticles or their binary mixture on the honey bee (*Apis millefera* L.). *Environmental Science and Pollution Research* 27:19004–19015. DOI: 10.1007/s11356-018-3314-2.

Negri I, Mavris C, Di Prisco G, Caprio E, Pellecchia M. 2015. Honey bees (*Apis mellifera*, L.) as active samplers of airborne particulate matter. *PLoS ONE* 10:1–22. DOI: 10.1371/journal.pone.0132491.

Neis PD, Ferreira NF, Fekete G, Matozo LT, Masotti D. 2017. Towards a better understanding of the structures existing on the surface of brake pads. *Tribology International* 105:135–147. DOI: 10.1016/j.triboint.2016.09.033.

Nicolson SW, Nepi M, Pacini E. 2007. *Nectaries and Nectar*. Dordrecht: Springer Netherlands. DOI: 10.1007/978-1-4020-5937-7.

Von Der Ohe W, Persano Oddo L, Piana ML, Morlot M, Martin P. 2004. Harmonized methods of melissopalynology. *Apidologie* 35:S18–S25. DOI: 10.1051/apido:2004050.

Olofsson TC, Alsterfjord M, Nilson B, Butler È, Vásquez A. 2014. *Lactobacillus apinorum* sp. nov., *Lactobacillus mellifer* sp. nov., *Lactobacillus mellis* sp. nov., *Lactobacillus melliventris* sp. nov., *Lactobacillus kimbladii* sp. nov., *Lactobacillus helsingborgensis* sp. nov. and *Lactobacillus kullabergensis* sp. nov., isol. *International Journal of Systematic and Evolutionary Microbiology* 64:3109–3119. DOI: 10.1099/ijs.0.059600-0.

Omode PE, Ademukola SA. 2008. Determination of trace metals in southern Nigerian honey by use of atomic absorption spectroscopy. *Spectroscopy Letters* 41:328–331. DOI: 10.1080/00387010802371239.

Österle W, Griepentrog M, Gross T, Urban I. 2001. Chemical and microstructural changes induced by friction and wear of brakes. *Wear* 251:1469–1476. DOI: 10.1016/S0043-1648(01)00785-2.

Özkan Y, Irende İ, Akdeniz G, Kabakçi D, Münevver S. 2014. Evaluation of the Comparative Acute Toxic Effects of TiO_2, Ag-TiO_2 and ZnO-TiO_2 Composite Nanoparticles on Honey Bee (*Apis mellifera*). *J. Int. Environmental Application & Science* 10:26–36.

Papa G, Capitani G, Capri E, Pellecchia M, Negri I. 2020. Vehicle-derived ultrafine particulate contaminating bees and bee products. *Science of The Total Environment*:141700. DOI: 10.1016/j.scitotenv.2020.141700.

Parmar TK, Rawtani D, Agrawal YK. 2016. Bioindicators: the natural indicator of environmental pollution. *Frontiers in Life Science* 9:110–118. DOI: 10.1080/21553769.2016.1162753.

Paull NJ, Krix D, Irga PJ, Torpy FR. 2020. Airborne particulate matter accumulation on common green wall plants. *International Journal of Phytoremediation* 22:594–606. DOI: 10.1080/15226514.2019.1696744.

Pellecchia M, Negri I. 2018. Particulate matter collection by honey bees (*Apis mellifera*, L.) near to a cement factory in Italy. *PeerJ* 2018:1–21. DOI: 10.7717/peerj.5322.

Persano Oddo L, Piazza MG, Pulcini P. 1999. Invertase activity in honey. *Apidologie* 30:57–65. DOI: 10.1051/apido:19990107.

Perugini M, Manera M, Grotta L, Abete MC, Tarasco R, Amorena M. 2011. Heavy Metal (Hg, Cr, Cd, and Pb) Contamination in Urban Areas and Wildlife Reserves: Honeybees as Bioindicators. *Biological Trace Element Research* 140:170–176. DOI: 10.1007/s12011-010-8688-z.

Pietrogrande MC, Bacco D, Ferrari S, Ricciardelli I, Scotto F, Trentini A, Visentin M. 2016. Characteristics and major sources of carbonaceous aerosols in $PM_{2.5}$ in Emilia Romagna Region (Northern Italy) from four-year observations. *Science of the Total Environment* 553:172–183. DOI: 10.1016/j.scitotenv.2016.02.074.

Pirovano G, Colombi C, Balzarini A, Riva GM, Gianelle V, Lonati G. 2015. $PM_{2.5}$ source apportionment in Lombardy (Italy): Comparison of receptor and chemistry-transport modelling results. *Atmospheric Environment* 106:56–70. DOI: 10.1016/j.atmosenv.2015.01.073.

Połka J, Rebecchi A, Pisacane V, Morelli L, Puglisi E. 2015. Bacterial diversity in typical Italian salami at different ripening stages as revealed by high-throughput sequencing of 16S rRNA amplicons. *Food Microbiology* 46:342–356. DOI: 10.1016/j.fm.2014.08.023.

Powell JE, Martinson VG, Urban-Mead K, Moran NA. 2014. Routes of acquisition of the gut microbiota of the honey bee *Apis mellifera*. *Applied and Environmental Microbiology* 80:7378–7387. DOI: 10.1128/AEM.01861-14.

Pozzer A, Bacer S, Sappadina SDZ, Predicatori F, Caleffi A. 2019. Long-term concentrations of fine particulate matter and impact on human health in Verona, Italy. *Atmospheric Pollution Research* 10:731–738. DOI: 10.1016/j.apr.2018.11.012.

Pruesse E, Quast C, Knittel K, Fuchs BM, Ludwig W, Peplies J, Glockner FO. 2007. SILVA: a comprehensive online resource for quality checked and aligned ribosomal RNA sequence data compatible with ARB. *Nucleic Acids Research* 35:7188–7196. DOI: 10.1093/nar/gkm864.

Rader R, Bartomeus I, Garibaldi LA, Garratt MPD, Howlett BG, Winfree R, Cunningham SA, Mayfield MM, Arthur AD, Andersson GKS, Bommarco R, Brittain C, Carvalheiro LG, Chacoff NP, Entling MH, Foully B, Freitas BM, Gemmill-Herren B, Ghazoul J, Griffin

SR, Gross CL, Herbertsson L, Herzog F, Hipólito J, Jaggar S, Jauker F, Klein AM, Kleijn D, Krishnan S, Lemos CQ, Lindström SAM, Mandelik Y, Monteiro VM, Nelson W, Nilsson L, Pattemore DE, Pereira NDO, Pisanty G, Potts SG, Reemer M, Rundlöf M, Sheffield CS, Scheper J, Schüepp C, Smith HG, Stanley DA, Stout JC, Szentgyörgyi H, Taki H, Vergara CH, Viana BF, Woyciechowski M. 2016. Non-bee insects are important contributors to global crop pollination. *Proceedings of the National Academy of Sciences of the United States of America* 113:146–151. DOI: 10.1073/pnas.1517092112.

Ravoet J, Reybroeck W, de Graaf DC. 2015. Pesticides for Apicultural and/or Agricultural Application Found in Belgian Honey Bee Wax Combs. *Bulletin of Environmental Contamination and Toxicology* 94:543–548. DOI: 10.1007/s00128-015-1511-y.

Raymann K, Moran NA. 2018. The role of the gut microbiome in health and disease of adult honey bee workers. *Current Opinion in Insect Science* 26:97–104. DOI: 10.1016/j.cois.2018.02.012.

Raymann K, Shaffer Z, Moran NA. 2017. Antibiotic exposure perturbs the gut microbiota and elevates mortality in honeybees. *PLoS Biology* 15:1–22. DOI: 10.1371/journal.pbio.2001861.

Ribeiro R de OR, Márwhile ET, de Jesus EFO, da Silva Carneiro C, Júnior CAC, de Almeida E, Filho VF do N. 2014. Determination of Trace Elements in Honey from Different Regions in Rio de Janeiro State (Brazil) by Total Reflection X-ray Fluorescence. *Journal of Food Science* 79. DOI: 10.1111/1750-3841.12363.

Rothman JA, Leger L, Kirkwood JS, McFrederick QS. 2019. Cadmium and Selenate Exposure Affects the Honey Bee Microbiome and Metabolome, and Bee-Associated Bacteria Show Potential for Bioaccumulation. *Applied and Environmental Microbiology* 85:1–18. DOI: 10.1128/AEM.01411-19.

Rühlmann J, Körschens M, Graefe J. 2006. A new approach to calculate the particle density of soils considering properties of the soil organic matter and the mineral matrix. *Geoderma* 130:272–283. DOI: 10.1016/j.geoderma.2005.01.024.

Ruttner F. 1988. *Biogeography and Taxonomy of Honeybees*. Berlin, Heidelberg: Springer Berlin Heidelberg. DOI: 10.1007/978-3-642-72649-1.

Sabree ZL, Hansen AK, Moran NA. 2012. Independent studies using deep sequencing resolve the same set of core bacterial species dominating gut communities of honey bees. *PLoS ONE* 7. DOI: 10.1371/journal.pone.0041250.

Satta A, Verdinelli M, Ruiu L, Buffa F, Salis S, Sassu A, Floris I. 2012. Combination of beehive matrices analysis and ant biodiversity to study heavy metal pollution impact in a post-mining area (Sardinia, Italy). *Environmental Science and Pollution Research* 19:3977–3988. DOI: 10.1007/s11356-012-0921-1.

Saunier JB, Losfeld G, Freydier R, Grison C. 2013. Trace elements biomonitoring in a historical mining district (les Malines, France). *Chemosphere* 93:2016–2023. DOI: 10.1016/j.chemosphere.2013.07.024.

Schloss PD. 2010. The Effects of Alignment Quality, Distance Calculation Method, Sequence Filtering, and Region on the Analysis of 16S rRNA Gene-Based Studies. *PLoS Computational Biology* 6:e1000844. DOI: 10.1371/journal.pcbi.1000844.

Schloss PD, Westcott SL, Ryabin T, Hall JR, Hartmann M, Hollister EB, Lesniewski RA, Oakley BB, Parks DH, Robinson CJ, Sahl JW, Stres B, Thallinger GG, Van Horn DJ, Weber CF. 2009. Introducing mothur: Open-Source, Platform-Independent, Community-Supported Software for Describing and Comparing Microbial Communities. *Applied and Environmental Microbiology* 75:7537–7541. DOI: 10.1128/AEM.01541-09.

Setti L, Passarini F, De Gennaro G, Barbieri P, Perrone MG, Borelli M, Palmisani J, Di Gilio

A, Torboli V, Fontana F, Clemente L, Pallavicini A, Ruscio M, Piscitelli P, Miani A. 2020. SARS-Cov-2RNA found on particulate matter of Bergamo in Northern Italy: First evidence. *Environmental Research* 188:109754. DOI: 10.1016/j.envres.2020.109754.

Shen J, Yuan L, Zhang J, Li H, Bai Z, Chen X, Zhang W, Zhang F. 2011. Phosphorus dynamics: From soil to plant. *Plant Physiology* 156:997–1005. DOI: 10.1104/pp.111.175232.

Smith KE, Weis D, Amini M, Shiel AE, Lai VWM, Gordon K. 2019. Honey as a biomonitor for a changing world. *Nature Sustainability* 2:223–232. DOI: 10.1038/s41893-019-0243-0.

Solayman M, Islam MA, Paul S, Ali Y, Khalil MI, Alam N, Gan SH. 2016. Physicochemical Properties, Minerals, Trace Elements, and Heavy Metals in Honey of Different Origins: A Comprehensive Review. *Comprehensive Reviews in Food Science and Food Safety* 15:219–233. DOI: 10.1111/1541-4337.12182.

Soltani N, Keshavarzi B, Sorooshian A, Moore F, Dunster C, Dominguez AO, Kelly FJ, Dhakal P, Ahmadi MR, Asadi S. 2018. Oxidative potential (OP) and mineralogy of iron ore particulate matter at the Gol-E-Gohar Mining and Industrial Facility (Iran). *Environmental Geochemistry and Health* 40:1785–1802. DOI: 10.1007/s10653-017-9926-5.

van der Steen JJM, de Kraker J, Grotenhuis T. 2012. Spatial and temporal variation of metal concentrations in adult honeybees (*Apis mellifera* L.). *Environmental Monitoring and Assessment* 184:4119–4126. DOI: 10.1007/s10661-011-2248-7.

Tang Z, Li W, Tam VWY, Xue C. 2020. Advanced progress in recycling municipal and construction solid wastes for manufacturing sustainable construction materials. *Resources, Conservation & Recycling: X* 6:100036. DOI: 10.1016/j.rcrx.2020.100036.

Tautz J. 2008. *The Buzz about Bees*. Berlin, Heidelberg: Springer Berlin Heidelberg. DOI: 10.1007/978-3-540-78729-7.

Ul-Hamid A. 2018. *A Beginners' Guide to Scanning Electron Microscopy*. Cham: Springer International Publishing. DOI: 10.1007/978-3-319-98482-7.

Vaknin Y, Gan-Mor S, Bechar A, Ronen B, Eisikowitch D. 2000. The role of electrostatic forces pollination. *Plant Systematics and Evolution* 222:133–142. DOI: 10.1007/BF00984099.

vanEngelsdorp D, Meixner MD. 2010. A historical review of managed honey bee populations in Europe and the United States and the factors that may affect them. *Journal of Invertebrate Pathology* 103:S80–S95. DOI: 10.1016/j.jip.2009.06.011.

Vasileiadis S, Puglisi E, Trevisan M, Scheckel KG, Langdon KA, McLaughlin MJ, Lombi E, Donner E. 2015. Changes in soil bacterial communities and diversity in response to long-term silver exposure. *FEMS Microbiology Ecology* 91:fiv114. DOI: 10.1093/femsec/fiv114.

Vojvodic S, Rehan SM, Anderson KE. 2013. Microbial Gut Diversity of Africanized and European Honey Bee Larval Instars. *PLoS ONE* 8. DOI: 10.1371/journal.pone.0072106.

Wang Y, Eliot MN, Wellenius GA. 2014. Short-term changes in ambient particulate matter and risk of stroke: A systematic review and meta-analysis. *Journal of the American Heart Association* 3:1–22. DOI: 10.1161/JAHA.114.000983.

Wang K, Li J, Zhao L, Mu X, Wang C, Wang M, Xue X, Qi S, Wu L. 2021. Gut microbiota protects honey bees (*Apis mellifera* L.) against polystyrene microplastics exposure risks. *Journal of Hazardous Materials* 402:123828. DOI: 10.1016/j.jhazmat.2020.123828.

World Health Organization. 2013. *Health effects of particulate matter. Policy implications for*

countries in eastern Europe, Caucasus and central Asia.

Wu T, Ma Y, Wu X, Bai M, Peng Y, Cai W, Wang Y, Zhao J, Zhang Z. 2019. Association between particulate matter air pollution and cardiovascular disease mortality in Lanzhou, China. *Environmental Science and Pollution Research* 26:15262–15272. DOI: 10.1007/s11356-019-04742-w.

Yadav S, Kumar Y, Jat BL. 2017. Honeybee: Diversity, Castes and Life Cycle. In: *Industrial Entomology*. Singapore: Springer Singapore, 5–34. DOI: 10.1007/978-981-10-3304-9_2.

Yang Y, Vance M, Tou F, Tiwari A, Liu M, Hochella MF. 2016. Nanoparticles in road dust from impervious urban surfaces: distribution, identification, and environmental implications. *Environmental Science: Nano* 3:534–544. DOI: 10.1039/C6EN00056H.

Younes M, Aquilina G, Castle L, Engel KH, Fowler P, Frutos Fernandez MJ, Gürtler R, Gundert-Remy U, Husøy T, Mennes W, Agneta Oskarsson PM, Rainieri S, Shah R, Waalkens-Berendsen I, Wölfle D, Gaffet E, Mast J, Peters R, Rincon AM, Fürst P. 2019. Scientific opinion on the proposed amendment of the EU specifications for titanium dioxide (E 171) with respect to the inclusion of additional parameters related to its particle size distribution. *EFSA Journal* 17. DOI: 10.2903/j.efsa.2019.5760.

Yun J-H, Lee J-Y, Hyun D-W, Jung M-J, Bae J-W. 2017. *Bombella apis* sp. nov., an acetic acid bacterium isolated from the midgut of a honey bee. *International Journal of Systematic and Evolutionary Microbiology* 67:2184–2188. DOI: 10.1099/ijsem.0.001921.

Zarić NM, Deljanin I, Ilijević K, Stanisavljević L, Ristić M, Gržetić I. 2018a. Honeybees as sentinels of lead pollution: Spatio-temporal variations and source appointment using stable isotopes and Kohonen self-organizing maps. *Science of The Total Environment* 642:56–62. DOI: 10.1016/j.scitotenv.2018.06.040.

Zarić NM, Ilijevic K, Stanisavljevic L, Grzetic I. 2018b. Use of honeybees (*Apis mellifera* L.)

as bioindicators of spatial variations and origin determination of metal pollution in Serbia. *Journal of the Serbian Chemical Society* 83:773–784. DOI: 10.2298/JSC171110018Z.

Zhou W, Apkarian R, Wang ZL, Joy D. 2006. Fundamentals of Scanning Electron Microscopy (SEM). In: *Scanning Microscopy for Nanotechnology*. New York, NY: Springer New York, 1–40. DOI: 10.1007/978-0-387-39620-0_1.

Zhou X, Taylor MP, Davies PJ. 2018. Tracing natural and industrial contamination and lead isotopic compositions in an Australian native bee species. *Environmental Pollution* 242:54–62. DOI: 10.1016/j.envpol.2018.06.063.

Zhu L, Qi S, Xue X, Niu X, Wu L. 2020. Nitenpyram disturbs gut microbiota and influences metabolic homeostasis and immunity in honey bee (*Apis mellifera* L.). *Environmental Pollution* 258:113671. DOI: 10.1016/j.envpol.2019.113671.

Zorlu T, Nurullahoğlu Z, Altuntaş H. 2018. Influence of Dietary Titanium Dioxide Nanoparticles on the Biology and Antioxidant System of Model Insect, *Galleria mellonella* (L.) (Lepidoptera: Pyralidae). *Journal of the Entomological Research Society* 20.

Ringraziamenti

Queste poche righe sono per ringraziare le persone a me care e che stimo particolarmente.

Il primo ringraziamento va alla mia tutor la Dr. Ilaria Negri che mi ha permesso di fare ricerca, dandomi fin dal primo giorno piena fiducia, permettendomi di fare esperienze formative importanti, condividendo con me la sua passione per la ricerca, per la didattica e tutta la sua esperienza, senza tralasciare mai il lato umano e i sentimenti. Ringrazio il Dr. Marco Pellecchia di Koinè, il Prof. Giancarlo Capitani e i dottori Paolo Gentile e Tiziano Catelani dell'Università Milano Bicocca per il supporto nelle analisi al SEM-EDX, aiuto nell'interpretazione dei dati e per aver condiviso con me il loro sapere.

Ringrazio i colleghi e amici del dipartimento DIANA, in particolare: la Dott.ssa Elisa Eufemi con cui ho collaborato sin dall'inizio di questa esperienza nella quale ho trovato una amica. Ringrazio tutti i miei colleghi e amici di dottorato, specialmente Maria, Federico, Roberta A. e Roberta Z., la segreteria e la scuola di dottorato Agrisystem.

Un grazie particolare va al Dr. Mario Barbato che mi ha insegnato, aiutata, supportata e sopportata tanto nella ricerca negli ultimi due anni e che per sua liberissima scelta continuerà a farlo.

L'ultimo grazie va a mia madre, ai miei fratelli, a mia zia Ivana, alla mia amica Serena e a tutti i miei amici di giù. Ovviamente un grazie va anche Ciro per essermi sempre stata vicino.